PRESENCE OF CELL-CYCLE DEPENDENT SUBSTRUCTURE AT LOW DOSE IN THE RADIATION SURVIVAL RESPONSE OF ASYNCHRONOUS V79-WNRE CELLS

by

MARK WILLIAM SKWARCHUK

B.Sc., University of Saskatchewan, 1987

A THESIS SUBMITTED IN PARTIAL FULFILLMENT OF

THE REQUIREMENTS FOR THE DEGREE OF

MASTER OF SCIENCE

in

THE FACULTY OF GRADUATE STUDIES

THE DEPARTMENT OF PHYSICS

We accept this thesis as conforming

to the required standard

THE UNIVERSITY OF BRITISH COLUMBIA

April 1990

In presenting this thesis in partial fulfilment of the requirements for an advanced degree at the University of British Columbia, I agree that the Library shall make it freely available for reference and study. I further agree that permission for extensive copying of this thesis for scholarly purposes may be granted by the head of my department or by his or her representatives. It is understood that copying or publication of this thesis for financial gain shall not be allowed without my written permission.

Department of Physics

The University of British Columbia
Vancouver, Canada

Date April 24, 1990

ABSTRACT

Survival studies using cell sorting techniques together with data averaging on asynchronously dividing V79-WNRE cells reveal statistically significant evidence of substructure in the radiation survival response at low dose (2 to 3 Gy) that cannot be adequately characterized by a single linear-quadratic function, $S = \exp(-\alpha D -\beta D^2)$. The data suggest a two-component response that is particularly evident when plotted in the linear form of the linear-quadratic equation, $-\ln(S)/D = \alpha + \beta D$. Application of other survival models (Single Hit + Multi Target and Repair-Misrepair) does not eliminate the substructure.

The substructure may result from subpopulations of cells at different stages of the cell cycle, which differ in their radiosensitivity, giving rise to a two-component survival response. In order to explore this hypothesis, studies were carried out with populations of partially synchronized cells. The mitotic selection technique was employed alone or in combination with 12 hours exposure to 1 mM hydroxyurea or 1 μg/ml aphidicolin to obtain large numbers of synchronized cells. G1/S phase populations obtained by mitotic selection followed by hydroxyurea or aphidicolin do not show the substructure found for asynchronous cells, thus supporting the hypothesis. G1 phase populations obtained by mitotic selection alone revealed substructure which could be characterized by a single fit to the RMR or SH+MT models. Structure was also present in the response of heterogeneous S/G2 phase populations synchronized by mitotic selection followed by hydroxyurea, but may not be present in the response of S phase populations synchronized by mitotic selection alone. The data are consistent with the hypothesis that the substructure is a result of sensitive (G1, G2 or M) and resistant (S) subpopulations of cells.

TABLE OF CONTENTS

LIST OF TABLES

LIST OF FIGURES

ACKNOWLEDGEMENTS

I have discovered that a Master's thesis is not the product of only one person's efforts. There are many individuals that I would like to thank and acknowledge for their invaluable assistance with this project.

I gratefully acknowledge the financial support I received in the form of a two year Natural Sciences and Engineering Research Council scholarship and the support provided by the Department of Physics and the British Columbia Cancer Research Center.

I wish to express my deepest gratitude to Dr. L. D. Skarsgard, my supervisor, for his encouragement, guidance and financial support throughout this project.

I would like to thank Dr. R. E. Durand for his many helpful suggestions in the course of this investigation.

I am grateful to Nancy Lepard and Denise McDougal for their enduring cooperation and technical expertise. I thank Adriana Vinczan for her many hours of laborious colony counting assistance. Special thanks to Susan MacPhail and Douglas Wilson for their encouraging words and optimism and for generally just "being there".

I thank my mother and my sister for always encouraging me in my endeavors and for their warm words of support over the years.

With special consideration I thank my (soon to be) wife Patricia for her unending love, understanding, perseverance and encouragement during the past $2\frac{1}{2}$ years. Without her gentle and loving support I could not have sanely completed this work. It is to Trish that I dedicate this thesis.

"The earth is the Lord's, and
all it contains,
The world, and those who
dwell in it.
For He has founded it
upon the seas,
And established it upon
the rivers."

(Psalm 24:1-2)

1. INTRODUCTION

1.1 RADIATION

With the discovery of the X-ray in 1895 by Roentgen and the subsequent explorations into the hidden world of the atom and nucleus, mankind has grappled with the potential benefit and hazard inherent in this form of invisible energy. Nearly a century after its fortuitous discovery, the physical basis of radiation is well understood, but its practical benefits continue to be explored and its potential for harm respected. The discipline of radiobiology has emerged to study the action of ionizing radiations on living things. The successful application of radiation to improve the human condition, particularly in its use for the treatment of cancer, has been a significant achievment of the scientific process in the twentieth century.

All human beings are exposed to radiation on a daily basis from natural and man-made sources. Naturally occuring radiations include (1) cosmic rays, (2) external gamma rays arising from the radioactivity of certain elements, principally uranium, potassium and thorium, that occur naturally in the earths crust, and (3) internal radiation arising from radioactive materials, principally potassium-40, carbon-14 and radon, that are naturally present in our bodies. In addition to the natural background radiation further exposures result from man-made materials and devices which include principally X-rays and radiopharmaceuticals in medicine, and to a much lesser extent exposure from smoke detectors, the atmospheric testing of nuclear weapons, accidents in nuclear power plants and various other sources. The absorbed dose of radiation received in a typical

lifetime from natural sources is essentially matched by the contribution from man-made sources, effectively doubling the average exposure dose (Johns and Cunningham 1983). It is thus of personal importance to have an understanding of the effects of radiation on biological systems.

Radiations may be classified into two categories, ionizing and non-ionizing radiation. Non-ionizing radiations, including ultraviolet, visible light, infrared and radiowaves, transfer enough energy to raise an electron of a target atom to a higher energy state but without ejecting it from the atom. Ionizing radiations, including X, gamma, beta and alpha-rays, protons and heavy ions, transfer sufficient energy to an atom to cause the ejection of one or more of the orbital electrons. The large, localized release of energy by ionizing radiation may cause the breakage or rearrangement of strong chemical bonds. The ejected electrons cause ionization and excitation of other electrons resulting in further ionizations and excitations until all of the available energy is expended. Damage to atoms and molecules by radiation may occur through a direct ionization of the atom or molecule or through an indirect reaction with primary radical species, principally those created through ionization of the water molecule. The mechanisms and types of damage resulting from non-ionizing and ionizing radiation are quite distinct. The effects of only ionizing radiation will be considered in this thesis.

The effects of radiation on biological systems became apparent soon after the discovery of the X-ray, with often tragic consequences for the pioneering scientists who were exposed to large doses of radiation. More recently, there has been considerable interest in the effects of low doses of radiation. Correlation has been suggested between low radiation doses and an increased incidence of some types of cancers, particularly leukemia

and lung cancer, for some groups of exposed persons such as atomic bomb survivors of Japan, radiologists, non-cancerous patients treated with radiation and miners of radioactive ore (Lewis 1957,UNSCEAR 1982, BEIR III). There is an apparent need to understand the fundamental mechanism(s) of radiation interaction with biological matter at low dose. Due to statistical and technological limitations, experimental results at low dose were typically available only by extrapolation from high dose data. It would be valuable to obtain statistically relevant data on the effects of radiation on mammalian cells using accurate experimental technique at low dose.

The "endpoint" may be defined as that effect measured at the end of an experiment. For the purposes of this thesis the endpoint used is the retention of proliferative capacity of mammalian cells. From this perspective, a viable cell is one that has retained its capacity for sustained proliferation. The "lethal" effect of radiation is then that effect which results in the loss of reproductive integrity. A "survivor" is a cell which, after receiving a dose of radiation, retains its reproductive integrity and is able to proliferate to produce a large clone or colony. The term "surviving fraction" (usually designated by S) refers to that fraction of cells that has "survived" a dose of radiation and has been able to generate a clone of like cells. These definitions will be used throughout this thesis (Hall 1988, Brosing 1983).

The term "absorbed dose" or simply "dose" refers to the energy absorbed from ionizing radiation per unit mass of the medium. The SI unit for dose is the gray (Gy) which represents the absorption of 1 joule of energy per kilogram of irradiated material. A recently abandoned, but commonly used, measure of absorbed dose is the rad, which is smaller than

the Gy by a factor of 100 (1 Gy = 100 rads = 1 J/kg) (Johns and Cunningham 1983).

1.2 MODELS OF CELLULAR INACTIVATION

The retention of reproductive integrity by members of an irradiated cell population may be assessed by the scoring of surviving (colony forming) cells; it is much more difficult to score the number of killed cells (Puck and Marcus 1956). The dose-effect relationship may then be described in terms of survival as a function of dose. The graphical representation of this relationship, usually presented with surviving fraction plotted on a logarithmic scale and dose plotted on a linear scale, is referred to as a "survival curve". The use of a logarithmic, rather than linear, scale for the plotting of survival allows for the practical visual examination of small levels of survival (less than 1%) that are associated with higher doses. As well, the dose-survival relationship may be well described on theoretical grounds by an exponential based model whose form may be more easily visualized on a logarithmic scale.

It would seem an unlikely prospect that the dose-survival relationship for a biologically heterogeneous population of cells could be adequately described by a simple algebraic expression (Alper 1979). It is nonetheless convenient to describe the survival response by such an expression even if it is only regarded as an approximation. Many different models and theories have been presented to describe mammalian cell survival. These models are usually based on some hypothesis as to the basic mechanism by which radiation produces biological damage or change and they often are expressed in a relativily simple algebraic form. Such expressions allow for the comparison of curves for cells of different lines

or for the same cell line irradiated under different conditions (Goodhead 1980).

Table I lists a few of the models most commonly cited in the literature. Their use for analysis of data in this thesis reflects their widespread application (but not necessarily suitability) in describing mammalian cell survival.

1.2.1 Simple Target Theory

The simplest form of target theory follows from the consideration that the inactivation of cells is a random process that can be described statistically by the Poisson distribution :

$$P_{a,n} = (a^n e^{-a}) / n! \qquad (1)$$

where $P_{a,n}$ is the probability of 'n' events occuring for 'a', the average number of random events (hits) in a cell or target. Assuming simple single hit, single target theory in which only a single event is sufficient to cause lethality, then only those cells that have received no hits (ie. n=0) will survive. For a large number of events, the surviving fraction is then equal to $P_{a,0}$, the probablity that a cell will receive no hits :

$$S = P_{a,0} = a^0 e^{-a} / 0! = e^{-a} \qquad (2)$$

If the average number of hits 'a' is proportional to the dose D (ie. a = kD) then the expression for the survival becomes

$$S = e^{-kD} \qquad (3)$$

where 'k' is the inactivation constant. The dose which gives on average one hit (or event) per target (the inactivation dose) is called D_o and may be found by equating equations 2 and 3 for a=1 and $D=D_o$:

$$e^{-kD} = e^{-1}$$

$$\text{or,} \qquad kD_o = 1$$

$$\text{therfore,} \qquad k = 1/D_o$$

Hence, equation 3 can be written in terms of D_o as

$$S = e^{-D/D_o} \tag{4}$$

Simple target theory results in an exponential that appears as a straight line when plotted on semi-logarithmic graph paper. Its applicability lies mainly in the description of the inactivation of enzymes and viruses (Alper 1979).

TABLE I
MODELS OF CELL INACTIVATION

MODEL	EQUATION
Single-Hit Single Target	$S = e^{(-D/D_o)}$
Single-Hit Multi Target	$S = 1 - [1 - e^{(-D/D_o)}]^n$
Single-Hit Multi Target with initial slope	$S = e^{(-D/D_1)}\{1 - [1 - e^{(-D/D_o)}]^n\}$
Linear-Quadratic	$S = \exp(-\alpha D - \beta D^2)$
Repair-MisRepair two parameter form	$S = e^{(-\delta D)}(1 + \delta D/\epsilon)^{\epsilon}$
Repair-Misrepair three parameter form	$S = e^{(-\delta D)}\ (1 + \delta D/\epsilon)^{\epsilon\phi}$

1.2.2 Shouldered Survival Models

Survival curves for mammalian cells irradiated with X-rays commonly display at low dose a region where there is a smaller proportion of cells killed per unit dose than after larger doses. The initial, low dose region is often referred to as the "shoulder" of the survival curve. Many survival models accommodate the appearance of a shoulder in the curve, often through underlying theories for its cause such as the accumulation or repair of damage.

The two parameter single hit, multi target model allows for an initial shouldered region with zero slope and terminating with an exponential at higher doses. The theory underlying the model assumes that the cells contain 'n' targets, each of which must be inactivated in order to cause cell lethality. Using the same definitions for the parameters as outlined previously, the probability that a target will not be inactivated as a result of a dose of radiation is e^{-D/D_o} and hence the probability that a target will be inactivated is $(1 - e^{-D/D_o})$. In order for the cell to be killed all n targets must be inactivated with a probability of $(1 - e^{-D/D_o})^n$, assuming an equal probability for each target. The probability of the cell surviving is the probability of not all of the targets being hit, given by

$$S = 1 - (1 - e^{-D/D_o})^n \qquad (5)$$

For high doses equation 5 reduces to

$$S = n\, e^{-D/D_o} \qquad (6)$$

which is a simple exponential. This model describes the survival response in terms of two parameters, n and D_o. The inactivation dose D_o is the dose which produces on average one hit per target and results in the reduction

of the survival by a factor of e^{-1} or 37% in the exponential region. Plotted in semi-logarithmic form, D_o may be found as the inverse of the slope of the terminal exponential region. Extrapolating the graph to the y-axis, the value of n may be found as the y-axis intercept. According to the theory of this model, n corresponds to the number of targets that need to be inactivated in order to cause cell lethality and hence n was originally referrred to as the target number. Since it has been found that n depends on the physiological condition of the cells, their stage in the cell cycle and upon irradiation conditions, the term extrapolation number was adopted to refer to the parameter n (Elkind and Whitmore 1967).

According to equation 5, the initial slope of the survival curve at zero dose should be zero, implying that the first small increment of dose received by the cells would not cause lethality. The concept of a threshold dose below which exposure would cause no permanent harm is implied by this theory. Most experimental data, however, exhibits a non-zero initial slope which is better accomodated by a number of different models.

The addition of a one-hit component to the single hit, multi target model by Bender and Gooch (1962) allows for a non-zero initial slope. The two component single hit, multi target (SH+MT) model

$$S = e^{-D/D_1} [1 - (1 - e^{-D/D_o})^n] \qquad (7)$$

contains three parameters D_1, D_o and n. The one hit component e^{-D/D_1} describes the possibility that a more densing ionizing particle may act as a single hit to either simultaneously inactivate all targets, or to simultaneously provide several hits on a target requiring more than one hit for inactivation (Alper 1979). The presence of three parameters may provide a better fit to the data, however it may be very difficult to

uniquely determine the values of the three parmeters without specifying one of them.

A survival model that has been suggested by several investigators on the basis of empirical as well as theoretical grounds is the linear-quadratic (LQ) model :

$$S = \exp(-\alpha D - \beta D^2) \tag{8}$$

This model allows for a non-zero initial slope and a continuously bending form at high dose. The model was first proposed by Sinclair empirically who observed that it provided a good fit to his data (Sinclair 1966).

Two theoretical formulations based on quite different sets of assumptions have followed resulting in the same form of the equation. Kellerer and Rossi based their rationale on the conclusion that the relative biological effectiveness (RBE) of neutrons compared to X-rays varied inversely with the neutron dose as follows (Kellerer and Rossi 1972, 1978) :

$$\text{RBE} \propto (\text{neutron dose})^{-1/2} \tag{9}$$

RBE may be defined as D_x/D_n, the ratio of doses of X-rays and neutrons required to give the same effect. Since RBE = D_x/D_n, substituting for the determined relation RBE α $D_n^{-1/2}$ gives

$$D_x/D_n = \text{constant} \cdot D_n^{-1/2}$$

$$\text{therefore,} \quad D_x = k \cdot D_n^{1/2}$$

$$\text{or,} \quad D_x^2 = k \cdot D_n \tag{10}$$

Kellerer and Rossi reasoned that for radiation of high LET (Linear Energy Transfer-the amount of energy released per unit path length of an

ionizing particle), lethal events accumulated linearly with dose according to single hit, single target theory. For radiation of low LET, lethal events were suggested to accumulate as the square of the dose, ie inactivation of a cell target required energy deposition by two independant electrons within the target volume. The two sublesions that result must then interact in order to inactivate the cell. Therfore, damage by high LET particles is directly proportional to dose and damage by low LET particles is proportional to the square of the dose. Both high and low LET components are present in the spectrum of primary electrons that result from the interaction of X-rays with matter. The two terms may be regarded as separately describing the intratrack events, by the linear term, and the intertrack events, by the quadratic term. The constants α and β then describe cell kill by the single-hit and double-hit mechanisms respectively.

Chadwick and Leenhouts arrived at the same equation based on their "Molecular Theory of Cell Survival" (Chadwick and Leenhouts 1973, 1985). Their assumption was that cell inactivation resulted from the induction of unrepairable double-strand breaks in the DNA. The breaks could occur either as a result of a single event occuring in both strands (and hence would be directly proportional to dose) or from separate events resulting in a single strand break in each of the two strands located in close proximity to each other (proportional to the square of the dose). The parameters α and β then represent the damage resulting from a single event double strand break or from the interaction of two single strand breaks in the DNA, respectively.

The LQ model has been shown by several investigators to provide a very good fit to many different types of data (Blakely 1985, Gillespie

et al 1975 a b, Hall 1988, Kellerer and Rossi 1972, 1978, Chadwick and Leenhouts 1985). There is some question, however, as to the nature of the survival response at high dose. Alper has suggested that there is considerable evidence in support of a terminal exponential region to shouldered survival curves (Alper 1979, 1980). The LQ equation may be regarded then as only a low dose approximation which could not adequately accomodate a terminal exponential. In her formulation, the proposed basic mechanism of cell killing by radiation is single-hit inactivation. The shoulder of the survival curve may be evidence of a repair process operating at the outset of the irradiation but becoming less effective at higher doses, until inactivation occurs without concomitant repair.

An example of a repair model is the Repair MisRepair (RMR) model of Tobias et al (Tobias et al 1980, 1985). The model assumes that the fate of a given lesion resulting from a dose of radiation is initially uncertain, but may over time be repaired, misrepaired or remain as a remnant lesion. The two parameter form of the RMR equation is :

$$S = e^{-\delta D} (1 + \delta D/\epsilon)^{\epsilon} \qquad (11)$$

where the parameter δ is the yield of uncommitted (to repair or misrepair) lesions per dose, and ϵ is the repair ratio of linear self-repair to quadratic mis-repair. Further, if the assumptions are made that the total time available for repair is fixed, perhaps due to progression through the cell cycle, and that linear self-repair is not a perfect process, then a three parameter form results :

$$S = e^{-\delta D} (1 + \delta D/\epsilon)^{\epsilon\phi} \qquad (12)$$

where ø is the probability that linear self-repair is eurepair (successful). Equation 11 has zero initial slope whereas equation 12 has non-zero initial slope indicating incomplete repair. Both forms of the equation bend continuously at high dose.

It is important to note that any of the survival models that allow for a non-zero initial slope can be expanded to give a polynomial of the form

$$\ln(S) = -(a + b\,D + c\,D^2 + d\,D^3 + \ldots) \qquad (13)$$

where a=0 since the data is usually normalized to S=1 at zero dose. At low dose, a good description of the data can usually be obtained by fitting to the first two parameters of the expansion, with a=0, which is in reality just the LQ equation. It should be noted also that the ability of a model to provide a good fit to the data does not verify the underlying assumptions of the model. It simply states that the data can be described by that particular algebraic expression.

1.3 THE CELL CYCLE

One of the fundamental characteristics of a living cell is its ability to reproduce. All new cells are formed from the reproduction of existing cells and the continued existence of a cellular species requires such a process in order to ensure its long term survival (Prescott 1978). Cell reproduction consists of the growth of the cell, the duplication of its chromosomes and its ultimate division into two identical daughter cells. Growth occurs as the cell synthesizes additional molecules of basic cell constituents such as proteins, enzymes, nucleic acids, carbohydrates, lipids and other components essential to the cell and its progeny. Chromosome duplication is necessary in order to provide each daughter cell with an identical complement of genetic material. Cell division, then, allows for the distribution of cytoplasmic parts and nuclear material to the daughter cells (Prescott 1978).

This process of growth, chromosome duplication and cell division occurs over a time course known as the "cell cycle" or "mitotic cycle". It begins with the formation of a daughter cell by division, continues through the processes of cell growth and chromosome duplication, and ends with the division of that cell into two new daughter cells. The time taken to complete one cell cycle is called the "generation time", "mitotic cycle time" or "cell cycle time". Most of the generation time is occupied by the period between divisions, called "interphase", during which time the cell doubles its mass and duplicates all of its contents in preparation for the next division. The division process itself occupies only a relatively small portion of the generation time. During this time, however, the processes of nuclear division, called "mitosis", and cytoplasmic division, called "cytokinesis", occur.

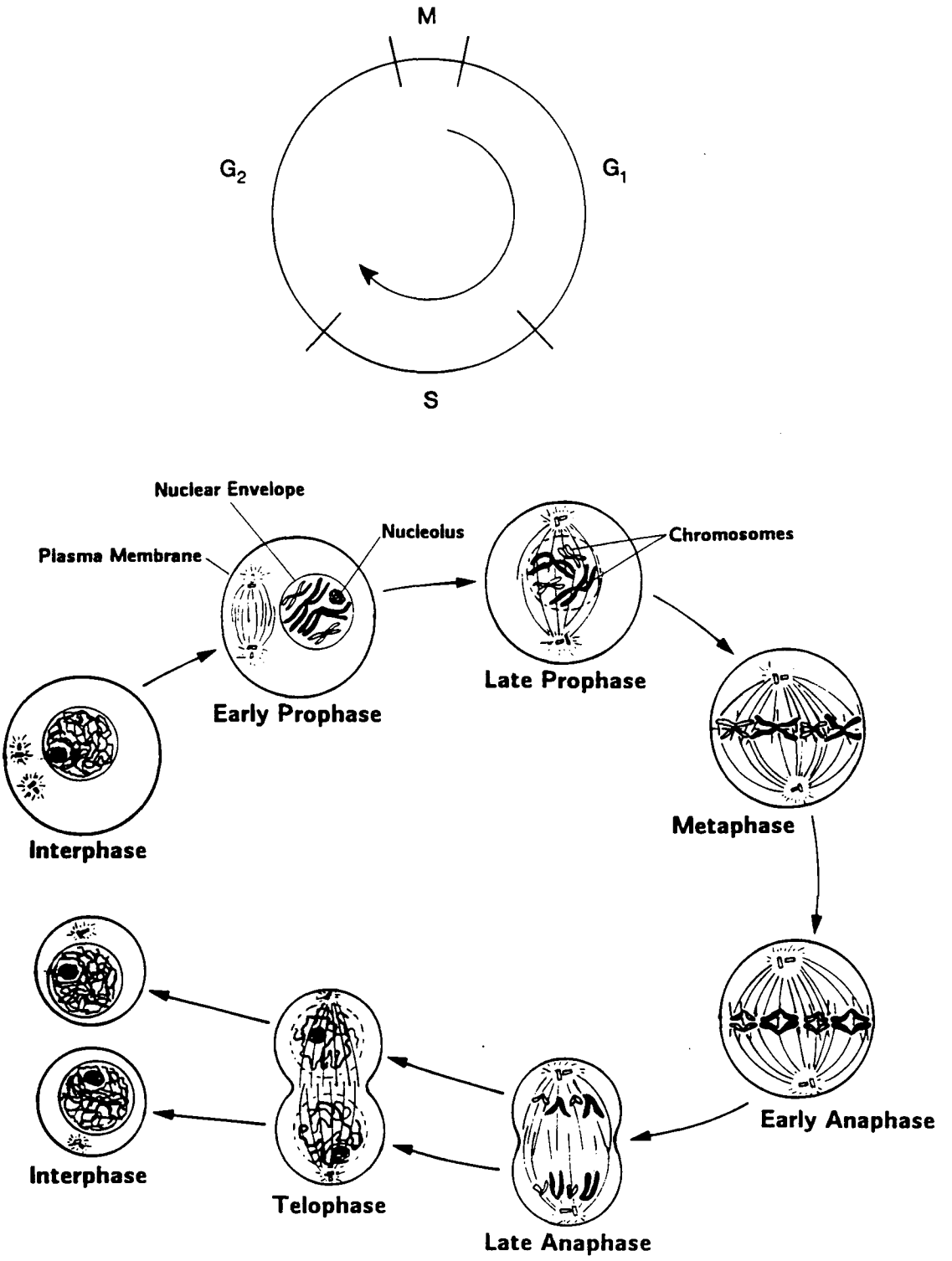

FIGURE 1. PHASES OF THE CELL CYCLE AND MITOSIS

a). The stages of the cell cycle for actively growing mammalian cells. M, mitosis; S, the DNA synthetic stage; G1 and G2, the gaps in DNA synthesis before and after S phase. b). The phases of mitosis : prophase, metaphase, anaphase and telophase. The configuration of the chromosomes at the various stages of mitosis are shown schematically.

1.3.1 Interphase

Howard and Pelc were the first to observe that interphase was composed of three separate phases (Howard and Pelc 1953). They determined that the process of DNA synthesis occured during a discrete time interval in the middle of interphase and that this phase was both preceeded and followed by gaps in DNA synthetic activity. They referred to these stages as S phase, the period of DNA synthesis, G1 phase, the first gap prior to DNA synthesis, and G2 phase, the second gap occuring after the DNA had been doubled but before division, which was referred to as M phase, the mitotic stage. Since cell reproduction is cyclically repeated for each generation of cells, it may be represented by a circle as shown in figure 1a. The circumference of the circle represents the overall generation time. The portion of the cycle time occupied by each phase of the cell cycle is labelled appropriately as G1, S, G2 or M.

The G1 phase begins with the end of the previous division and continues to the onset of chromosomal DNA synthesis. Cellular growth begins in G1, with the synthesis of structures and macromolecules continuing throughout the S and G2 phases. No specific events occur in G1 that would uniquely characterize it in the same way that S phase is uniquely characterized by DNA synthesis. Preparations for initiating DNA synthesis probably are carried out in G1. In addition to general cell growth, G1 also contains stop-start signals that determine whether the cell will proceed through S and G2 to the next division or remain temporarily or permanently arrested in G1 (Prescott 1978, Becker 1986).

The S phase begins with the initiation of DNA synthesis and continues to the completion of this process. It is during this time that the

genetic information is doubled in preparation for the equal division of the chromosomes in mitosis. DNA synthesis occurs semiconservatively and is accompanied by the synthesis of histone proteins that immediately bind to the DNA.

The G2 phase begins with the termination of DNA synthesis and ends with the initiation of mitosis. It is also a period of continued general growth without any uniquely characterizing events. It is likely that G2 phase is occupied by preparations for mitosis and cytokinesis, in particular the production of those factors involved in condensing the interphase chromosomes and required for construction of the mitotic apparatus.

1.3.2 Mitosis

The beginning of mitosis is visually evident by the progressive condensation (thickening and coiling) of the duplicated interphase chromosomes and ends with the subsequent separation of the two daughter cells (cytokinesis). The events of mitosis may be further subdivided into four phases : prophase, metaphase, anaphase and telophase, as illustrated in figure 1b.

Prophase is marked by the appearance of the chromosomes as they progressively condense and become visible when viewed under a light microscope. During S phase, each chromosome has duplicated so that they consist of two sister chromatids joined together at a point called the centromere. By late prophase, the nuclear envelope has begun to fragment, the nucleoli disappear and most of the nuclear proteins and all of the RNA are released into the cytoplasm. A structure called the mitotic spindle begins to appear at the poles of the nucleus. Its fibers appear to aid the condensed chromosomes to align along the equator (metaphase plate) of the

nucleus during metaphase. During anaphase, the sister chromatids begin to separate as they are drawn away from each other and toward opposite spindles, and hence to opposite ends of the cell. At the same time, the spindle poles also begin to migrate in opposite directions along with the separated daughter chromosomes which arrive at the poles of the spindle by the beginning of telophase. The daughter chromosomes begin to uncoil in telophase and revert to their interphase appearance. The spindle fibers disappear, the nuclear envelope reforms, nucleoli begin to reappear and the RNA and proteins originally from the nucleus return to the two daughter nuclei. The final event in cell division is cytokinesis where the cytoplasm is divided between the daughter cells. The cells are then able to independently progress through their own cell cycles.

It has been observed by many investigators that several properties of a cell appear to relate to its position in the cell cycle (Mitchison 1971, Mazia 1961). In particular, the radiosensitivity of a population of cells appears to vary as a function of cell cycle position as was first shown by Terasima and Tolmach in 1961 for the human cell line HeLa. Shortly thereafter in 1963, Sinclair and Morton showed that Chinese hamster cells in late S phase were most resistant to the effects of radiation, while those at or close to mitosis were the most sensitive. The reason for this variation is still not clearly understood although it may relate to the fixation or repair of damage to the DNA or to a variation in the levels of naturally occuring sulfhydryl compounds in the cell that act as radioprotectors. In order to make such measurements, however, populations of uniform age specificity must be obtained, which is the topic of the following section.

1.3.3 Synchronized Populations Of Cells

An asynchronous population in exponential growth is comprised of cells in all of the stages of the cell cycle. They are usually present in quantities related to the fraction of the total generation time occupied by that stage. Results obtained using asynchronous populations, then, reflect the heterogeneity of the constituent cells and may be considered as an age-averaged response. Observation and interpretation in many situations may be greatly simplified by using cell populations of uniform age. It is of great benefit to obtain cell cultures that have been synchronized with respect to some point in the cell cycle (Klevecz 1975).

The methods used to obtain synchronous cultures may be divided into two broad classes. The first are induction synchrony techniques in which all of the cells of a culture are induced to divide sychronously by some treatment, and the second are selection synchrony techniques, in which a certain segment of a cell population that is at a particular stage of the cell cycle is separated off and grown as a separate synchronous culture (Mitchison 1971).

An example of a selection synchrony technique is mitotic selection. The technique is based on the structural changes that accompany the progress of a mammalian cell from interphase to mitosis. Interphase cells growing on the surface of a culture vessel remain spread out and are quite firmly attatched. During mitosis, however, they round up in the shape of a sphere and become very loosly attatched to the surface by thin cytoplasmic strands, as shown in figure 4a. The constituents of the microtubules, tubulin, that bind the interphase cells firmly to the vessel surface are recruited in mitosis to form the spindle apparatus, hence causing the

mitotic cell to round up and be less firmly attatched. The mitotic cells are thus easily removed from the vessel surface by shaking the culture vessel resulting in a shear force of growth medium that dislodges the dividing cells with minimal disturbance to interphase cells.

The resulting population of mitotic cells may then be removed and grown as a synchronous culture, although a slight degree of contamination by interphase cells is common. This technique was first used by Terasima and Tolmach and is considered the method of choice for producing synchronous cultures from cells growing on solid surfaces (Terasima and Tolmach 1961). Since the resulting population is synchronized in mitosis, within a short time they will progress into G1 phase and continue to proceed through the cell cycle. However, decay in the synchrony occurs rather quickly due to variation in the generation time for individual cells. The process of mitotic selection may be combined with an induction synchrony technique in order to further increase the quality of the synchronized population.

An example of an induction synchrony technique is the addition of a chemical inhibitor to a population of cells (Ashihara and Baserga 1979, Grdina et al 1984, Hall 1988, Mitchison 1971, Nias and Fox 1971, Stubblefield 1968). An inhibitor generally acts at one stage of the cell cycle causing an accumulation of cells at this point so that after release from the inhibitor the population is able to progress synchronously. Two inhibitors of DNA synthesis are hydroxyurea and aphidicolin. Addition of these drugs to a cell population causes accumulation at the G1/S border. Removal of the drugs results in a population highly synchronized at the G1/S border that can then be allowed to progress to the desired stage in the cell cycle.

Hydroxyurea acts both as an inhibitor of DNA synthesis and as a cytotoxic agent to those cells synthesizing DNA at the time of drug addition. Hydroxyurea blocks DNA synthesis by inhibiting the reduction of ribonucleoside diphosphate (NDP) molecules to deoxyribonucleoside diphosphate (dNDP) molecules which are the precursors of DNA. The enzyme that catalyzes this reaction, ribonucleotide reductase, contains a free radical that is essential for catalysis of the reduction. Hydroxyurea acts to quench the free radical and hence block the action of the enzyme in catalyzing the reduction of NDP molecules to dNDP. The result is that the pool of dNDP molecules necessary for DNA replication is not created and progression from G1 to S phase is thus blocked. An accumulation of cells at the G1/S border results (Sinclair 1967, Stryer 1988).

Aphidicolin, a fungal diterpenoid, acts as an inhibitor of DNA synthesis but appears not to have the same cytotoxic effect on S phase cells as hydroxyurea when low concentrations of the drug are present. Aphidicolin blocks DNA synthesis by inhibiting DNA polymerase-α which is the primary enzyme involved in nuclear DNA replication. The functioning of polymerase-β, involved in the repair of nuclear DNA, and of polymerase-Γ, involved in the replication of mitochondrial DNA, appear unaffected by the actions of aphidicolin. Similar to the result of hydroxyurea, exposure of mammalian cells to aphidicolin results in a block in the progression of cells from G1 into S phase, hence there is a subsequent accumulation of cells at the G1/S border (Ikegami et al 1978, Iliakis 1982, 1989, Pedrali-Noy and Spadari 1979).

It is important to note, however, that although both hydroxyurea and aphidicolin result in an accumulation of cells at the G1/S border, the

mechanism for their action is quite different. Separate enzymes involved in different aspects of DNA replication are blocked by the two drugs.

Exposure to these or one of the many other inhibitory drugs that align a population at a certain stage of the cell cycle is typically carried out for a period equal to the generation time of the cell. During this time, other cellular processes proceed normally so that unbalanced growth and a perturbation in metabolism after release are likely consequences of this method. Hence, a selection technique such as mitotic selection which induces minimal or no perturbation in the resulting population, is considered to be an ideal method in theory. However, many investigators have found that populations synchronized by exposure to hydroxyurea or aphidicolin show little effect of the drug or the state of unbalanced growth in the response of the population to radiation (Sinclair 1967).

1.4 IMPORTANCE OF LOW DOSE STUDIES

Studies on the effects of low doses of radiation on biological systems have recently been of interest to both the general public, who are concerned with the possible health effects resulting from exposure to low levels of radiation, and to the scientific community, which is also interested in understanding the basic mechanisms of radiobiolgy. With a better understanding of radiobiological mechanisms, improvements may then be applied to radiation protection, radiotherapy and the modelling of radiation interactions with matter.

Cancer incidence in Canada has been estimated at over one hundred thousand new cases per year (not including skin cancer) or about 7 new cases per 1000 people (National Cancer Institute 1989). Of these cases, about 50% have been controlled by the three major modalities,

surgery, radiotherapy and chemotherapy. Radiotherapy alone or in combination with the other modalities is, thus, an important treatment for the control of cancer for a large segment of the general population.

In order to determine the survival response of a cell population, a radiobiologist usually irradiaties a sample in a series of dose increments within a very short period of time on the order of minutes. Samples for analysis are withdrawn after each dose increment. The accumulation of the increments up to each dose point represents an acute or single exposure to radiation. A radiotherapist, however, usually delivers a very large dose (50 to 80 Gy) in a series of much smaller fractions (1.5 to 3 Gy) administered daily several days a week over a period of several weeks. It has been shown both *in vitro* and *in vivo* that if sufficient time for repair is allowed between successive fractions a great deal of the sublethal radiation damage will be repaired (Elkind and Sutton 1958, Elkind and Sutton 1960, Elkind and Whitmore 1967, McCulloch and Till 1962). A population of cells exposed to a series of dose fractions responds to each fraction as though it were delivered from the initial region of the survival response. Hence, from the radiotherapist's perspective, survival responses obtained at high dose from a single acute exposure may be of little practical value to the clinical situation where the response to much lower doses (1.5 to 3 Gy) is more relevant. An experimental technique which could accurately determine the survival response and model parameters at low dose could be of great benefit for optimization of treatment protocols.

During the past few years widespread concern has been expressed regarding the health effects of low levels of ionizing radiation. Studies on humans and on laboratory animals indicate that there are three health

effects that need to be examined at low levels of exposure : cancer induction, birth abnormalities (from *in utero* exposure) and genetic effects (Hendee 1984, AAPM #18 1986). Direct measurement of the health effects due to low dose exposure would be desirable but have been inconclusive due to the long latent periods associated with most radiation induced injury in humans and because of the statistically complicated nature of the injury expression above normal incidence. Estimates of risk at low dose are usually, then, extrapolated from more reliable data at high dose according to a linear, linear-quadratic or quadratic dose-response relationship. Information regarding the relationship between dose and injury expression (presuming a correlation between the cell killing, carcinogenic and genetic effects of radiation) is thus of importance, especially data obtained at low doses (BEIR III 1980, UNSCEAR 1982).

Accurate survival data at low doses is also important for the examination of the various models of cellular inactivation. These models make predictions about the cellular response at low dose which can be tested by accurate experimental results. For example, the two-parameter single hit, multi target model has an initial zero slope, indicating that a threshold dose may need to be received by a cell prior to exhibiting radiation damage. In contrast, the linear-quadratic model has a non-zero initial slope indicating that any dose will cause damage, although the damage may be quite small. Precise measurement of the cellular response to low doses of radiation would help discriminate between the two predictions.

Measurements of cell survival data in the low dose region may also be valuable for accurate determination of certain model parameters which in many instances are estimated from high dose data under assumptions that

may not be valid. Over the past decade, there has been considerable evidence generated indicating that there may be strong correlation between those parameters that describe the initial region of the *in vitro* survival response of human tumour cell lines and the clinical radioresponsiveness of the corresponding tumours (Fertil et al 1981, 1985, Deacon et al 1984). The parameters which provided the best correlation were the initial slope, α, the surviving fraction at 2 Gy, S_2, and the mean inactivation dose, $\overline{D}$ (Fertil 1984). Other parameters used extensively in the past and based on the single hit, multi target model are the extrapolation number n, the average dose for one hit per target D_o and the quasi threshold dose D_q, which is the dose corresponding to the intersection of the high dose exponential with the survival fraction at S=1. As well, the ratio α/β derived from the linear-quadratic parameters α and β has particular significance in calculations related to fractionated doses used in radiotherapy (Douglas and Fowler 1975, Fowler 1987). It would be of enormous benefit to obtain accurate measurements of such parameters, particularly in the clinically relevant dose range of 1.5 to 3 Gy.

1.5 PURPOSE OF THE THESIS

The importance of obtaining accurate survival data in the low dose region has recently been indicated by the results of Skarsgard et al in measuring the response of an asynchronous culture of V79-171 cells (Skarsgard et al 1990 a,b,c) The survival data indicated the prescence of substructure in the response at low dose in the form of a discontinuity in the survival curve at 2.8 Gy that could not be adequately characterized by a single fit to the linear-quadratic or any other model of cell inactivation. The data suggested a two-component character to the response which led to the fitting of the low dose and high dose data

separately to the LQ equation. This resulted in a good fit to the data and a consistent divergence between the low dose and high dose fits. Statistical analysis of the fit parameters also revealed that the structure was reproducible.

The purpose of this thesis is : 1). to obtain and examine the radiation response of an asynchronously dividing population of V79-WNRE cells, 2). to determine if a similar type of substructure as observed previously for V79-171 cells is present in the asynchronous response of V79-WNRE cells, 3). to examine possible hypotheses to explain the substructure if it is observed. This includes examining the data with respect to various models of cellular inactivation. As well, it includes the determination and examination of the survival response of cell populations of uniform age synchronized at some point in the cell cycle.

2. MATERIALS AND METHODS

2.1 CULTURE TECHNIQUE

The cultured cell line used for all of the *in-vitro* biological experiments reported here was the cell line V79-WNRE, which was kindly provided by Dr. J. D. Chapman. The V79-WNRE is a strain of the Chinese hamster lung cell line V79-379-A (modal chromosome number of 21) which has been adapted to spinner culture (Chapman et al 1970, 1972).

The V79-WNRE cells were routinely grown in suspension culture in minimum essential medium S-14 (Ca^{++} free : Gibco 410-1400, Grand Island, N.Y.) supplemented with fetal bovine serum (7% by volume : Gibco), penicillin (80 units/ml), streptomycin (80 units/ml), and sodium bicarbonate (2.2 g/l). (Chapman 1975) Cultures were grown in a spinner vessel (Bellco Hanging Bar Spinner Flask, Bellco Glass Inc.) and were pre-gassed with 95% air, 5% CO_2 prior to growth at 37 ^{o}C in an incubator (Biomedic) on a stir table. The cell culture was maintained at a concentration of between $2x10^4$ and $3x10^5$ cells/ml through daily dilutions. The cell doubling time was 9-10 hours during asynchronous exponential growth.

The cells could be transferred from spinner culture to monolayer culture with ease. Monolayer cultures were maintained in minimum essential medium F-15 (containing Ca^{++} : Gibco 410-1500), supplemented with fetal bovine serum (12.5% by volume : Gibco), penicillin (80 units/ml), streptomycin (80 units/ml) and sodium bicarbonate (2.2 g/l). Cultures were grown at 37 ^{o}C in a humidified atmosphere of 95% air, 5% CO_2.

Spinner culture was used to grow cells on a day-to-day basis. Cells were transferred to monolayer when needed for asynchronous radiation experiments and for the seeding of the tissue culture roller bottles used for mitotic selection.

2.2 SYNCHRONY TECHNIQUE

For the experiments with synchronous cells, a variation on the mitotic selection technique of Terasima and Tolmach (1963) was employed either alone, to obtain a population of mitotic/early G1 phase cells, or in combination with hydroxyurea or aphidicolin, to obtain a population of G1/S phase cells.

2.2.1 Table-Shake Method

The early synchrony work of Terasima and Tolmach involved a simple procedure of gently pipetting fresh medium over a monolayer of cells, resulting in the release of those cells in mitotis. In an effort to obtain a greater number of released cells that were more homogeneously in mitosis, this technique was modified to involve the shaking of several flasks of cells simultaneously on a reciprocating shaker table (Brosing 1983, Gillespie 1975, Petersen et al 1968, Sinclair and Yu 1967). This approach was initially followed to obtain synchronized populations of cells in the present work.

The following procedure was employed : Three days prior to mitotic selection, $5x10^4$ cells were seeded into each of 6 plastic tissue culture (TC) flasks (growth area of 75 cm^2/flask : Falcon Tissue Culture Products) in minimum essential medium (MEM) F-15 containing 10% fetal bovine serum

(FBS). (The FBS concentration in the MEM F-15 was later increased to 12.5%.) The plated cells were placed in an incubator and fed one day prior to mitotic selection with 15 ml of fresh MEM F-15. The shake-off procedure was conducted in a 37 ^{o}C warm room. A horizontal shaker table was used to swirl the overlying medium over the monolayer of cells. Six flasks at a time were shaken (combined surface area of 450 cm^2) for a 5 minute interval at 124 vibrations/minute with a stroke length of 4.5 cm. The overlying medium was collected in a chilled 4 ^{o}C vessel and replaced with 10 ml of pH and temperature equilibrated MEM S-14 (suspension medium) (Gillespie 1975). The flasks were then placed in the warm room for 10 minutes prior to the next shake-off.

This procedure was repeated up to 14 times in order to examine the yield and quality of the selected populations.

2.2.2 Mitotic Selection Using The Talandic Cell Cycle Analyzer

The technique actually employed to obtain large numbers of mitotic or early post-mitotic cells for the synchronized cell experiments involved using a Talandic Cell Cycle Analyzer (Talandic Research Corp., 2500 E. Foothill Blvd., Pasadena, CA) (Klevecz 1972, 1975). The system may act in either a fully-automated or manually-operated capacity to produce populations of tissue culture cells of uniform age using the mitotic selection technique. The cell cycle analyzer removes mitotic cells from exponentially growing asynchronous cultures on the inner surface of roller bottles by the gentle shearing effect of medium over the monolayer. The advantage of using this system is that a high yield may be achieved by using up to four roller bottles each with a large number of cells seeded onto a

combined surface area of 7000 cm^2. As well, the 'harvest' can be repeated at intervals as brief as 20 minutes.

The system configuration used for our requirements consisted of a sequence controller, a culture rotator and a sampling/feeding pump, as shown in figure 2 . The sequence controller coordinated the systems' timing functions such as the number of harvest cycles of an experiment, the duration of each harvest cycle and the duration of the mitotic selection, sampling and feeding periods within each cycle. The culture rotator apparatus consisted of up to four roller bottles mounted horizontally and driven by Teflon derotator caps. Sampling and feeding was carried out through Teflon-tipped stainless steel tubing mounted within the derotator caps. The original apparatus harvested mitotic cell suspensions by dragging the sample tube along the lower surface of the roller bottle. As well, feeding with new medium was from a tube elevated 4 cm above the roller bottle surface. Since both of these processes were thought to dislodge interphase cells and leave behind the uncollected cells to contaminate later rolls, the sampling tube was modified to both collect cells and feed fresh medium against the vertical end of the roller bottles. A single pump and length of tubing was then used to perform both the sampling and feeding procedures. The culture rotator controller could be used to vary the rotation speed of the bottles from 0.1 to 300 rpm.

The system allows for complete automation of all of the above features, but was used manually in order to have more complete control of its functioning. Although not used, the system does allow for the use of a batch sample collector to automatically deliver the total volume of the roller bottles after each selection into one of 24 sterile flasks. It may also be noted that this system has been widely used by several investigators using

many different cell lines with good success (Blakely 1985, Klevecz 1975, Ngo et al 1988).

A detailed and labour intensive process was followed to produce a synchronized population of cells. The following is an outline of the steps involved.

2.2.2.1 Preparation of the Roller Bottles

During the initial synchronous cell experimental period, long glass roller bottles (1950 cm^2/bottle, 10 cm diameter, 62 cm length) were used for cellular growth and mitotic selection. These bottles had the advantage of being reusable, but the disadvantage of having to ensure an accomodating surface for cell attatchment. Bottles were cleaned by hand using standard glassware cleaner (Sparkleen), scrubbed, rinsed 10-12 times with distilled water, then allowed to sit or rotate overnight containing a solution of 0.1 M sodium carbonate. The bottles were thoroughly rinsed 10-12 times with double distilled water before sterilization. The proper preparation of the roller bottle surface represented a critical phase of the synchronization procedure (Klevecz 1975, Monahan 1974).

It was consistently observed that cells seeded onto such a surface produced large cell aggregates attatched to the surface. After some hours in roller culture, these clumps developed 'tails' (and often a pair of V-shaped 'comet tails') along the circumference of the roller bottle surface. These 'tails' presumably developed under the influence of the fluid currents as the medium passed over the cell clumps. The clumping may have contributed to the number of non-mitotic cells present in the harvested populations, so in an effort to remedy the problem a switch was made to the use of plastic roller bottles (Falcon #3035). This switch alone

did not solve the problem, but through the optimization of cell attatchment parameters (discussed later) the clumping problem was eliminated and consistently uniform monolayers were observed (with only the occasional smaller clumps present). Preparation of the plastic roller bottles involved rinsing the inner surfaces of the bottles twice with 50 ml of MEM F-15 (lacking FBS and sodium bicarbonate) to remove any plastic debris to which cells could have attatched to produce clumps.

2.2.2.2 Seeding the Roller Bottles

The following steps pertain to the seeding of the plastic roller bottles. A word regarding the glass roller bottles follows at the end of this section.

Twenty-four hours prior to the seeding of the roller bottles, 40-44 hours prior to the beginning of an experiment, cells in spinner culture were diluted to a concentration of about $4x10^4$ cells/ml to reach a final concentration of 2.0-2.5 $x10^5$ cells/ml the next day. About 1 litre of cells at this final concentration was required to seed the four roller bottles. The cell suspensions were cooled on ice to minimize clumping, placed into two to four 500ml glass centrifuge vessels, and centrifuged at 600 rpm (90 g's) for 8 minutes (Sorvall RC-3 general purpose centrifuge). The supernatant was aspirated and the cells were resuspended in 50 ml of MEM F-15 using vigorous vortexing of the cell suspension for 5 to 8 seconds to disperse the cells. A cell count was performed and the cells were observed under a microscope for the prescence of clumps. Into each of four standard glass bottles containing 250 ml of prewarmed, pH balanced MEM F-15 was placed $5x10^7$ cells that had been passed through a mesh filter to remove large cell clumps. The cell suspensions were mixed by

hand swirling with any surface bubbles being aspirated prior to seeding. The contents of one of these bottles was then carefully poured into one plastic roller bottle. Caution was exercised to minimize the creation of surface bubbles which were observed to disrupt the delicate cell attatchment process leading to streaking of the monolayer. The roller bottle was then gassed for about 40 seconds with 95% air, 5% CO_2 and a sterile derotator cap was inserted into the open end of the roller bottle. The roller bottle was then attatched to the culture rotator apparatus and allowed to rotate at 0.3 rpm in a 37 ^{o}C warm room. This procedure was repeated until all four bottles were seeded, gassed and rotating. The roller bottles were allowed to rotate at 0.3 rpm for one hour during which time the bottles were gently mixed every 15 minutes by raising and lowering either end of the rotator apparatus by 4 cm in order to evenly disperse the cells in suspension. After this cell attatchment period the medium from each of the bottles was pumped out, fresh prewarmed MEM F-15 was pumped in and the rotation speed increased to 1 rpm. It was observed that between 80-95% of the cells would attatch during this time.

The procedures during the cell attachment phase were implemented to stop the formation of long (3 cm) V-shaped cell clumps that were observed on the surface of both the glass and plasic roller bottles prior to these measures. It was thought that those cells which never attached to the vessel surface may have clumped together in suspension while at slow rotation speed and attached at some later point, and grown into the observed clumps. By removing those cells that did not attach and by increasing the rotation speed to 1 rpm to avoid nutrient deprivation, uniform monolayers were consistently observed with only much smaller clumps occasionally present.

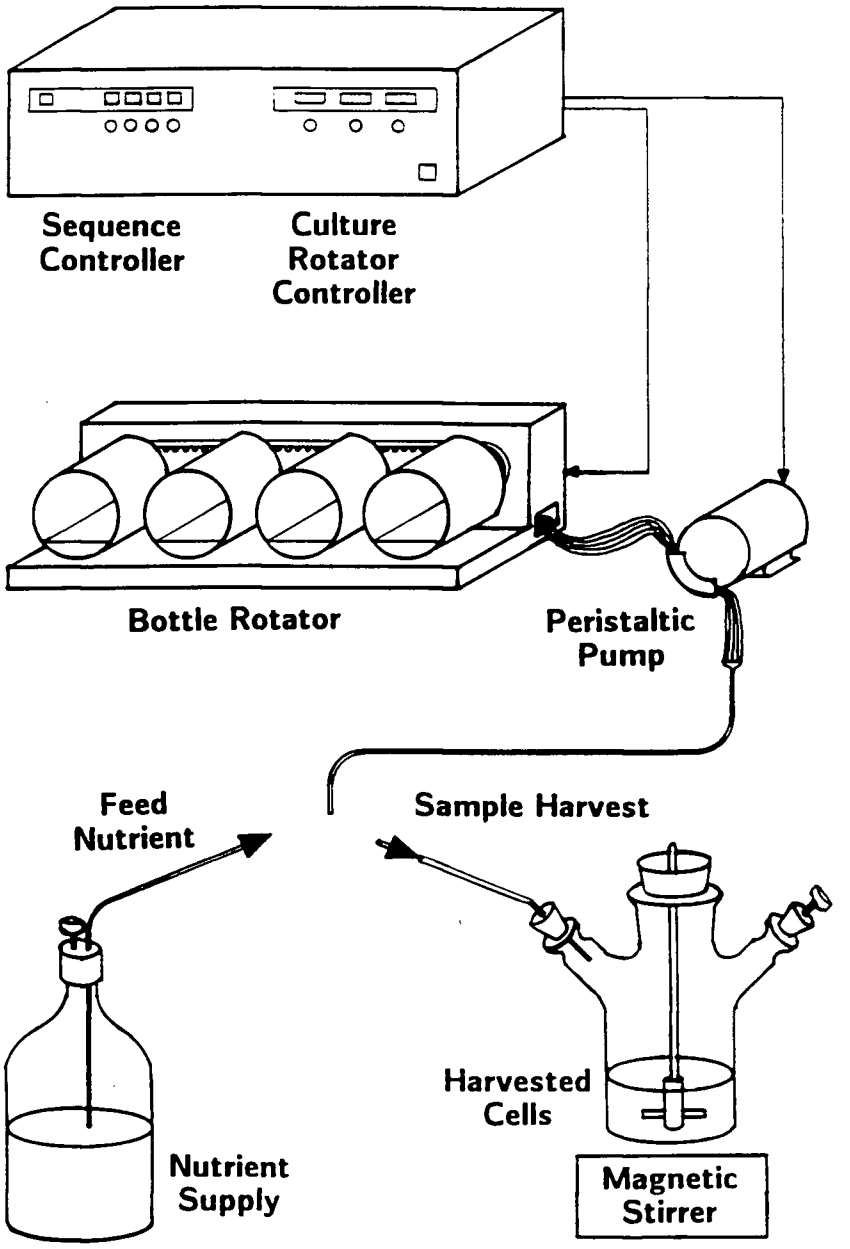

FIGURE 2 : DIAGRAM OF TALANDIC CELL CYCLE ANALYZER

Cells synchronized by mitotic selection were obtained using a Talandic Cell Cycle Analyzer. The system consisted of a sequence controller, a culture rotator and a sampling/feeding pump. A population of mitotic cells was obtained by increasing the rotation speed of the roller bottles to 200 rpm for 5-6 minutes. Harvests could be repeatedly obtained at intervals as brief as 20 minutes.

The roller bottles were allowed to grow undisturbed for 14-18 hours prior to any mitotic selection work. After this growth period, the monolayer had covered 40-70% of the bottle surface area.

Glass roller bottles (used in the early experiments with synchronized cells) were treated similarily with a few notable exceptions. The cells used to seed the roller bottles were grown using monolayer culture in sixteen 175 cm^2 plastic TC flasks and were removed from the flask surface by incubating in a 0.1% trypsin solution at 37 ^{o}C for 6 minutes. The cell suspension was centrifuged, the supernatant was discarded, the cells were resuspended in MEM F-15 and $15x10^7$ cells were placed into each roller bottle. The bottles rotated at 0.3 rpm for the entire length of the growth period prior to any mitotic selection work.

2.2.2.3 Obtaining Mitotic Cells

The mitotic selection process consisted of a series of harvest cycles each lasting 25-30 minutes. Within each harvest cycle a higher rotation rate of 200 rpm occurred for 5-6 minutes; then rotation was decreased to 1 rpm while the medium containing the suspended mitotic cells was aspirated from each bottle (sample time 2 min.) ; 25 ml of pre-warmed MEM S-14 was fed into each bottle and pumped out in order to flush the lines and to pick up any cells left over from the sampling (flush time 1 min.) ; 125 ml of MEM S-14 was then fed to each bottle (feed time 2 min.) ; during the remainder of the harvest cycle (15-20 min.) the bottles were left undisturbed rotating at 1 rpm.

For experiments involving cells synchronized by mitotic selection alone, the first ten populations harvested were not used since cellular debris and small cell clumps were present in these populations. For

experiments involving mitotic selection followed by a drug block, the first three populations harvested were discarded.

2.2.3 Mitotic Selection Followed By A Drug Block

Experiments were also conducted on cells synchronized using the combined methods of mitotic selection followed by a drug block. Mitotic cells, obtained from two harvests pooled together and held on ice, were centrifuged for 7 minutes at 600 rpm (90 g's), decanted, and resuspended in MEM F-15 containing hydroxyurea at concentrations of 1 mM or 2 mM, or aphidicolin at concentrations of 1 µg/ml or 3 µg/ml. The suspension of cells was then plated into two 175 cm^2 TC flasks with $1.2x10^7$ cells in 50 ml and one 75 cm^2 TC flask with $5x10^6$ cells in 20 ml. The flasks were placed in a humidified 37 ^oC incubator for 12 hours prior to release from the drug.

Hydroxyurea (BDH Chemicals : molecular weight 76.06 g/mol) is readily soluble in water and aqueous media. A 10 mM solution was initially prepared in MEM F-15 and allowed to mix on a 37 ^oC stir table for 10 minutes. The solution was sterile filtered and either a 1 mM or 2 mM solution was made after the appropriate dilution (Fox et al 1987, Sinclair 1967).

Aphidicolin (Sigma Chemicals : anhydrous molecular weight 338.5 g/mol) was initially dissolved in dimethyl sulphoxide (DMSO) at 1 mg/ml of DMSO, since it is not water soluble. Since small quantities of the aphidicolin were required (0.1-0.4 mg) and since the drug is a possible carcinogen and mutagen, great care was taken not to come into direct contact with the drug by adding the DMSO directly into the drug vial using a syringe. The drug was mixed by hand in its container and allowed

to sit for 10 minutes at 37 ^{o}C. A 4 µg/ml solution was then prepared in MEM F-15, allowed to mix for 10 minutes at 37 ^{o}C, sterile filtered, then diluted to a final concentration of 1 µg/ml. The final concentration of DMSO in the MEM F-15 was 0.1%, which has been reported by others not to influence cell growth or radiation response. A 3 µg/ml solution was also prepared in a similar manner with a final DMSO concentraion of 0.1%. (Fox et al 1987, Ikegami et al 1978, Iliakis et al 1982).

2.3 EXPERIMENTAL TECHNIQUE

Experiments were conducted on both asynchronous and synchronous poplulations of cells to determine their response to radiation as a function of radiation dose.

2.3.1 Experiments Using Asynchronous Cells

Asynchronous cell cultures were prepared by loading $5x10^5$ cells in 40 ml MEM F-15 into 175 cm^2 TC flasks 46-50 hours prior to an experiment. Three flasks were required for each survival response and usually 2 to 5 such responses were performed in succession on a typical experiment day. The flasks were incubated at 37 ^{o}C in a humidified atmosphere containing 95% air, 5% CO_2,. The overlying medium from each flask was replaced 24 hours later with an equal volume of fresh prewarmed MEM F-15. After 46-50 hours since the original seeding, the monolayer was observed to cover 50-70% of the growth surface of the flasks, ensuring an exponentially growing poplulation. Cells were harvested by trypsinization : the overlying medium was decanted, 10 ml of 0.1% trypsin was added to each flask, swirled and poured off; another 10 ml of trypsin was added, swirled

and poured off; 2 ml of trypsin was then added; the flask was incubated at 37 ^{o}C for 6 minutes followed by gentle agitation to release the cells from the flask surface; the trypsin was neutralized by adding 8 ml of MEM F-15 (high FBS content). The cell suspension was centrifuged, the supernatant decanted and the cells resuspended in MEM S-14 lacking sodium bicarbonate. Between 45-55 ml of the cell suspension at a concentration of 4-6 x10^5 cells/ml was then loaded into a water-jacketed spinner flask maintained at 37 ^{o}C. Irradiations were then performed as described in section 2.3.3.

2.3.2 Experiments Using Synchronized Cells

2.3.2.1 Cells Synchronized By Mitotic Selection Alone

Populations of cells synchronized by mitotic selection alone were obtained as described in section 2.2.2.3. One harvest of cells was pumped directly from the roller bottles into a large spinner flask (Bellco) which was then gassed with 95% air, 5% CO_2 and placed on a spinner table at 37 ^{o}C. When the cells had progressed to the desired stage in the cell cycle they were centrifuged and resuspended in MEM S-14 lacking sodium bicarbonate. Between 45-55 ml of the cell suspension at a concentration of 3-5 x10^5 cells/ml was then loaded into a water-jacketed spinner flask maintained at 37 ^{o}C. Irradiations were performed as described in section 2.3.3.

It was observed that several hours after mitotic selection many of the daughter cell doublets were still present in the population, although the cells themselves had progressed over time beyond their original mitotic stage. Experiments were also conducted on populations that were reduced to a single cell suspension by exposure to trypsin. After a synchronized

population had progressed to the desired stage in the cell cycle it was centrifuged and resuspended in 10 ml of 0.1% trypsin for 4 minutes. After neutralizing the trypsin with 30 ml of MEM F-15, the cells were centrifuged again and resuspended in MEM S-14 lacking sodium bicarbonate. Between 45-55 ml of the cell suspension at a concentration of 3-5 $x10^5$ cells/ml was then loaded into a water-jacketed spinner flask maintained at 37 ^oC. Irradiations were then performed as described in 2.3.3.

2.3.2.2 Cells Synchronized By Mitotic Selection + A Drug Block

Populations of cells synchronized by mitotic selection followed by a drug block were obtained as described in section 2.2.3. After the 12 hour exposure, the cells were released from the inhibitory effects of the drug block by pouring off the drug-containing medium, rinsing twice with MEM F-15 (lacking FBS and sodium bicarbonate), and feeding with fresh MEM F-15 (with FBS and sodium bicarbonate). The flasks were placed in a 37 ^oC incubator. When the cells had progressed to the desired stage in the cell cycle, they were harvested by trypsinization, centrifuged and resuspended in MEM S-14 lacking sodium bicarbonate. Between 45-55 ml of the cell suspension at a concentration of 4-6 $x10^5$ cells/ml was then loaded into a water-jacketed spinner flask maintained at 37 ^oC. Irradiations were then performed as described in section 2.3.3.

2.3.3 Irradiation And Plating Procedure

A cell suspension prepared as described in sections 2.3.1 and 2.3.2 in a water-jacketed spinner flask was mounted near the head of the X-ray source (Philips, 250 kVp X-rays, HVL 1.5 mm Cu) as shown in figure 3a. A magnetic stir motor placed beneath the flask holder maintained a stir rate of 350-360 rpm. The cell suspension was kept at 37 ^oC using a circulating

water bath connected to the water jacket of the spinner flask. The cells were gassed for 15 minutes prior to and during irradiation with humidified air at 37 ^{o}C. A dose rate of 2.30 Gy/minute was determined using Fricke ferrous sulphate dosimetry (Fricke and Hart 1966). The dose rate was also measured periodically by secondary ionization measurements using a Victoreen model 500 electrometer.

After control samples were removed, the irradiation proceeded with two samples withdrawn after each dose increment. Between 29 and 35 samples were removed during the irradiation time which took less than 15 minutes to complete. Samples were vortex mixed at low speed, placed on ice and taken to the cell sorter.

A cell sorter (Beckton-Dickinson 440) was used to deliver a known number of cells from each sample by identifying the cells on the basis of light scattering without the use of a cell stain. Three aliquots were dispensed from each sample into 5 ml test tubes containing 4 ml of MEM F-15. Each aliquot was plated into a 100 mm petri dish with 14 ml of MEM F-15 to produce about 500 colonies/petri dish after 6 days incubation. For higher dose samples (8-12 Gy), only 2 aliquots were dispensed per sample since the larger cell numbers needed at such high doses required considerably longer sorting time.

After incubation, the medium was poured off from each dish and 6 ml of cold malachite green stain was added. Six minutes later, the stain was poured off and the dishes were rinsed under cold running water. Colonies containing greater than 50 cells were then counted.

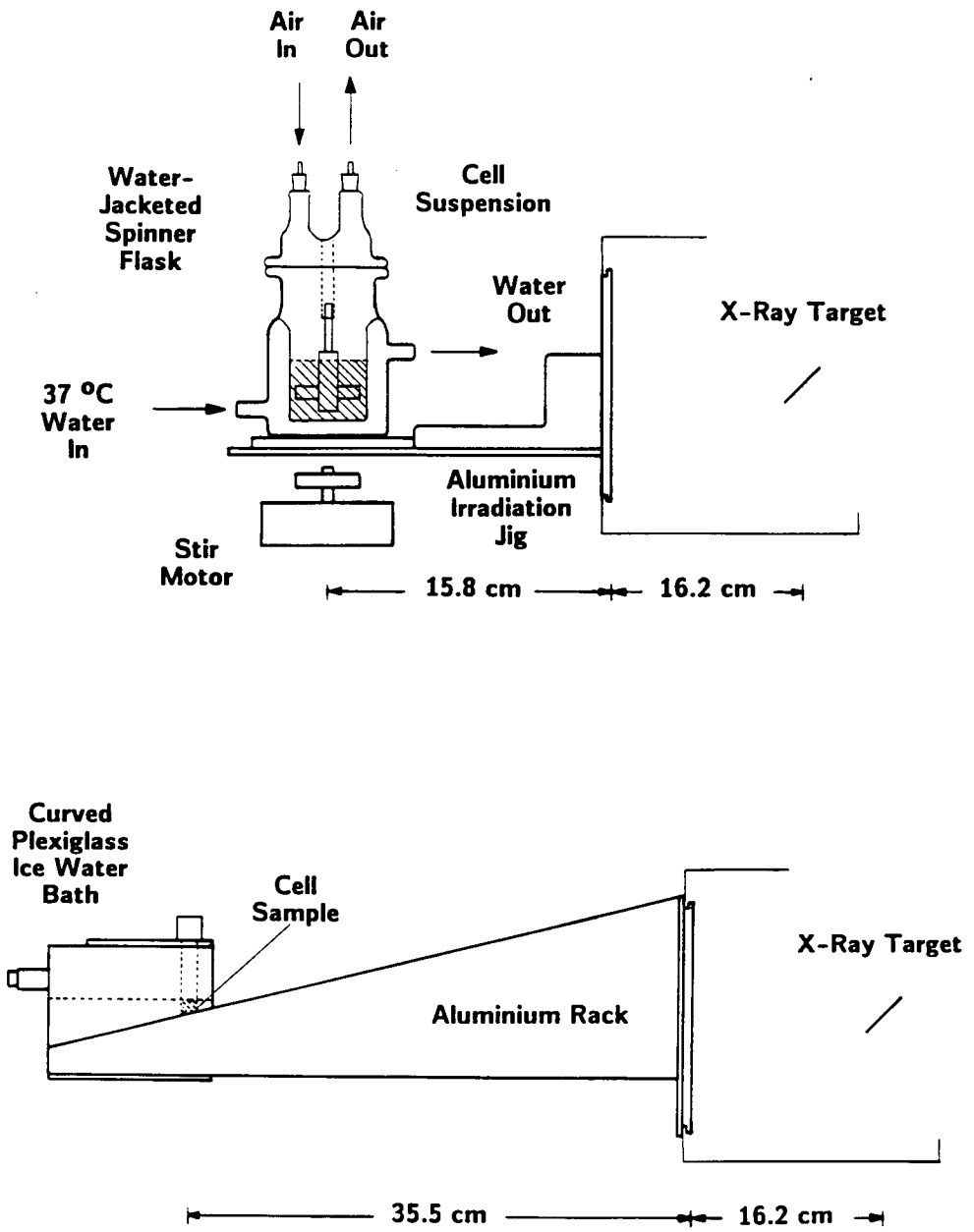

FIGURE 3 : DIAGRAM OF IRRADIATION SET-UP

(a) The irradiation vessel was placed on an aluminum rack attached to the head of the X-ray unit (Philips 250 kVp). A stir motor beneath the vessel stirred the 37 ^{o}C suspension at 350-360 rpm. A dose rate of 2.30 Gy/min was obtained at a distance of 32 cm from the X-ray tube target.
(b) The response of synchronized cells to a single dose of radiation was measured by placing a 5 ml test tube containing the cell suspension in a plexiglass and aluminum rack attatched to the head of the X-ray unit. A dose rate of 1.27 Gy/min was obtained at a distance of 40 cm from the X-ray tube target. Samples were irradiated on ice water.

2.3.4 Calculation Of Surviving Fraction

The endpoint considered in this thesis is the retention of proliferative capacity of mammalian cells. This may be determined by measurement of the fraction of cells that have survived a dose of radiation ie. the surviving fraction, S, given by :

$$S(D_i) = PE(D_i)/PE(D=0) \tag{14}$$

where $PE(D_i)$ is the "plating efficiency" at a given dose D_i. The plating efficiency may be defined as that fraction of cells seeded that grow into colonies :

$$PE(D_i) = \#\text{ of colonies counted } / \#\text{ of cells originally seeded} \tag{15}$$

Division by PE(D=0), the plating efficiency of an unirradiated sample for dose D=0 Gy, normalizes the plating efficiencies and results in a quantity defined as the surviving fraction.

The data that follow in the Results and Discussion sections are the averaged surviving fractions for a stated number of repeated experiments of a certain type. The value of the surviving fraction at a given dose is thus the arithmetic mean of the individual responses for that particular dose, given by :

$$S(D_i) = \{ \sum_{i=1}^{N} S(D_i) \} / N \tag{16}$$

for N, the number of individual responses. The standard error in the mean was calculated using the expression :

$$\delta S(D_i) = \{ \langle \sum_{i=1}^{N} [S(D_i) - \bar{S(D_i)}]^2 \rangle / \langle N (N - 1) \rangle \}^{\frac{1}{2}} \tag{17}$$

The error bars attatched to the data points are standard errors of the mean. Points for which an error bar is not shown indicate that the standard error is smaller than the size of the data point symbol.

2.3.5 Calculation Of The RMS Deviation Of A Curve Fit To The Data

Throughout this thesis the various models of cellular inactivation, discussed in section 1.2, were applied to survival data as a means of characterizing the observed responses. In order to test and compare the ability of the survival equations to adequately describe the survival response (but not necessarily their underlying assumptions) a calculation was routinely performed of the RMS (Root Mean Square) deviation of the fitted curve to the data. The RMS deviation was calculated using the following expression :

$$RMS = \{ \sum_{i=1}^{N} [\ln(S_{fi}) - \ln(S_{oi})]^2 / N \}^{\frac{1}{2}} \qquad (18)$$

where, S_{oi} = observed survival value at a given dose D_i (obtained from experimental results)

S_{fi} = fitted survival value at a given dose D_i (obtained from a particular survival equation)

Calculation of the difference between the logarithm of the observed and fitted survivals allowed for an equal weighting of the differences at a particular dose point regardless of the level of survival.

This somewhat crude goodness-of-fit test provided a means of comparing the fit of different survival models to the same survival data. Roughly, a lower value of the RMS deviation indicated a better fit to the data.

2.3.6 Statistical Analysis : T-Tests Versus Nonparametric Tests

Throughout this thesis, statistical methods are used to determine the level of significance represented by the differences between LQ model fit parameters, α or β, obtained from separately fitting low and high dose data. The methods used include :

1). Students' t-test (paired analysis)

2). Students' t-test (unpaired analysis)

3). Sign-rank test (nonparametric)

4). W-test (nonparametric)

Appendix A contains specific information regarding how the tests are applied. The t-tests assume that the samples being compared are normally and independently distributed. The validity of this assumption cannot accurately be tested with the sample sizes considered in this thesis (3 to 8 pairs per sample). As a result, nonparametric tests, that do not make assumptions regarding the shape of the distribution, have also been applied. Results from both types of analysis are shown in the Results and Discussion.

2.4 PROCEDURES FOR DETERMINING THE DEGREE OF SYNCHRONY

To determine the degree of synchrony of a population synchronized by the described techniques three methods were routinely employed. These include the staining of mitotic cells for the determination of mitotic index, the measurement of the radiosensitivity of the population to a single dose of radiation and the examination of flow cytometry histograms of DNA distribution for a population of synchronized cells.

2.4.1 Determination of Mitotic Index

Into a 25 ml glass test tube on ice was placed 2-4 $x10^6$ cells that had been synchronized using mitotic selection only. The cell suspension was centrifuged (6 min., 600 rpm), resuspended in 10 ml of cold 0.025 M sodium citrate (hypotonic solution) and placed on ice for 15 min. To the cell suspension, an equal volume of cold Carnoy fixative (75% ethanol, 25% acetic acid) was slowly added. The cell suspension was recentrifuged (6 min., 1200 rpm-360 g's), resuspended in 10 ml cold Carnoy and held on ice for at least 10 minutes. At this point samples were accumulated and processed simultaneously at a later time. After fixation, the cell suspension was recentrifuged (6 min., 1200 rpm-360 g's) and resuspended in 0.5 ml cold Carnoy. One or two drops of the cell suspension were applied to a clean microscope slide and allowed to air dry for 30 minutes. Prepared slides were stained in Acetic-Orcein stain for 20 minutes, rinsed in 50% acetic acid and sealed by placing two drops of diluted Acetic-Orcein stain on each slide, applying a cover slip and sealing the outer edges of the cover slip to the slide with hot paraffin (Brosing 1983, Freshney 1983).

The Acetic-Orcein stain was prepared by adding 10 g powdered orcein stain (Sigma) to 500 ml of 50% acetic acid (with boiling chips !) and refluxing for 3-5 hours. This was filtered prior to use.

Mitotic cells were identified by the obvious presence of condensed chromosomes. Interphase nuclei were nearly uniform in uptake of the stain, but showed evidence of a darker stained nucleolus.

2.4.2 Single Dose Response of Synchronized Cells

The response of cycling, synchronized cells to a single dose of X-radiation delivered at various times throughout the cell cycle gives an indication of the degree of synchrony present in the population (Sinclair and Morton 1965).

The following procedures apply to cells synchronized by mitotic selection only. Immediately following the mitotic selection procedure, a single harvest of cells was placed in a spinner culture flask (Bellco). A cell count was performed, the flask was gassed with 95% air, 5% CO_2 and it was placed on a stir table at 37 ^{o}C. After the appropriate time interval, an aliquot of cell suspension (at $1x10^5$ cells/ml) was removed. Part of the suspension was loaded into a 5 ml plastic test tube, placed in a test tube irradiation rack, shown in figure 3b, and irradiated for a total dose of 8 Gy at a dose rate of 1.27 Gy/minute. Irradiations were performed at 4 ^{o}C. Cells were plated from the irradiation tube so that approximately 500 colonies per petri dish would have grown after 6 days incubation at 37 ^{o}C. The cell concentration in the irradiation tubes was determined using a Coulter Counter. After incubation, the medium was carefully removed and the petri dishes were stained as described in section 2.3.3. Colonies containing greater than 50 cells were then counted.

In preparation for a single dose response of cells synchronized by mitotic selection followed by a drug block, the cells were handled as described in section 2.2.3 except that 1.3-1.5 $x10^6$ cells in 5 ml of medium (with drug) were seeded into several 25 cm^2 plastic TC flasks. One flask was prepared for each time examined in the cell cycle response. After 12 hours of exposure, all flasks were released from the drug by discarding

the overlying medium, rinsing twice with 5 ml of prewarmed MEM F-15 (lacking FBS and sodium bicarbonate) and then incubating in fresh MEM F-15 (with FBS and sodium bicarbonate). At the desired time interval cells were removed from a flask by trypsinizing. After neutralizing the trypsin with MEM F-15 the cell suspension was centrifuged at 600 rpm for 6 minutes, the supernatant discarded and the cells resuspended in 8-10 ml of fresh MEM F-15 (final concentration $2x10^5$ cells/ml). An aliquot of cell suspension was then loaded into a 5 ml plastic test tube, placed into a test tube irradiation rack (figure 3b) and irradiated for a total dose of 8 Gy at 1.27 Gy/minute. Irradiations were performed at 4 ^{o}C. Cells were plated from the irradiation tube so that approximately 500 colonies per petri dish would have grown after 6 days incubation at 37 ^{o}C. The cell concentration in the irradiation tubes was determined using a Coulter Counter. After incubation, the medium was carefully removed and the petri dishes were stained as described in section 2.3.3. Colonies containing greater than 50 cells were then counted.

2.4.3 Histograms of the DNA Distribution

Flow cytometry histograms of cell populations synchronized by mitotic selection alone or by mitotic selection followed by a drug block were obtained as a monitor of the progression of these populations through the cell cycle. A Fluorescence Activated Cell Sorter (FACS - Becton Dickinson 440) was utilized to measure DNA content at various times after mitotic selection or after release from the drug block (Fox et al 1987, Fried et al 1980).

At hourly time intervals after harvest, an aliquot of cells was removed from the population synchronized by mitotic selection alone to

provide two samples containing $1x10^6$ cells and $2x10^6$ cells respectively in separate test tubes. To the smaller of the two samples was added $1x10^6$ 'marker' cells. These were plateau-phase cells that acted as a G1-marker and were obtained by trypsinizing a tissue culture flask containing a confluent monolayer of cells.

In the case of populations synchronized by mitotic selection followed by a drug block, at hourly time intervals after release from the drug, a flask was trypsinized to provide two cell samples containing $2x10^6$ cells in one test tube and $1x10^6$ cells with $1x10^6$ marker cells in another test tube.

The samples were centrifuged (6 min., 600 rpm), the supernatant carefully discarded, the residual medium wiped from the test tube and the cells resuspended in a cold ethidium bromide solution. Optimal sample preparation was at a final concentration of 1-2 $x10^6$ cells/ml of ethidium bromide. Samples were stored on ice a minimum of 10 minutes prior to analysis which consisted of filtering the samples and measuring the fluorescence spectra with the flow cytometer using 488 nm excitation.

The ethidium bromide solution was prepared at a concentration of 75 μM in a neutral saline citrate buffer of 0.0034 M citric acid (monohydrate) and 0.01 M NaCl. The solution also contained 0.1% Non Idet P40 detergent which lysed cell membranes.

3. RESULTS

3.1 EVALUATING THE DEGREE OF SYNCHRONY

3.1.1 Mitotic Index

The mitotic index of a population of cells is defined to be that fraction of the population that is in any stage of mitosis (prophase, metaphase, anaphase or telophase) at some particular time (Becker 1986). The mitotic index has traditionally been used as a measure of the quality of synchrony (ie. homogeneity in mitosis) of a population of cells that has been synchronized just prior to or during mitosis. Cells synchronized by the mitotic selection technique are particularily suited, then, to analysis by this method. However, cells synchronized at the G1/S border by mitotic selection followed by a drug block are less suited to such an analysis since the high degree of synchrony characteristic of this technique is usually not maintained several hours later when the population reaches mitosis. Other techniques are employed for their analysis.

A population of cells was synchronized by the mitotic selection technique as described in section 2.2.2. Microscope slides of fixed and stained cells were prepared as described in section 2.4.1. The slides were then observed using a microscope for the prescence of cells in mitosis. Cells in prophase to early-telophase were easily identified by the obvious prescence of darkly-stained condensed chromosomes. Cells that did not clearly exhibit chromosomes were more difficult to classify. Cells that fall into this category could include those from mid-telophase, G1, S and G2

phases. Many such cells were typically observed and were classified based upon several criteria discussed in the following paragraphs.

In prophase as the chromosomes condense and the nuclear envelope begins to dissipate, the nucleoli become progressively more dispersed so that by late-prophase nucleoli are no longer visible (Becker 1986, Prescott 1978, Wheatley 1982, Willmer 1964). The reverse process occurs in telophase when the chromosomes decondense and both the nuclear envelope and the nucleoli reappear. One nucleolus is present per chromosome (21 for WNRE cells). As they enlarge, the nucleoli quickly fuse into a single large nucleolus that is characteristic of an interphase nucleus. The nucleolus is the only clearly visible feature in the nucleus of interphase cells stained by the described technique. Hence, the identification of a nucleolus (or the lack thereof) in a stained nucleus is one basis for classifying those cells that do not exhibit chromosomes as being telophase/early G1 or interphase. As well, the morphological texture of a telophase or early post-mitotic nucleus is more granular in its appearance compared to interphase nuclei "due to the long time taken by chromosomes to fade into inter-mitotic chromatin" (Willmer 1964). Further, it was observed that the nuclear area of the many cells that did not exhibit chromosomes was usually equivalent in size to the nucleus of the more clearly distinguishable early-telophase cells and smaller than the nucleus of a distinctive interphase cell. This may have indicated that the cells that did not exhibit nuclear detail may have recently progressed from early to late-telophase. Finally, it was observed that many of the cells synchronized by mitotic selection were present as doublets. Stained preparations often contained many of these doublets, thought to be mitotic daughter pairs, neither of which clearly exhibited chromosomes.

Hence, four criteria were established for the classification of cells not exhibiting chromosomes as being either late-telophase/early G1 or interphase :

1). the prescence of a darkly stained nucleolus in the nucleus of an interphase cell

2). the granular texture of the telophase nucleus

3). the similarity in nuclear area of the cell to that of an early telophase cell

4). the prescence of the cell as a member of a doublet

Although none of these criteria singularly defined the cells in question, usually most were satisfied simultaneously giving confidence to their proper classification. This was particularly the case with the large number of late-telophase/early G1 cells and with the few cells with a large visible nucleolus which were fairly easy to classify. Cells with properties intermediate to both classifications were more troublesome and have been classified separately as "probably mitotic" or "probably interphase".

Table II shows results for the determination of the mitotic index of populations synchronized by mitotic selection alone. For each sample at least one thousand cells were scored. Note that although the mitotic index itself is quite low (8.6-41.3 %), when combined with those cells determined as clearly or probably in late-telophase/early G1 (54.9-87.9 %) the index of synchrony becomes 96.2-97.7 %. It should be noted that all of the clearly mitotic cells were scored as a single cell rather than as two cells, as is sometimes carried out in the literature. Within a short time, when all of the mitotic cells and daughter cell doublets would have completed division and progressed beyond mitosis, the index of synchrony by the four criteria

above would then have increased to 96.8-98.3 % in early G1. Stained cell preparations indicated that within 30 to 45 minutes after mitotic selection the mitotic index drops to about 1 %.

There is a particular tendency for the V79 cell lines, when synchronized by mitotic selection, to detatch as a daughter cell doublet in anaphase, telophase or just past mitosis and to remain as a doublet for several hours after harvest (Gillespie 1975, Sinclair and Yu 1967, Klevecz 1975). The mitotic index may misrepresent the true synchrony of the population since the cells selected by this procedure probably represent a spread in time of no greater than the length of mitosis (determined by Gillespie et al to be about 30 minutes) within the cell cycle (Gillespie 1975). The index of synchrony including those cells in late-telophase/early G1 provides a more realistic description of the quality of synchrony. As well, since clearly mitotic cells were scored as a single, rather than double, cell the value for the mitotic index and index of synchrony is rather conservative compared to other analysis in the literature.

TABLE II
Values of Mitotic Index and Index of Synchrony
(percentage in each category)

Sample Number	Mitotis	Telophase/ early G1	Probably Telophase/ early G1	Interphase	Probably Inter.	Index of Synch.
1	41.3	51.9	3.0	2.1	1.7	96.2
2	34.1	61.6	2.0	1.6	0.7	97.7
3	8.6	86.5	1.4	1.8	1.7	96.5

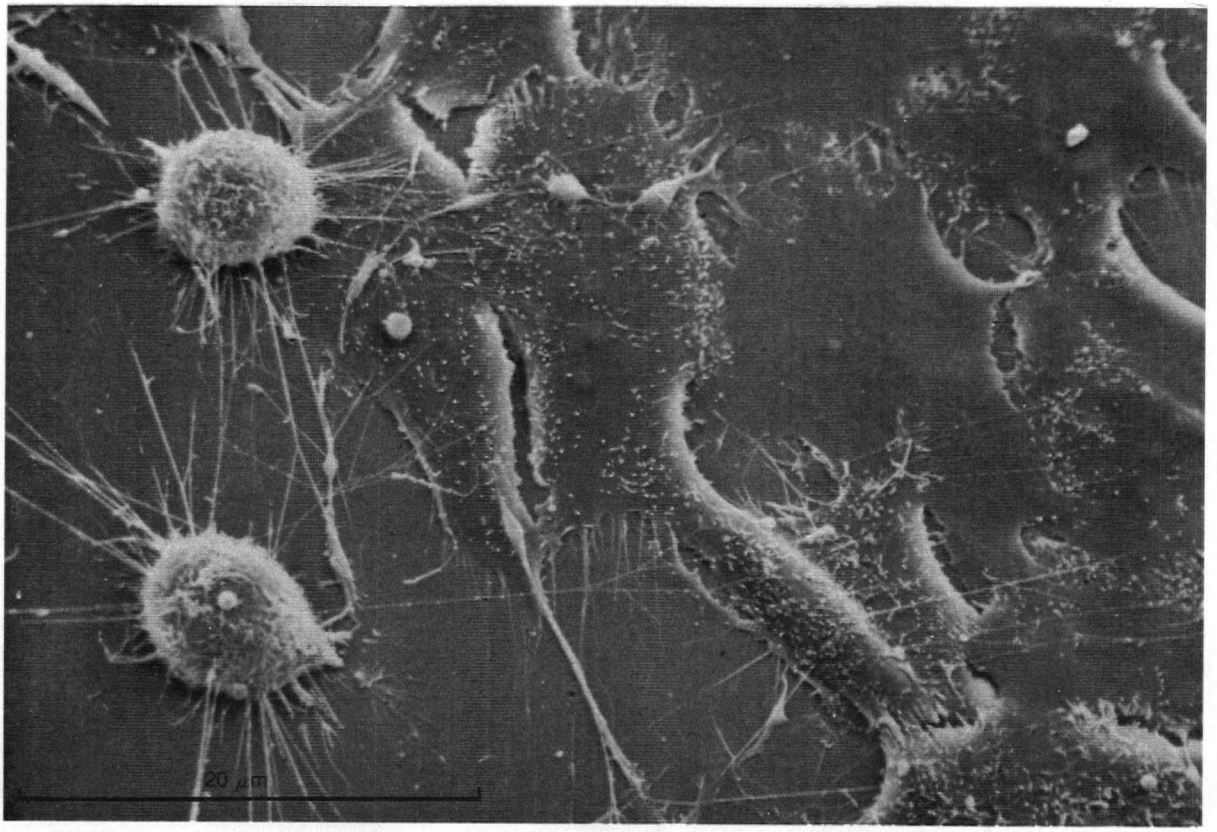

FIGURE 4 : PHOTOGRAPHS OF CELLS IN MITOSIS AND INTERPHASE

Interphase cells are spread out and are firmly attatched to the surface of the culture vessel. In mitosis, the cells become spherical in shape and are loosely attatched to the vessel surface by thin strands of tubulin. (scanning electron micrograph, reprinted with the permission of Dr. D.M. Prescott)

3.1.2 Single Dose Response of Synchronized Cells

The variation in cellular radiosensitivity as a function of position in the cell cycle (the "age response") was noted by Sinclair and Morton in 1963 using a V79 subline. Their results indicated that the cells were most sensitive when irradiated at or near the mitotic phase of the cell cycle and were most resistant when irradiated during late S phase (Sinclair and Morton 1963, 1965). An asynchronous population, being a mixture of cells at all stages of the cell cycle, should exhibit a constant radiosensitivity as a function of time. The response of synchronized cells to a constant dose of radiation over the cell cycle may qualitatively provide an indication of the quality of synchrony of the population.

Cells were synchronized and prepared for single dose irradiation studies as described in section 2.4.2. The response of the synchronized populations to a constant dose, 8 Gy, of 250 KVp X-radiation is shown in figure 5 for populations synchronized by mitotic selection alone or followed with 1 mM hydroxyurea or 1 µg/ml aphidicolin.

The experimental technique used to obtain the responses involving hydroxyurea or aphidicolin ensured that a single cell suspension was irradiated and plated. However, suspensions of cells synchronized by mitotic selection alone often contained between 40 - 80 % visible doublets that remained doublets up to several hours after selection. It was necessary, then, to correct the surviving fraction for the average number of cells per colony forming unit (CFU) plated in order to obtain the single cell response. The average single cell survival, s, is related to the survival, f, for a mixed population of multiple cell CFU's by the expression (Sinclair and Morton 1965)

$$f = \sum_i \phi_i \langle 1-(1-s)^i \rangle \qquad (19)$$

where ϕ_i is the fraction of the CFU's having i cells. An approximation to equation 19 may be made :

$$f = 1-(1-s)^N \qquad (20)$$

$$\text{or,} \qquad s = 1-(1-f)^{1/N} \qquad (21)$$

where N is the average viable cell multiplicity = $\Sigma\, \phi_i \cdot i$. The above assumes that each cell of a CFU survives independantly of other cells. Equation 21 was applied to the survival response of cells synchronized by mitotic selection alone assuming an average of 60 % doublets (ie. N=1.6) in the population (between 40 - 80 % doublets were typically observed) to obtain the single cell survival shown in figure 5.

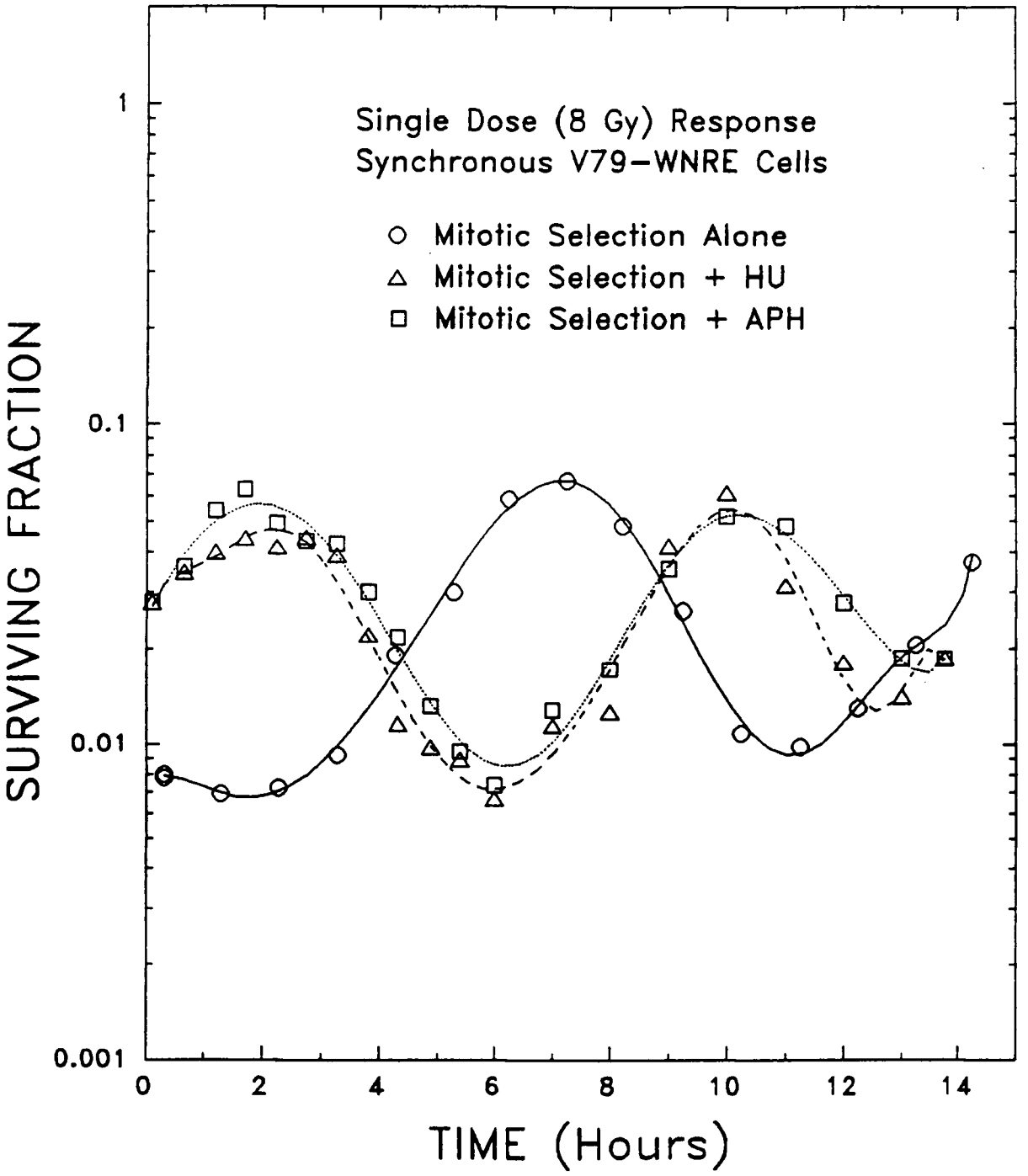

FIGURE 5 : SINGLE DOSE (8 GY) IRRADIATION PROFILE

The response of synchronized cells to a constant dose (8 Gy) of radiation as a function of time after mitotic selection alone (O), or after release from 12 hour exposure to 1 mM hydroxyurea (Δ) or 1 μg/ml aphidicolin (□) preceeded by mitotic selection. The response of cells synchronized by mitotic selection alone has been corrected for the large number of doublets present in the population using equation 16 for N=1.6. The lines represent the 10^{th} order regression fit to the response of cells synchronized by mitotic selection alone (————), or followed by hydroxyurea (- - - - -) or aphidicolin (·····).

3.1.3 Fluorescence Analysis of DNA Distributions

The variation in DNA content of a cell as it traverses the cell cycle may be exploited to provide information on the quality and position of a synchronized population. Since the V79-WNRE is a diploid cell type the DNA content gradually increases from 2n (where n=21 for V79-WNRE) at the beginning to 4n at the conclusion of the synthesis (S) phase of the cell cycle and remains at 4n during G2 phase. Upon division at mitosis, half of the 4n chromosomes are equally distributed to each of the daughter cells, returning the cells to the 2n state for the entirety of G1 phase.

The DNA content of a population of cells may be determined using a fluorochrome that binds stoichiometrically to the DNA of the cells. When the probe molecules are excited at a specific frequency by a laser, fluorescence is emitted that is proportional in intensity to the DNA content (Fried et al 1980).

Using a Fluorescence Activated Cell Sorter (FACS) cell preparations stained with ethidium bromide were excited by a 488 nm laser to fluoresce at > 580 nm. Histograms of cell populations synchronized by mitotic selection alone or followed by either hydroxyurea (1 or 2 mM) or aphidicolin (1 or 3 μg/ml) are shown in figure 6. The two vertical lines represent positions of the 2n and 4n peaks respectively. All populations appear to be highly synchronized initially. Cell populations synchronized by mitotic selection alone maintain a high degree of synchrony especially during the first two hours. The population loses some degree of synchrony as it passes through the cell cycle as evidenced by the enlarged S phase tail at 11 hours. Populations synchronized by mitotic selection followed by hydroxyurea appear to be equally well synchronized

following release from either 1 or 2 mM hydroxyurea, although the population receiving 2 mM is delayed slightly in its progression through S phase to G2. Blocking with 1 or 3 µg/ml aphidicolin appears to produce equally synchronized populations although the population receiving 3 µg/ml is also delayed slightly in its progression through S phase to G2. Both 1 mM hydroxyurea and 1 µg/ml aphidicolin work well in synchronizing cells at the G1/S border although the synchrony appears to be better maintained by 1 µg/ml aphidicolin after one complete cell cycle as indicated by the T=10 hour histograms.

At T=0 for populations synchronized at the G1/S border one might expect the distributions to lie on the G1 peak. The histograms for hydroxyurea and aphidicolin at T=0, however, appear shifted to the right of the G1 peak as if the populations were synchronized in early S phase rather than at the G1/S border. This is not an uncommon occurrence for populations pre-treated with a drug prior to staining with a fluorochrome. The observed shift is more likely due to a greater uptake of ethidium bromide stain in the DNA double helix of the cells possibly resulting from the opening up of more potential binding sites on the DNA by the hydroxyurea or aphidicolin pretreatment (conversation with Dr. R.E. Durand). In either case, the initial populations appear well synchronized at their particular position in the cell cycle whether it is classified as the G1/S border or early S.

In an effort to quantitatively determine the percentages of cells in G1, S or G2/M phases at a particular time, a computer program (written by Dr. R. E. Durand) was used to analyze the histograms. The G1 population was characterized by fitting a gaussian distribution to the ascending half of the maximum peak of the histogram and calculating the area under the

gaussian bounded on either side of the peak by two standard deviations. To eliminate fitting the gaussian to tail noise, all data to the left of the point representing 5% of the peak maximum was ignored. The G2/M population was similarily characterized by fitting a gaussian distribution to the descending half of the data centered at the channel number corresponding to a specified G2/G1 channel number ratio. The S phase population included all cells not falling under either of the fitted guassian distributions. An example of a computed fit to a histogram is shown in figure 7. The G1, S and G2/M regions are bounded by a dashed, solid and dotted line respectively. The percentage of the population in each of the three phases was computed from the area under the three curves.

The histograms for populations synchronized by mitotic selection alone or followed by 1mM hydroxyurea or 1 ug/ml aphidicolin were analyzed for phase percentage in G1, S or G2/M. The program is best suited for analyzing asynchronous histograms containing a maximum at the G1 peak, a large proportion of the cells in S phase and a smaller G2/M peak. Most of the histograms of synchronized cells contain only one prominent peak located on or between the G1 and G2 position markers which the program would wrongly interpret as the G1 peak regardless of channel number. At best the program can be used to provide a rough estimation of the percent number of cells represented by the prominent peak. At time T=0 the percentage of cells determined to lie under the prominent peak for populations synchronized by mitotic selection alone or followed by 1 mM hydroxyurea or 1 µg/ml aphidicolin was analyzed to be 92.88%, 95.36% and 93.47% respectively. Although not definitive, these figures do suggest a high degree of synchrony for the initial populations.

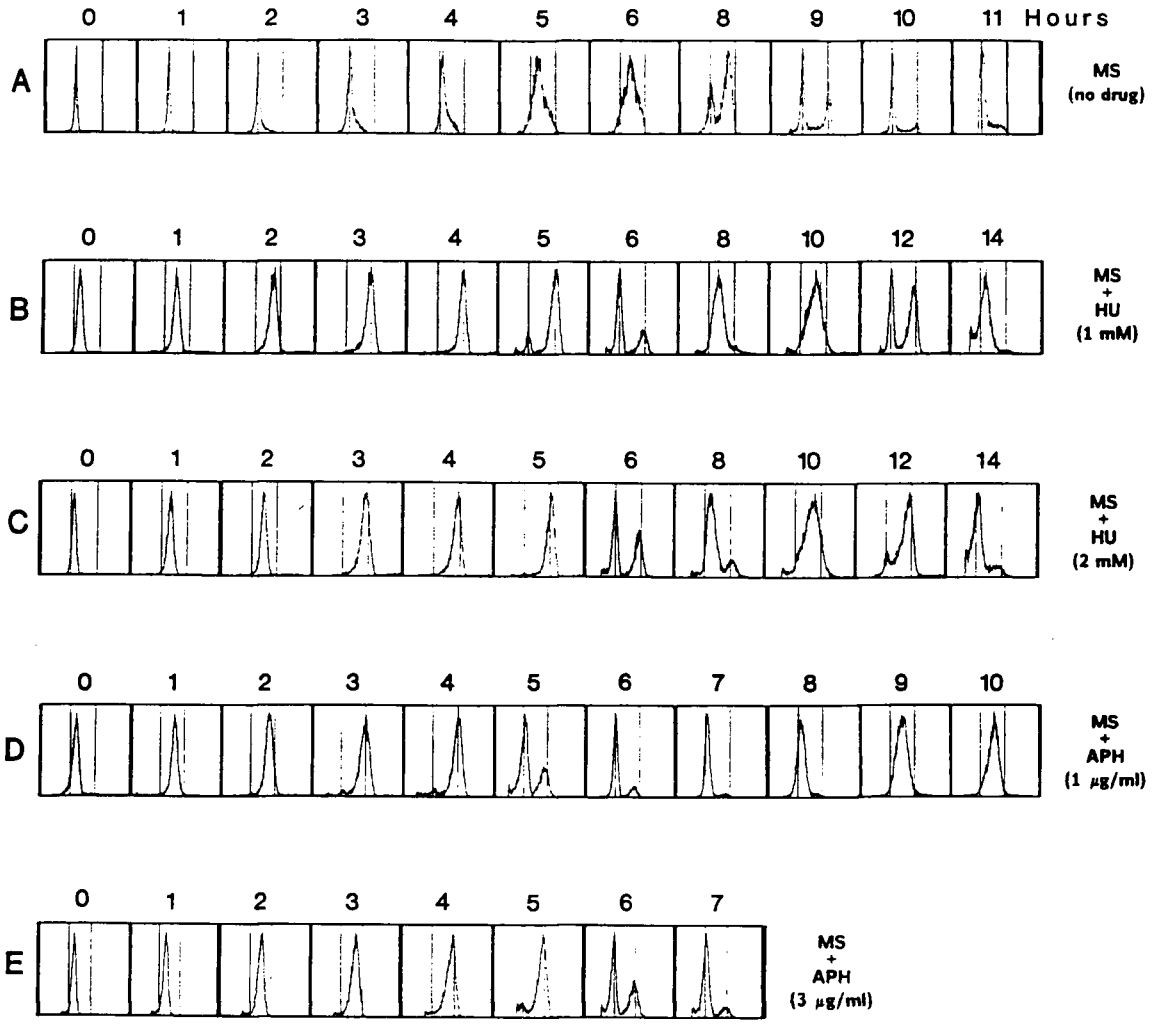

FIGURE 6 : FLOW CYTOMETRY DISTRIBUTIONS AFTER SYNCHRONY
The distribution of DNA content at various times after synchrony procedures. A : Populations synchronized by mitotic selection alone. B to E : Mitotic selection followed by 12 h exposure to a drug block, with release at 0 h. B : 1 mM hydroxyurea. C : 2 mM hydroxyurea. D : 1 µg/ml aphidicolin. E : 3 µg/ml aphidicolin. The vertical lines show the positions of the 2n (G1) and 4n (G2) peaks. The time after synchronization is shown above each of the histograms.

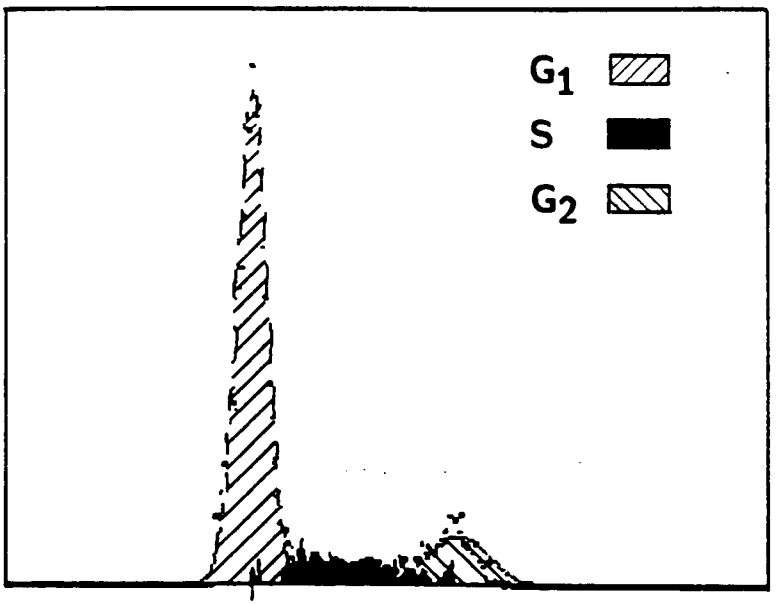

FIGURE 7 : COMPUTED FIT TO A DNA HISTOGRAM

A DNA histogram of a previously synchronized population of cells was computer fitted to the experimental data points (circles) in order to determine the approximate percentage of cells in G1, S or G2/M.

3.2 ASYNCHRONOUS CELL EXPERIMENTS

Previous studies on asynchronously dividing V79-171 cells indicated the prescence of substructure in the radiation survival response at low dose (less than 4 Gy in air) (Skarsgard et al 1990 b,c). In an effort to further explore the cause of the substructure, similar studies were carried out on V79-WNRE cells. The V79-WNRE cell line was chosen for its adaptability to both spinner and monolayer culture making it well suited for both asynchronous studies and synchronous studies using mitotic selection where it was known to provide a good shake-off yield at harvest.

Using the cell sorter assay, radiation survival experiments were conducted on asynchronously dividing populations of V79-WNRE cells. Two series of such experiments were carried out under aerobic conditions over the dose range 0 to 12 Gy. The initial series (or "series 1") included 5 experiments using a dose increment of 0.5 Gy for samples between 0 and 4 Gy. In an effort to more accurately define the low dose region of the survival response, a second series of 8 experiments ("series 2") was conducted eight months after the termination of the first series using a dose increment of 0.4 Gy for samples between 0 and 4 Gy. This allowed for the addition of four more experimemtal samples representing two dose points over the low dose range.

3.2.1 Initial Series of Asynchronous Experiments

Data from 5 experiments of the initial asynchronous series were averaged and fitted to the linear-quadratic (LQ) equation $S = \exp(-\alpha D - \beta D^2)$ over the dose range 0 to 12 Gy as seen in figure 8. The same data may alternatively be replotted as $-\ln(S)/D$ vs. D, the linear form of the LQ equation, $-\ln(S)/D = \alpha + \beta D$, where S is equal to the surviving fraction

and D is equal to the dose, as seen in figure 9 (Skarsgard 1990 b,c). It is clear, particularly in figure 9, that the quality of the LQ fit over the full dose range is poor with most of the low dose points lying off the fitted curve. This result suggested that the data may be better characterized by fitting the low dose (0-3 Gy) and high dose (3-12 Gy) data separately to the LQ equation as seen in figures 10 and 11. These same data and LQ fits are shown in figures 12 and 13 plotted on an expanded scale up to 4 Gy. It can be seen that there is a consistent divergence between the low dose and high dose fits, evidence of a 2-component character in the response. Comparing figures 9 and 11 it is clear that a single, full dose LQ fit to the data is not adequate to describe the asynchronous survival response of V79-WNRE cells. If the data were truly representative of a single LQ function, then it should follow a single straight line of slope beta and y-axis intercept alpha, when plotted in the form $-\ln(S)/D$ vs D. The straight line fit to the data shown in the $-\ln(S)/D$ vs D plots is the same fit as in the S vs D plots, ie., the data in both cases have been fit by the method of least squares to the equation $\ln(S) = -\alpha D - \beta D^2$.

Further evidence of a two component character in the survival response is found from statistical analysis of the values of alpha and beta for the low dose and high dose fits of the individual experiments. A Student's t-test and two nonparametric tests (see appendix A) were applied to the low and high dose values of alpha and beta to determine whether differences between the low dose distributions of alpha or beta and high dose distributions of alpha or beta are statistically significant. Results from the analysis are shown in table III. For the initial series of asynchronous experiments the low and high dose values of alpha were determined to be significantly different at the P=0.0675 (t-test paired

analysis), P=0.0369 (t-test unpaired analysis), P<0.001 (rank-sum test) and P=0.056 (W-test) levels. For beta, the low and high dose values were found to be significantly different at the P=0.0596 (t-test paired analysis), P=0.0421 (t-test unpaired analysis), P<0.001 (rank-sum test) and P=0.008 (W-test) levels. These P values reflect a high degree (about 93-99%) of confidence that the low or high dose values of alpha or beta are not subsets of a larger distribution of alpha's or beta's but represent distributions statistically different from each other.

A goodness of fit test was applied to the LQ fit of the data over the full dose (0-12 Gy), low dose (0-3 Gy) and high dose (3-12 Gy) ranges. The test consisted of a simple calculation of the RMS deviation of the logarithm of the actual data from the logarithm of the fitted points of the LQ survival curve at the dose values of the data. For the full dose fit, the RMS deviation was found to be 0.0346 (unitless). The deviation decreased to 0.00952 by fitting to the low dose data and to 0.0331 by fitting to the high dose data separately. These figures, shown in table VI, reassert that the response is best characterized by separate fits to the low dose and high dose data.

The division between low and high dose was chosen as 3 Gy based upon an analysis of the RMS deviations of the various possible fits to the data indicating, for a two-component fit, that the lowest RMS deviations were obtained for fits between 0 to 3 Gy and 3 to 12 Gy. Larger RMS deviations were obtained when the division between low and high dose was tested at 2, 2.5, 3.5 or 4 Gy.

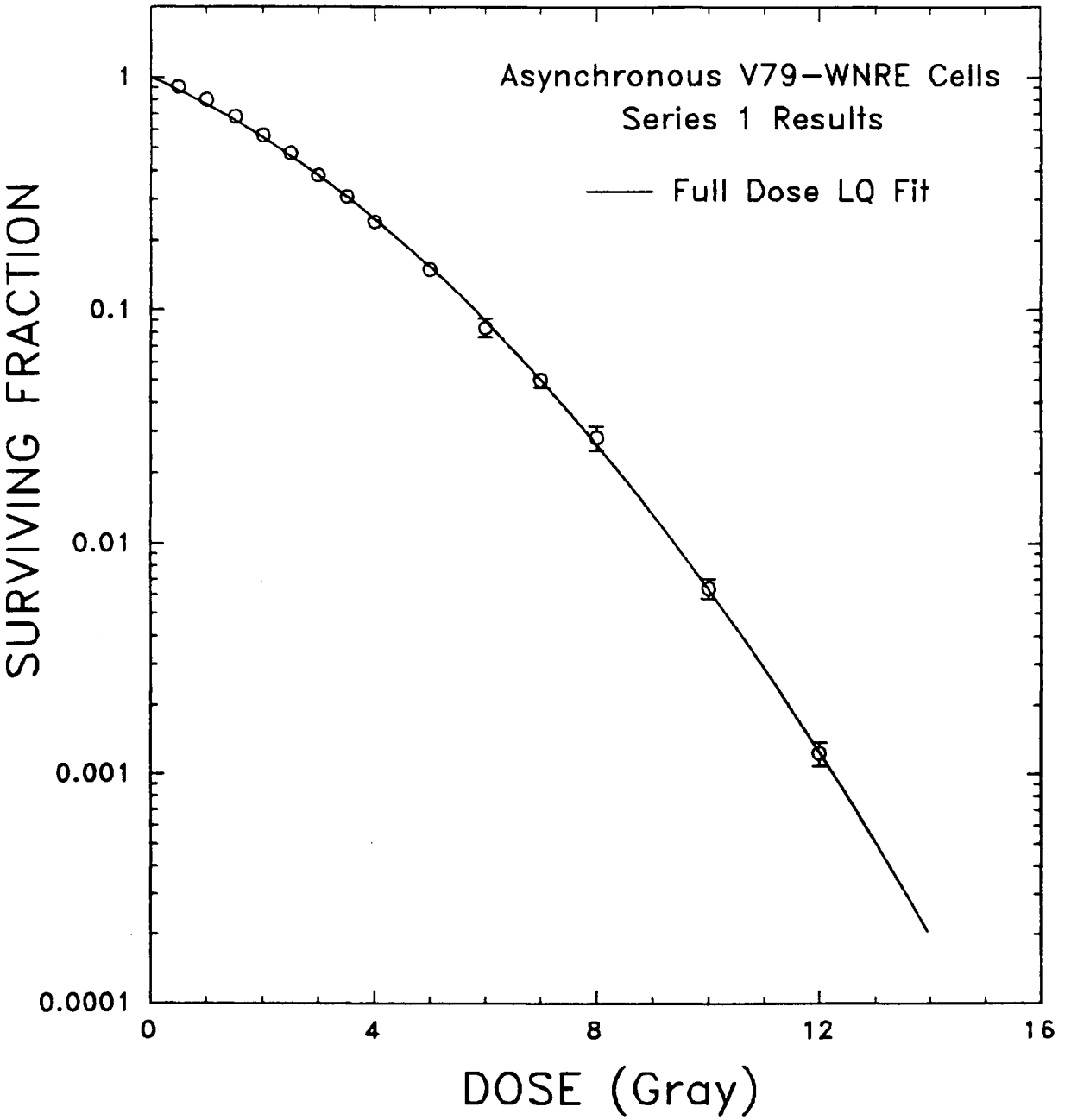

FIGURE 8 : INITIAL SERIES OF ASYNCHRONOUS EXPERIMENTS - I

Survival data obtained from asynchronously growing V79-WNRE cells irradiated at 37 ^{o}C in suspension culture under aerobic conditions (3-6x10^5 cells/ml in MEM S-14; X-ray source : Philips 250 kV_p, HVL 1.5 mm Cu, dose rate 2.295 Gy/min.). Cell sorting was used to determine the number of cells for plating into petri dishes. After a 6 day incubation period, colonies were stained and counted, the surviving fraction S was then determined. Data are the average of five experiments from the initial asynchronous series. Error bars are the standard error in the mean. Solid lines represent the least-squares fit of the data over the full dose range (0 to 12 Gy) to the LQ equation. Data and best fits are plotted in the form $S = \exp(-\alpha D-\beta D^2)$. Note that all fits to the LQ model in this thesis have been made to the equation $\ln(S) = -\alpha D-\beta D^2$ for curves plotted either as S vs. D or $-\ln(S)/D$ vs. D.

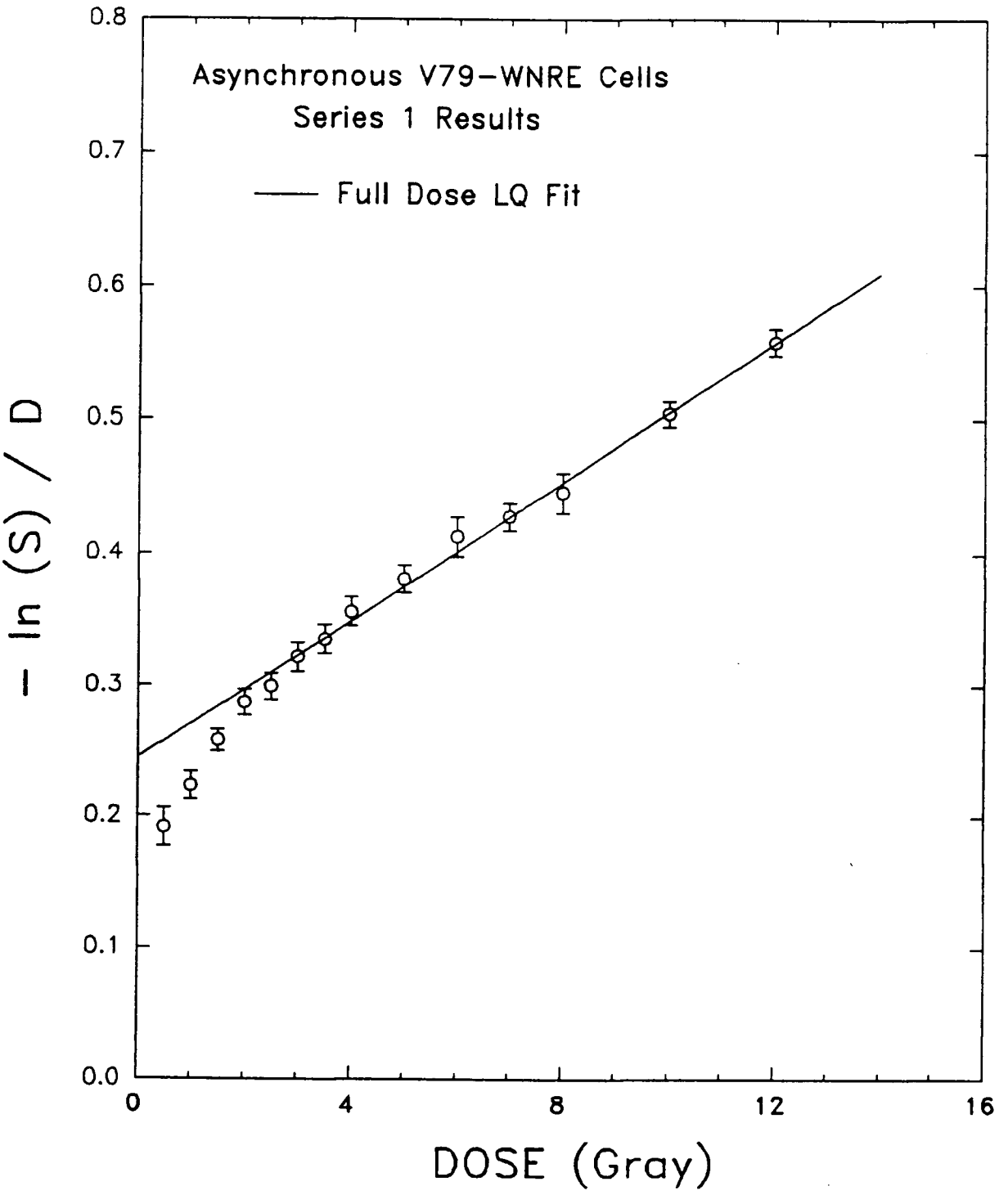

FIGURE 9 : INITIAL SERIES OF ASYNCHRONOUS EXPERIMENTS - II

The same survival data shown in figure 8 for the average of five experiments from the initial asynchronous series are replotted in the form $-\ln(S)/D = \alpha + \beta D$. When plotted in this form the parameters α and β of the LQ fit are clearly visualized as the y-axis intercept and slope, respectively. The solid line represents the least-squares fit of the data over the full dose range (0 to 12 Gy) to the LQ equation.

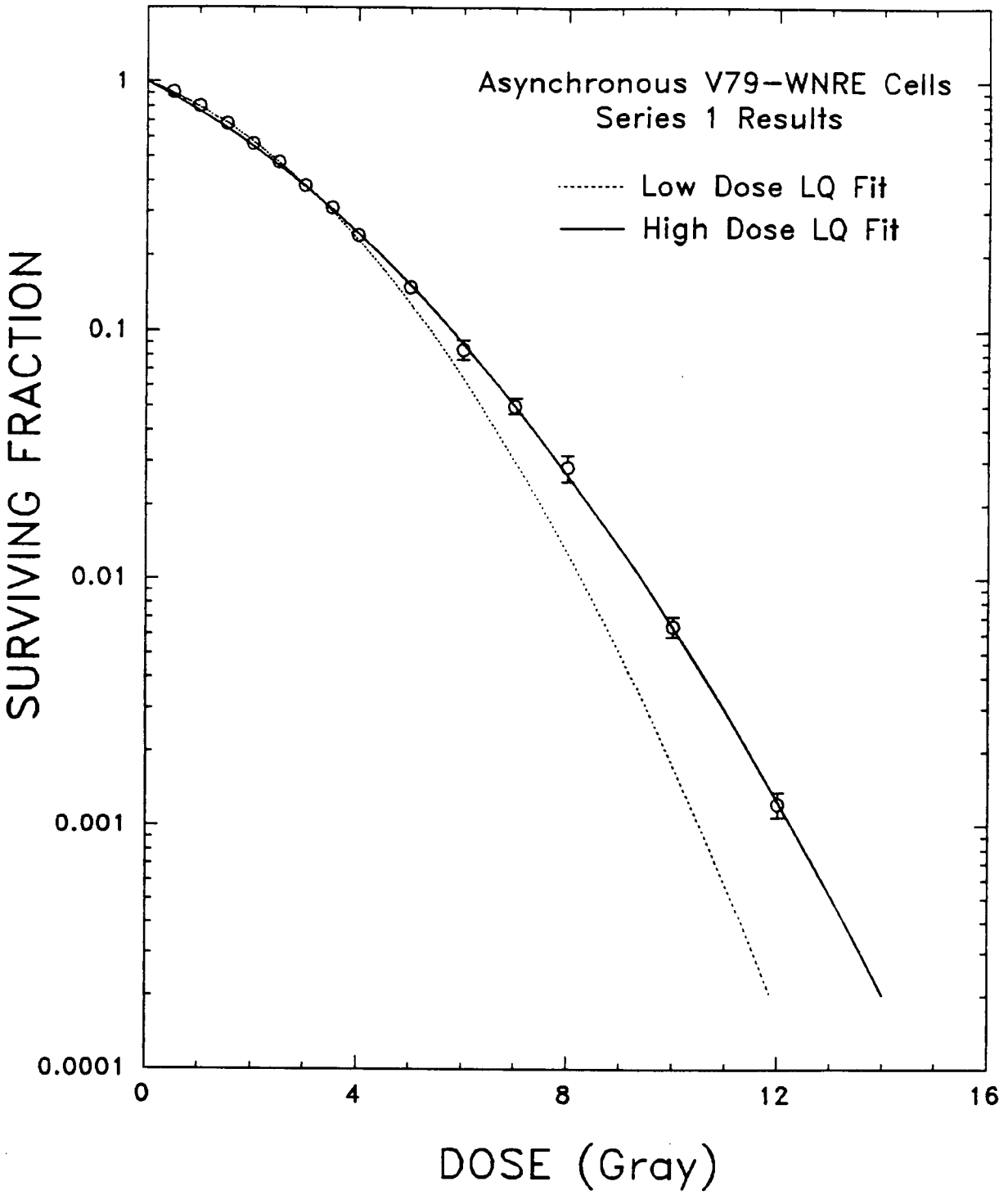

FIGURE 10 : SEPARATE FITS TO SERIES 1 ASYNCHRONOUS DATA - I

The same data as shown in figure 8 have been fitted separately to the LQ equation over the low dose (0 to 3 Gy) region (-----) or the high dose (3 to 12 Gy) region (———). Data and separate low and high dose LQ fits are plotted in the form $S = \exp(-\alpha D - \beta D^2)$.

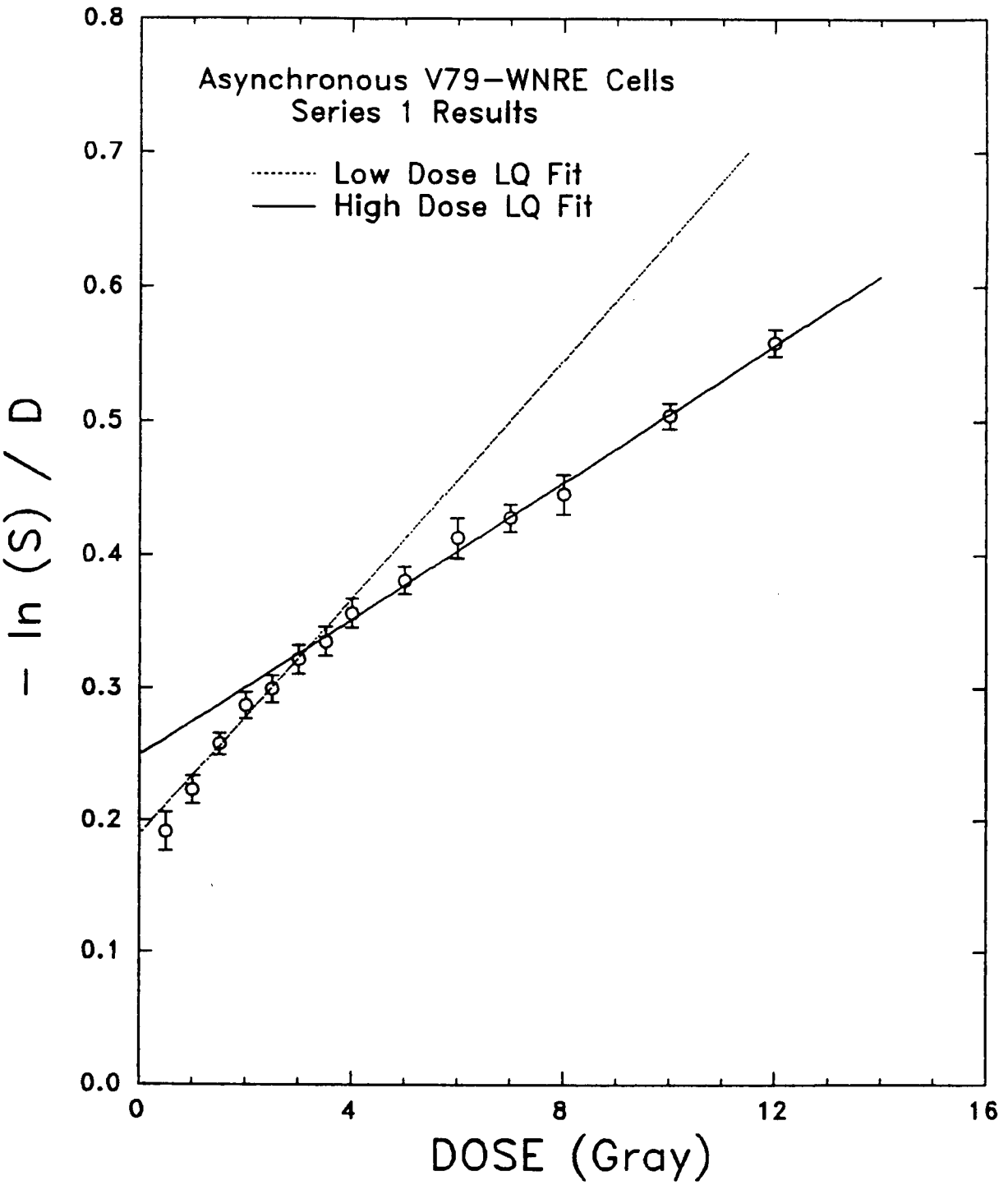

FIGURE 11 : SEPARATE FITS TO SERIES 1 ASYNCHRONOUS DATA - II

The same data as shown in figure 8 have been fitted separately to the LQ equation over the low dose (0 to 3 Gy) region (-----) or the high dose (3 to 12 Gy) region (———). Data and separate low and high dose LQ fits are plotted in the form $-\ln(S)/D = \alpha + \beta D$.

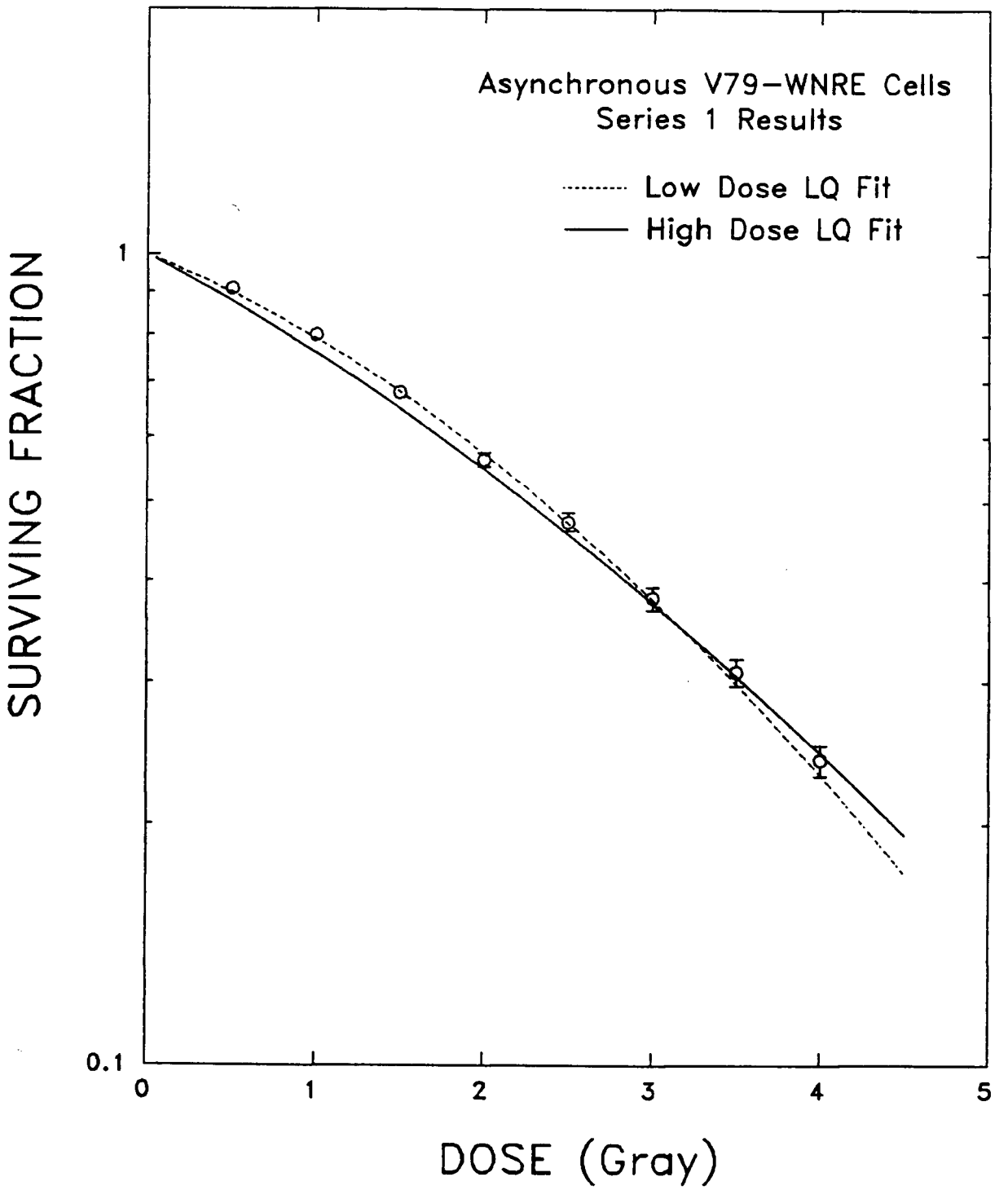

FIGURE 12 : LOW DOSE SURVIVAL SERIES 1 ASYNCHRONOUS DATA - 1

The data and separate low dose (0 to 3 Gy) and high dose (3 to 12 Gy) fits to the LQ equation as shown in figure 8 for the average of five experiments of the initial asynchronous series are replotted over the dose range 0 to 4 Gy in the form $S = \exp(-\alpha D - \beta D^2)$.

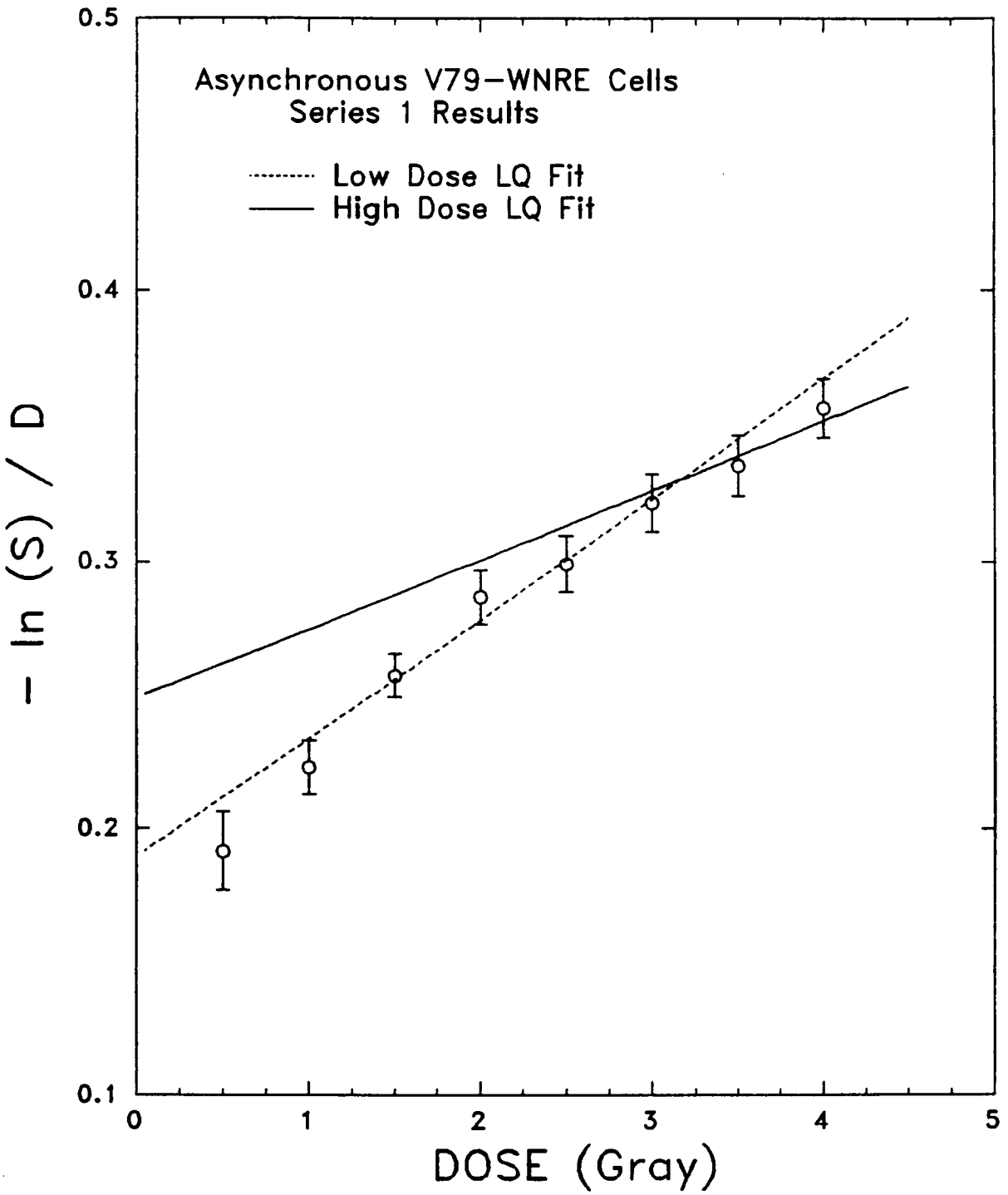

FIGURE 13 : LOW DOSE SURVIVAL SERIES 1 ASYNCHRONOUS DATA - II

The data and separate low dose (0 to 3 Gy) and high dose (3 to 12 Gy) fits to the LQ equation as shown in figure 8 for the average of five experiments of the initial asynchronous series are replotted over the dose range 0 to 4 Gy in the form $-\ln(S)/D = \alpha + \beta D$.

3.2.2 Second Series of Asynchronous Experiments

Data from 8 experiments of the second asynchronous series were averaged and fitted separately to the LQ equation over the low dose (0-2 Gy) and high dose (2-12 Gy) ranges as seen in figure 14. The same data and LQ fits are replotted in the form -ln(S)/D vs. D in figure 15. The differences in the asynchronous responses of the initial and second series of experiments are most evident by comparing figures 11 and 15. The low dose region appears to be more sensitive and the high dose region more resistant in the second series compared to the initial series. In spite of the obvious differences between the two sets of data it is still clear that the low dose and high dose data are best represented by fitting the data separately to the LQ equation.

A similar statistical analysis was carried out on the low dose and high dose values of α or β. The results, shown in table III, indicate that for the second series of asynchronous experiments the low and high dose values of α were statistically different at the P=0.042 (t-test paired analysis), P=0.087 (t-test unpaired analysis), P=0.078 (rank-sum test) and P=0.115 (W-test) levels. For β, the low and high dose values were found to be significantly different at the P=0.013 (t-test paired analysis), P=0.0091 (t-test unpaired analysis), $P < 0.001$ (rank-sum test) and $P < 0.001$ (W-test) levels. These P values indicate, for α, a confidence of between 88.5 % and 95.8 % that the low and high dose values of α represent statistically different populations. For β, there is between 98.7 % and 99.9 % confidence that the low and high dose values of β represent statistically different populations.

TABLE III
STATISTICAL SIGNIFICANCE OF THE DIFFERENCES BETWEEN THE LOW DOSE AND HIGH DOSE VALUES OF α AND β
ASYNCHRONOUS CELL EXPERIMENTS

	Full Dose Mean	Low Dose Mean	High Dose Mean	P_{pair}	P_{unp}	P_{sr}	P_W
Series 1 (5 Expts)							
α ($\times 10^{-1}$ Gy^{-1})	2.447	1.893	2.498	0.067	0.037	<0.001	0.056
β ($\times 10^{-2}$ Gy^{-2})	2.607	4.508	2.599	0.059	0.042	<0.001	0.008
Series 2 (8 Expts)							
α ($\times 10^{-1}$ Gy^{-1})	2.457	2.179	2.451	0.042	0.087	0.078	0.115
β ($\times 10^{-2}$ Gy^{-2})	2.294	4.902	2.299	0.013	0.0091	<0.001	<0.001

(Note : P values stated were determined from Students' t-test paired analysis (P_{pair}), Students' t-test unpaired analysis (P_{unp}), the signed-rank test (P_{sr}) and the W-test (P_W), as described in Appendix A).

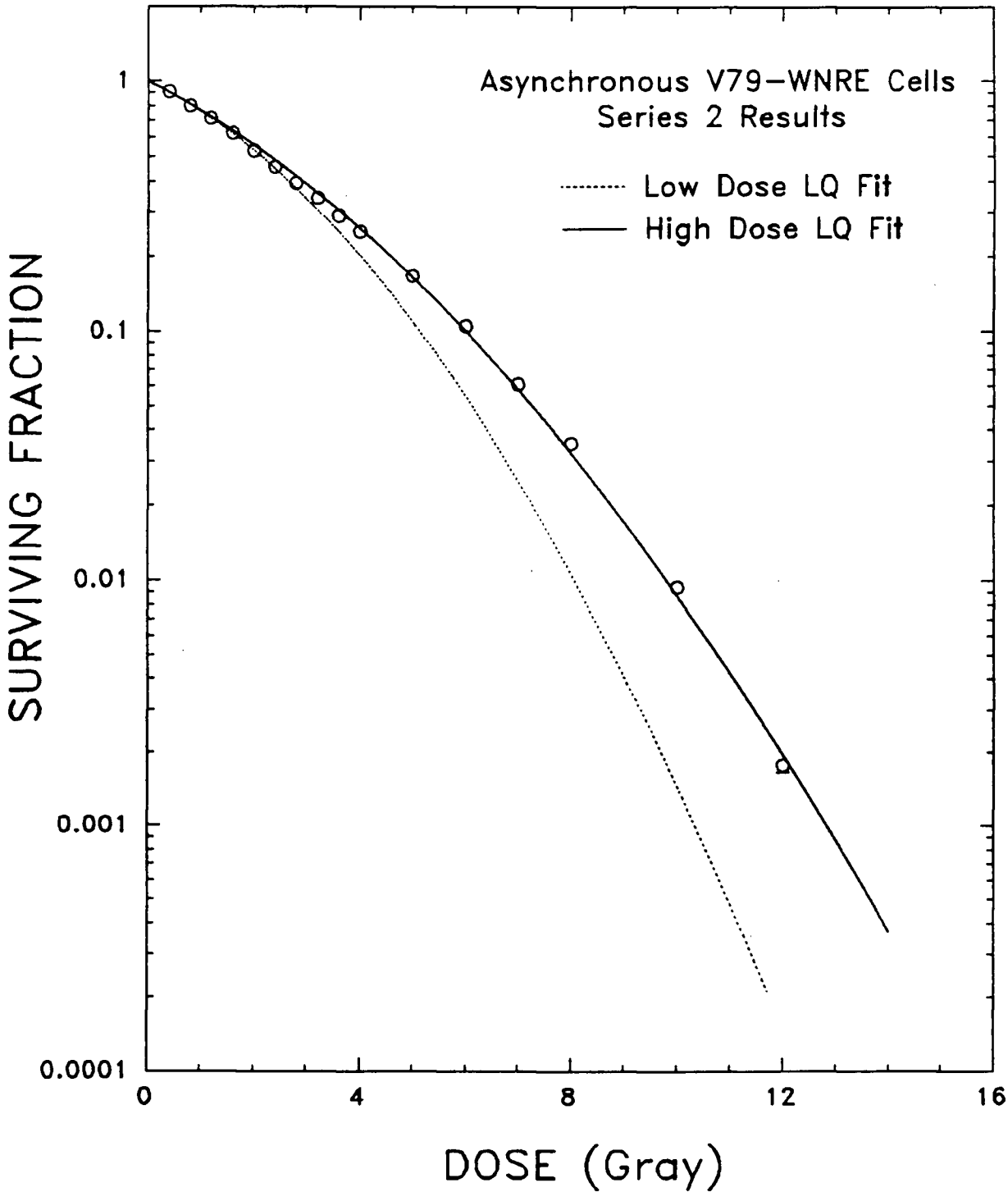

FIGURE 14 : SECOND SERIES OF ASYNCHRONOUS CELL EXPERIMENTS - I

Asynchronous cells were handled as described in figure 8. Data are the average of eight experiments obtained during the second series of asynchronous experiments. Data have been fitted separately to the LQ equation over the low dose (0 to 2 Gy) region (-----) or the high dose (2 to 12 Gy) region (————) Data and separate low and high dose LQ fits are plotted in the form $S = \exp(-\alpha D - \beta D^2)$.

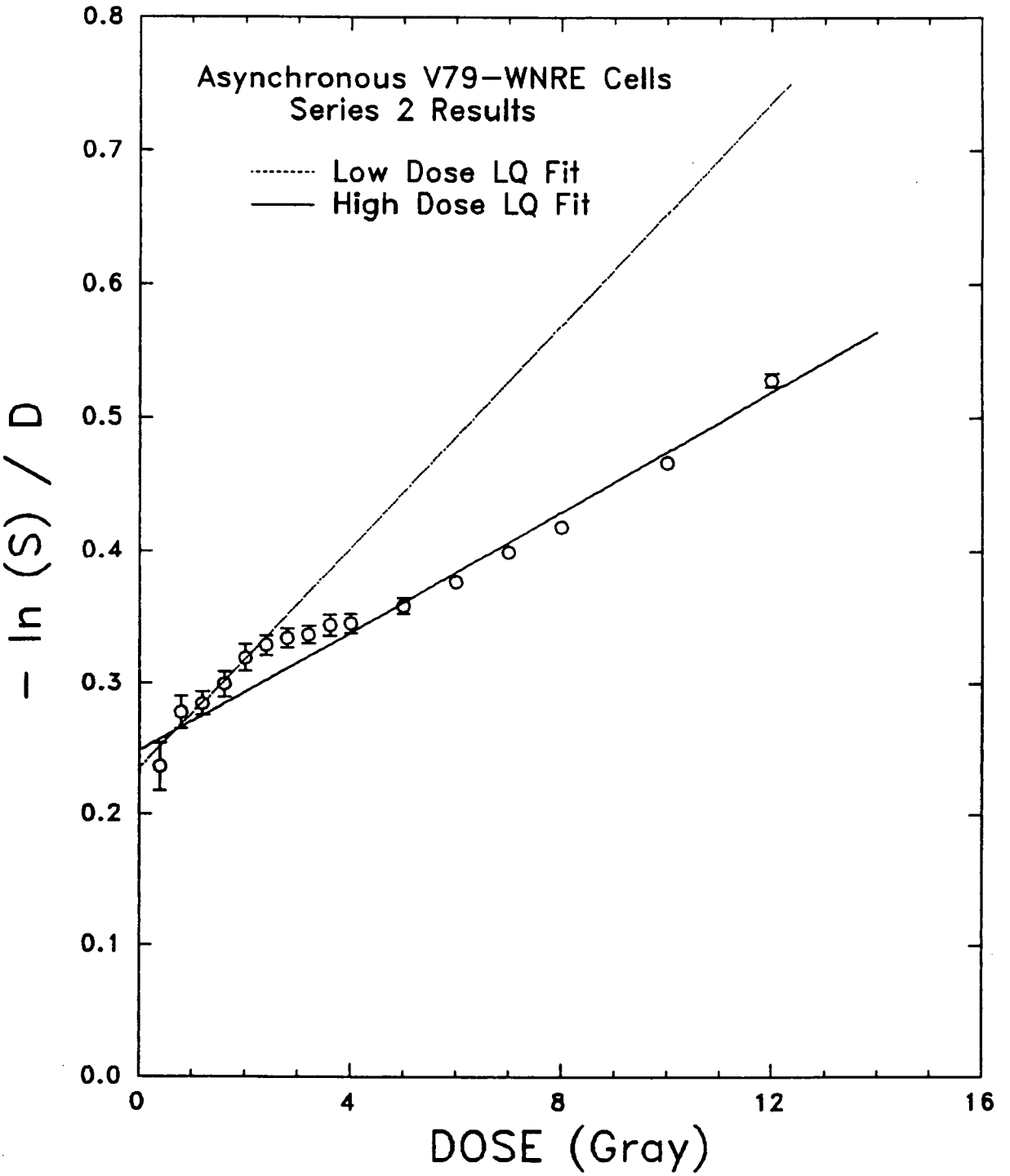

FIGURE 15 : SECOND SERIES OF ASYNCHRONOUS CELL EXPERIMENTS -II

Asynchronous cells were handled as described in figure 8. Data are the average of eight experiments obtained during the second series of asynchronous experiemnts. Data have been fitted separately to the LQ equation over the low dose (0 to 2 Gy) region (-----) or the high dose (2 to 12 Gy) region (————) Data and separate low and high dose LQ fits are plotted in the form $-\ln S/D = \alpha + \beta D$.

The reason for the differences between the initial and second series of asynchronous survival responses is not immediately apparent. A period of about eight months lapsed between the last experiment of the initial series and first experiment of the second series, during which time most of the experiments involving synchronized cells were performed. Natural "biological drift" would tend to shift the response uniformly across the entire dose range rather than the skewed displacement observed.

A more likely explanation may be found by examining the FACS produced measurements of cellular light scattering shown in figure 16 for a typical experiment from each of the initial and second series of asynchronous experiments. The histograms show light scattering intensity as a function of channel number (particle volume). They are used to establish "gates" for the minimum and maximum particle volumes that the FACS will sort into the plating samples. The distribution of particle volumes prior to gating is shown in figures 16a and 16c. In order to eliminate cellular and other debris, characterized by the tails of the particle volume distribution, the gates shown in figures 16b and 16d were established. All particles having volumes lying between the gates were classified as single cells and became candidates for sorting into the plating sample test tube. Figure 16d from the second series shows an increase in the width of the gate compared to figure 16b from the initial series. The increase in gate width appears mainly to include those particles from the forward tail of the distribution. If the additional particles being included by this enlarged gating are non-viable debris, the cell sorter would interpret each particle of debris as a viable single cell resulting in a decrease in the plating efficiency. The zero dose plating efficiency (and standard error) for the initial series of asynchronous experiments was 81.4

± 1.3 %, and for the second series was 75.5 ± 0.9 %, indicating that the above hypothesis may be true, although other factors are likely involved. The -ln(S)/D vs D plot is particularly sensitive to slight variations in the zero dose plating efficiency, especially in the low dose region of the plot. A small decrease in the zero dose plating efficiency alone would produce an overall increase in the survival response, which would be observed as a downward shift in the low dose region of the -ln(S)/D vs D plot. This is quite opposite to the upward shift in the low dose region observed for the second series of asynchronous experiments.

The observed shift would be more easily explained by an increase in the proportion of sensitive cells in the asynchronous population, leading to an increase in the low dose region of the -ln(S)/D vs D plot, but would not account for the slight downward shift in the high dose region. An increase in the proportion of sensitive cells could occur if some of the cells grown as monolayer on the tissue culture flasks were overcrowded and restricted from normal cell cycling. This would lead to cells maintained at G_0 which are very sensitive in their radiation response. Great effort was taken to ensure that the tissue culture flasks used for asynchronous radiation experiments were between 40-70 % confluent in order to eliminate inducing the cells into G_0. There were no obvious differences in this regard between the flasks used for the initial or second series of experiments, although larger 175 cm^2 TC flasks were used for the second series while 75 cm^2 TC flasks were used for the initial series.

As part of the normal experimental procedure, preparations of ethidium-bromide stained cells from the irradiated asynchronous population were obtained for each experiment. The preparations were analyzed to determine the distribution of DNA content for the population of

asynchronous cells. Histograms of relative number of cells vs. channel number (DNA content) for some of the initial and second series of asynchronous experiments are shown in figure 17. An increase in the number of sensitive G1 or G_o cells would be reflected in an increase in the prominent G1 peak. The histograms for both series of experiments show roughly the same distribution of cells throughout the cell cycle indicating no obvious differences between the populations used for any of the experiments.

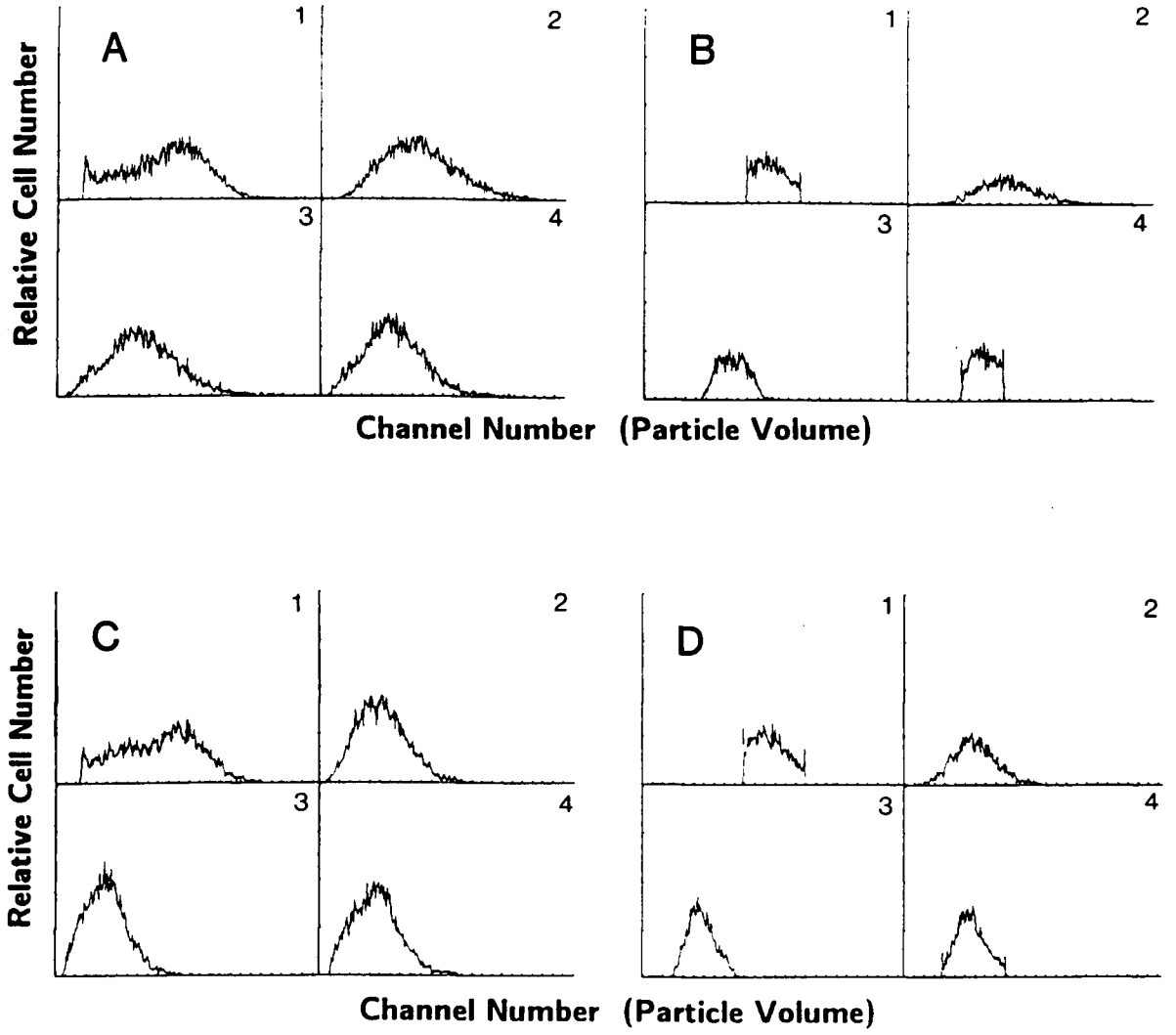

FIGURE 16 : PARTICLE VOLUME DISTRIBUTIONS

Histograms of the light scattering intensity as a function of channel number (particle volume) for cellular populations were routinely measured for each experement as part of the cell sorting procedure. These were used to establish 'gates' of minimum and maximum particle volumes for the sorted cell samples. The distribution of particle volumes prior to gating is shown for a). the initial series and c). the second series of asynchronous experiments. The position of the established gates is shown for the same particle volume distribution for b). the initial series and d). the second series of asynchronous experiments.

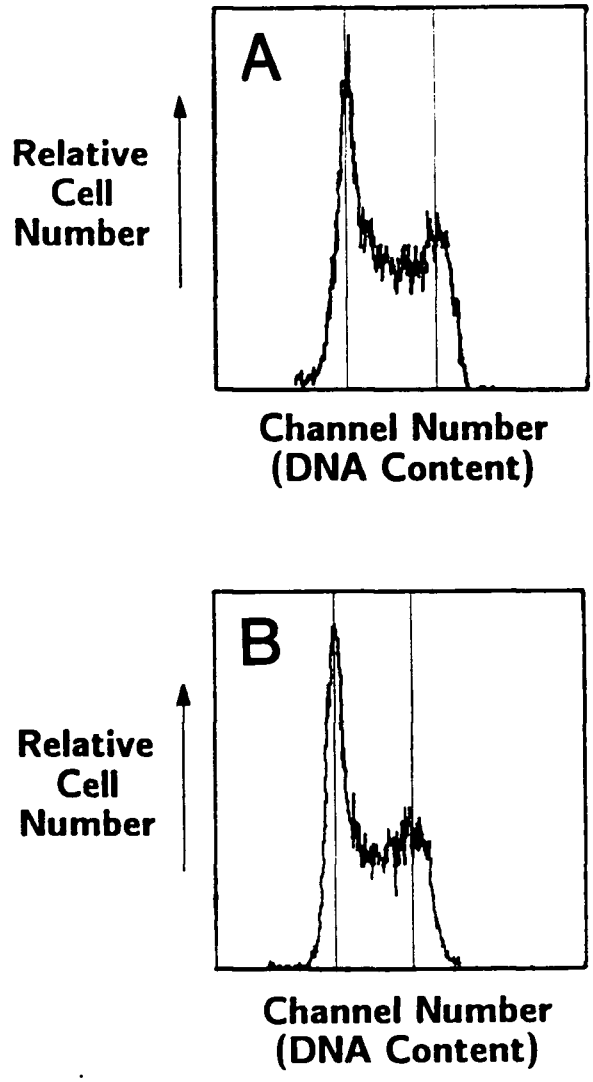

FIGURE 17 : DNA DISTRIBUTION OF ASYNCHRONOUS CELL POPULATIONS

The distribution of DNA content for the irradiated asynchronous populations of cells was determined as part of the routine procedure of an asynchronous experiemnt. Histograms of relative cell number vs. channel number (DNA content) from some of the asynchronous experiments are shown for a). the initial series , and b). the second series. The samples indicate no obvious differences in the populations used for either series of experiments. The vertical lines represent the approximate positions of the 2n (G1) and 4n (G2) peaks.

3.3 SYNCHRONOUS CELL EXPERIMENTS

In order to determine whether the observed substructure was the result of differential killing of subpopulations of cells with different radiosensitivities (hypothesis 3, section 4.3 of the Discussion), the radiation survival response of homogeneous populations of synchronized cells was measured using the same kind of experimental technique utilized with the asynchronous populations. It was desirable to obtain populations that were homogeneous both in their radiation sensitivity and in population size within the cell cycle. Heterogeneities in either respect could result in a response influenced by the constituent subpopulations.

The hypothesis may be tested by applying statistical analysis (see appendix A) to the low and high dose parameters α and β derived from the reponses of synchronized cells. For the hypothesis to be valid, differences in the parameters should not be statistically significant, assuming that the LQ model adequately characterizes the response of the synchronized populations being examined.

3.3.1 Cells Synchronized By Mitotic Selection Alone

3.3.1.1 Response Of G1 Phase Cells

Using the cell sorter assay, radiation survival experiments were conducted on cell populations synchronized by mitotic selection alone. Two series of such experiments were carried out. The first series included 4 experiments conducted on cells initially grown on the inner surface of glass roller bottles prior to mitotic selection. Irradiations for 3 of the experiments were conducted one hour after roll off, which includes about 30 minutes of cell handling (centrifugation, resuspension, preparation of

irradiation flask), and 30 minutes of unperturbed cellular growth at 37° C in spinner culture. The fourth experiment was conducted two hours after roll off which includes 30 minutes of cell handling and 90 minutes of unperturbed growth at 37° C. It was consistently observed that large cellular clumps formed on the inner surface of the glass roller bottles. In an attempt to eliminate the clumping, which was suspected of contributing interphase cell contaminants, cells were grown on the inner surface of plastic roller bottles. A second series including four experiments was conducted on cells cultured in these bottles prior to mitotic selection. Irradiations for 2 of the experiments were conducted one hour and for the other 2 experiments two hours after roll off under the same conditions described for the first series of experiments. Examination of the single dose irradiation profile, figure 5, indicates that the populations were irradiated in G1 phase and that the response to 8 Gy was relatively uniform up to 2 hours after mitotic selection.

The responses for both series of experiments and times were roughly equivalent and have been averaged together and fitted to the LQ equation over the dose range 0 to 12 Gy as seen in figures 18 and 19. The quality of a single fit over the full dose range is poor, with most of the low dose points lying above and the high dose points lying below the best fit curve. This result suggested that the data may be better characterized by fitting the low dose (0-3.2 Gy) and high dose (3.2-12 Gy) data separately to the LQ equation as seen in figure 20. The same kind of divergence seen in the asynchronous response is also seen in figure 20 for a homogeneous population of cells in G1. The same data replotted in the form $-\ln(S)/D$ vs. D is shown in figure 21. Comparing figures 21 to figure 19, for the 0 to 12 Gy fit, it is clear that a single LQ fit is not adequate to describe the

survival response of V79-WNRE cells synchronized by mitotic selection alone and allowed to progress to G1.

Statistical analysis of the values for α or β from low or high dose fits to the LQ model clearly indicate that the low dose values of α or β are significantly different from the high dose values. Results from the analysis are shown in table IV. The low and high dose values of α were determined to be significantly different at the $P<0.001$ level for both the paired and unpaired t-tests as well as for both nonparametric tests. For β, the low and high dose values were also found to be significantly different at the $P<0.001$ level for both the paired and unpaired t-tests as well as for both nonparametric tests. These P values reflect an extremely high degree (>99.9%) of confidence that the low and high dose values of α or β represent statistically different distributions from each other.

A goodness of fit test consisting of a calculation of the RMS deviation of the actual data from the fitted points of the LQ survival curve was carried out for the low dose, high dose and full dose LQ best fits. For the full dose fit, the RMS deviation was found to be 0.157 (unitless). The deviation decreased to 0.0217 by fitting to the low dose data and to 0.115 by fitting to the high dose data separately. These figures reassert that the response is best characterized by separate fits to the low dose and high dose data.

3.3.1.2 Response of G1 Phase Cells Exposed to Trypsin

The cell populations synchronized by mitotic selection alone contained a large number (40-80 %) of visible cell doublets that remained even several hours after harvest. The cell sorting procedure used for all of the irradiation experiments ensured that only single cells were selected for the

plating samples. In order to increase the efficiency of the sorting procedure, which was reduced by the presence of the high number of doublets, and in order to ensure that no doublets actually were sorted into the plating samples, synchronized populations were irradiated that had been treated with trypsin to break up doublets as described in section 2.3.2.1. Figure 22 shows the average of two experiments on cells that were synchronized by mitotic selection alone, allowed to progress to G1 phase in spinner culture for 1 hour, treated with trypsin and irradiated 2 hours after harvest. Separate fits to the low dose (0-3.2 Gy) and high dose (3.2-12 Gy) data indicate that substructure is still present in the response at low dose. The substructure observed in figures 20 and 21 for populations synchronized by mitotic selection alone irradiated 1 to 2 hours after harvest was not eliminated by reducing the population to a single cell suspension.

3.3.1.3 Response of S-Phase Cells

Experiments were also conducted on populations synchronized by mitotic selection alone and allowed to progress to S phase in spinner culture. Figure 23 shows the radiation survival response for the average of two experiments of populations irradiated 6.5 hours after harvest, which includes 30 minutes of cell handling time. The data, replotted in figure 24 as $-\ln(S)/D$ vs. D, exhibits very little of the structure seen in the response of asynchronous cells, although with only 2 experiments no conclusions can be drawn.

TABLE IV
STATISTICAL SIGNIFICANCE OF THE DIFFERENCES BETWEEN THE LOW DOSE AND HIGH DOSE VALUES OF α AND β
SYNCHRONOUS CELL EXPERIMENTS
MITOTIC SELECTION ALONE

	Full Dose Mean	Low Dose Mean	High Dose Mean	P_{pair}	P_{unp}	P_{sr}	P_W
G1 Phase Cells (8 Expts)							
α ($\times 10^{-1}$ Gy^{-1})	4.514	2.055	4.642	<0.001	<0.001	<0.001	<0.001
β ($\times 10^{-2}$ Gy^{-2})	2.168	9.221	2.234	<0.001	<0.001	<0.001	<0.001
S Phase Cells (2 Expts)							
α ($\times 10^{-1}$ Gy^{-1})	0.347	0.518	0.303				
β ($\times 10^{-2}$ Gy^{-2})	2.946	2.632	2.990				

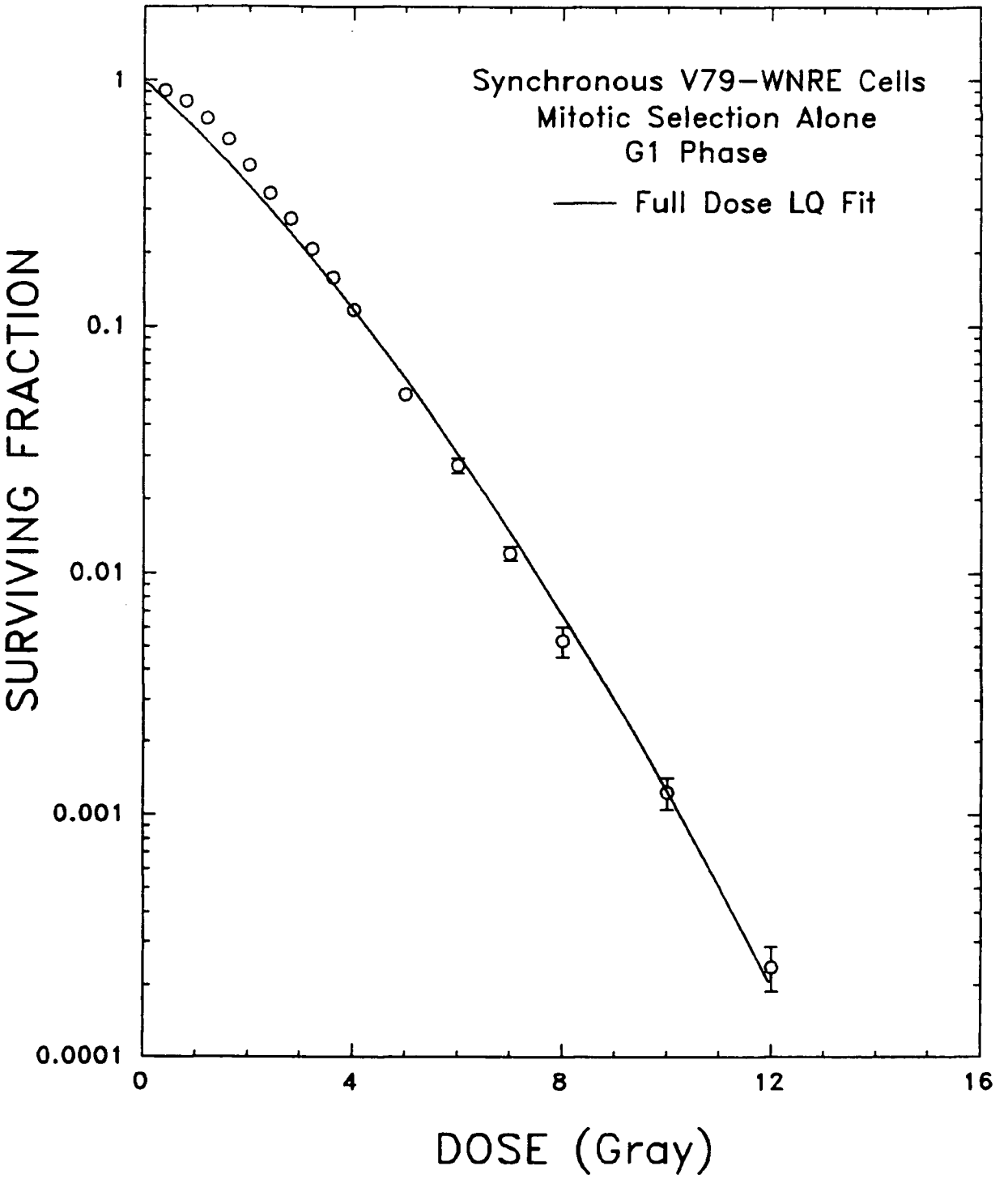

FIGURE 18 : MITOTIC SELECTION G1 PHASE CELL IRRADIATION - I

Survival data obtained from the average of eight experiments of cell populations synchronized by mitotic selection and irradiated in G1 phase one to two hours after harvest. Experimental conditions are as described in figure 8. Data and the full dose (0 to 12 Gy) LQ fit are plotted in the form $S = \exp(-\alpha D - \beta D^2)$

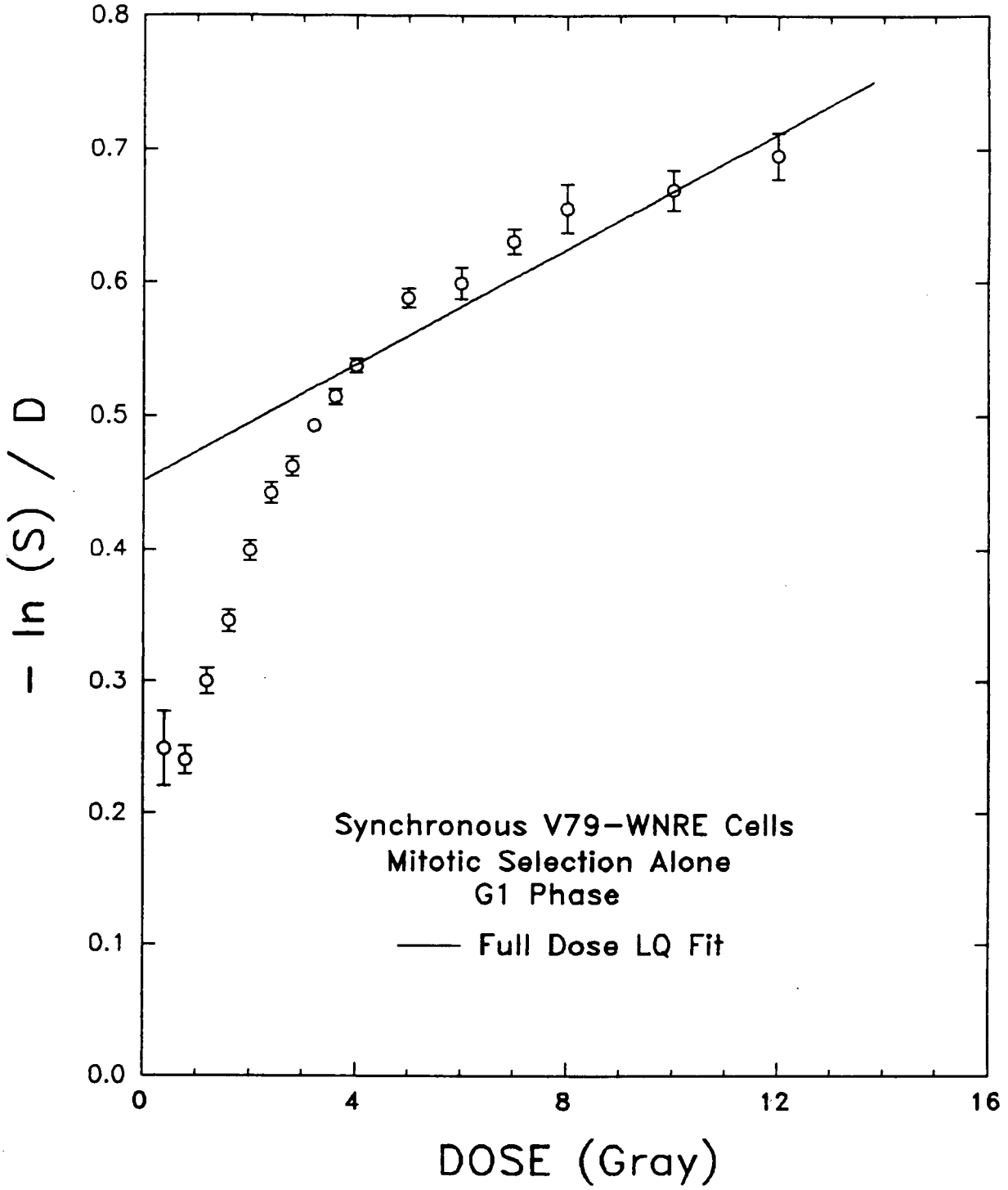

FIGURE 19 : MITOTIC SELECTION G1 PHASE CELL IRRADIATION - II

Survival data obtained from the average of eight experiments of cell populations synchronized by mitotic selection and irradiated in G1 phase one to two hours after harvest. Experimental conditions are as described in figure 8. Data and the full dose (0 to 12 Gy) LQ fit are plotted in the form $-\ln S/D = \alpha + \beta D$.

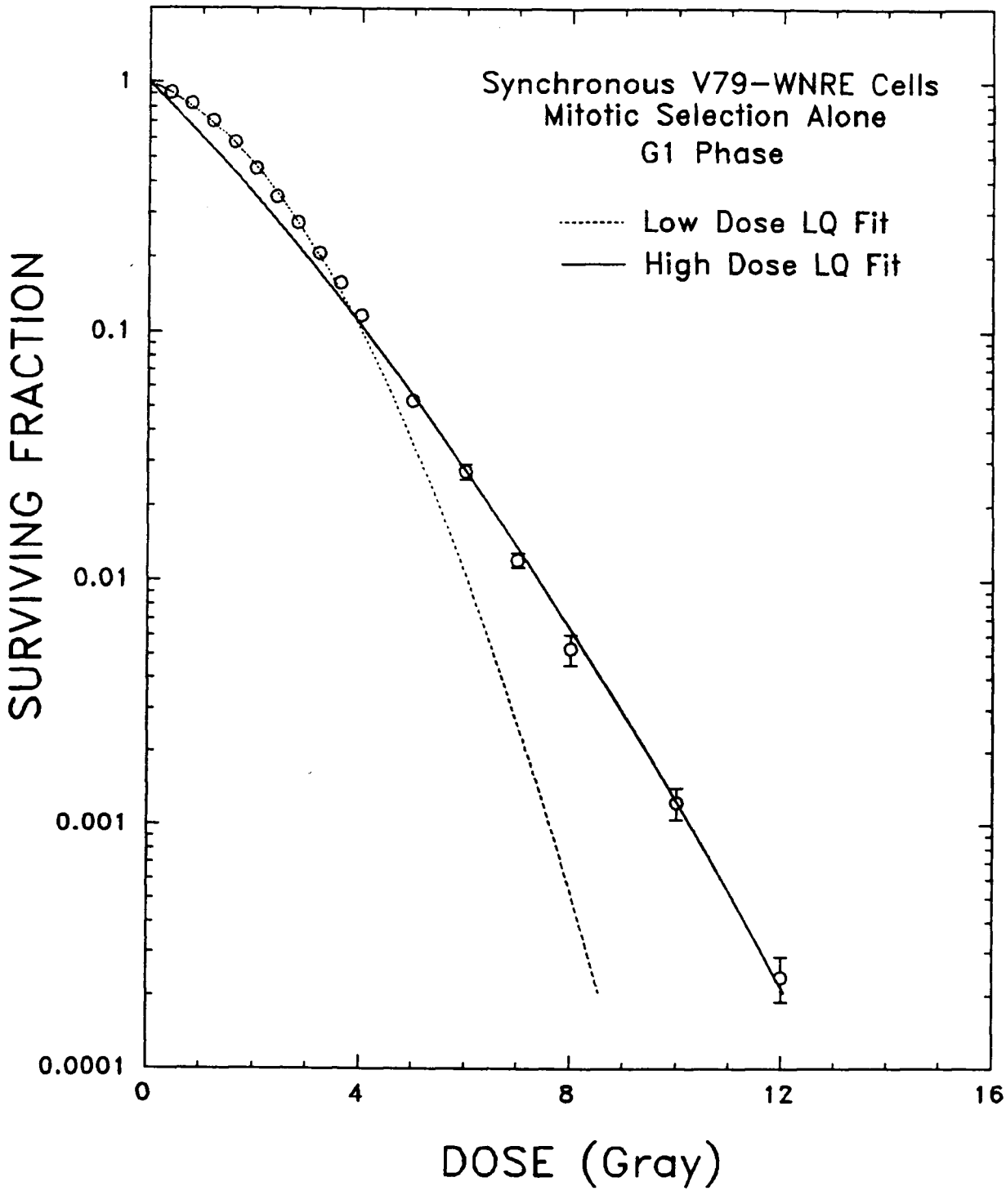

FIGURE 20 : SEPARATE FITS TO MITOTIC SELECTION G1 DATA - I

The same data shown in figure 18 have been fitted separately to the LQ equation over the low dose (0 to 3.2 Gy) region (------) or the high dose (3.2 to 12 Gy) region (————). Data and separate low and high dose LQ fits are plotted in the form $S = \exp(-\alpha D-\beta D^2)$.

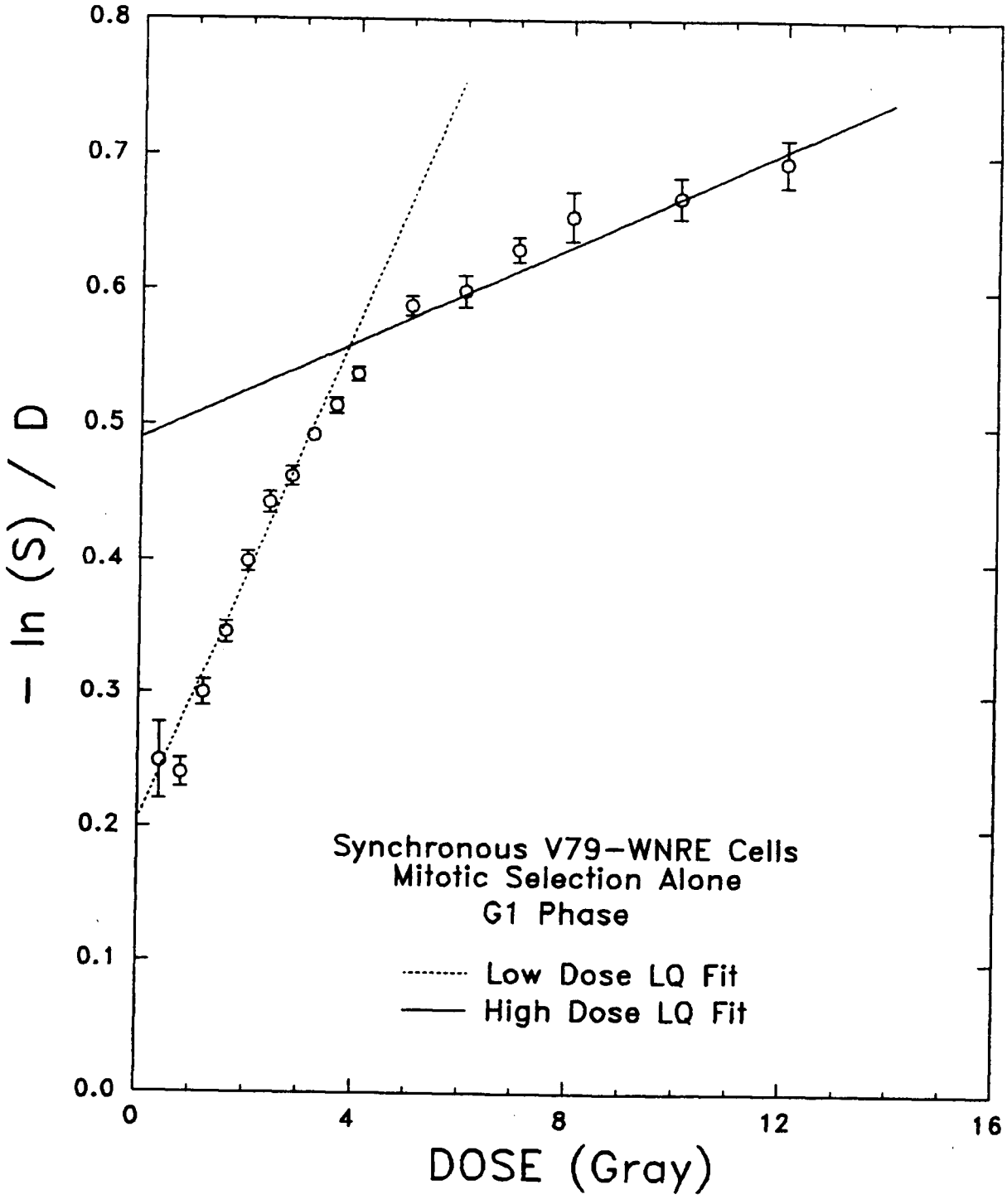

FIGURE 21 : SEPARATE FITS TO MITOTIC SELECTION G1 DATA - II

The same data shown in figure 18 have been fitted separately to the LQ equation over the low dose (0 to 3.2 Gy) region (------) or the high dose (3.2 to 12 Gy) region (————). Data and separate low and high dose LQ fits are plotted in the form $-\ln S/D = \alpha + \beta D$.

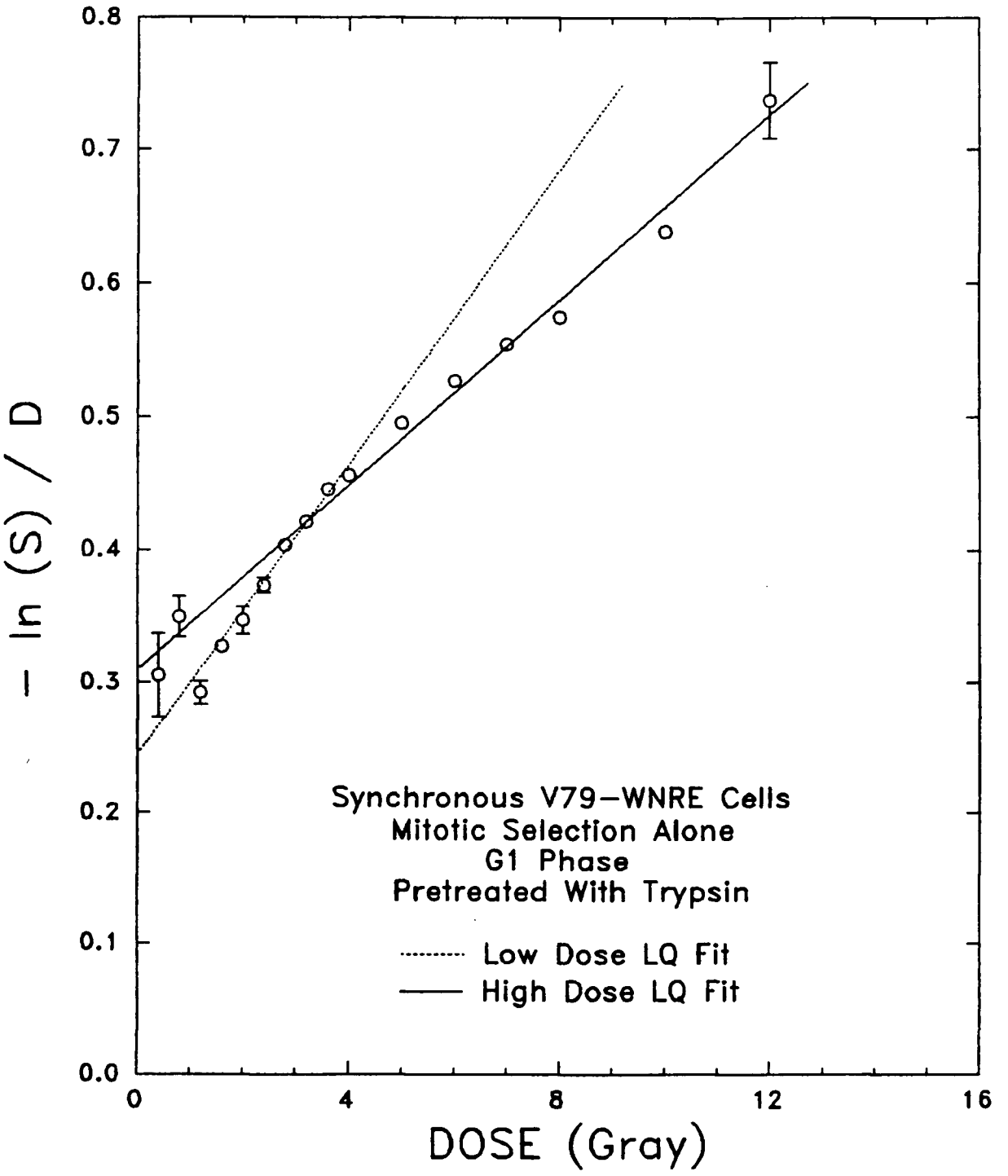

FIGURE 22 : G1 PHASE CELLS PRETREATED WITH TRYPSIN

Survival data obtained from the average of two experiments of cell populations synchronized by mitotic selection and treated with trypsin prior to irradiation in G1 phase. The mitotic selection procedure results in a large number (40 to 80 %) of daughter cell doublets being present in the synchronized population. After progressing to G1 phase, the population was reduced to a single cell suspension by the addition of trypsin prior to irradiation. Data and separate low dose (0 to 3.2 Gy) and high dose (3.2 to 12 Gy) LQ fits are plotted in the form $-\ln S/D = \alpha + \beta D$

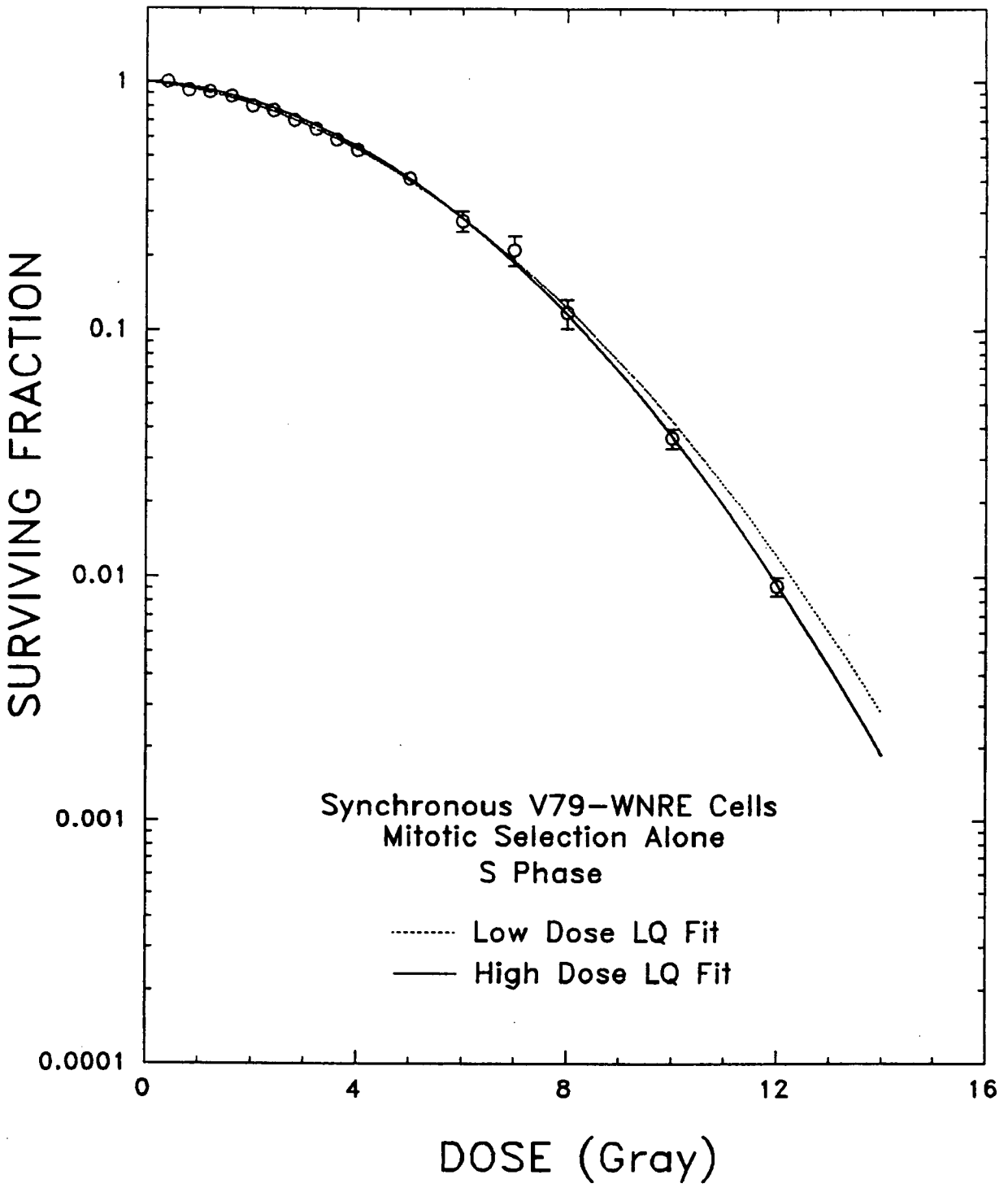

FIGURE 23 : MITOTIC SELECTION S PHASE CELL IRRADIATION - I

Survival data obtained from the average of two experiments of cell populations synchronized by mitotic selection and irradiatied in S phase 6.5 hours after harvest. Experimental conditions were as described in figure 8. Data and separate LQ fits to the low dose (0 to 3.2 Gy) region (------) and high dose (3.2 to 12 Gy) region (————) are plotted in the form $S = \exp(-\alpha D - \beta D^2)$.

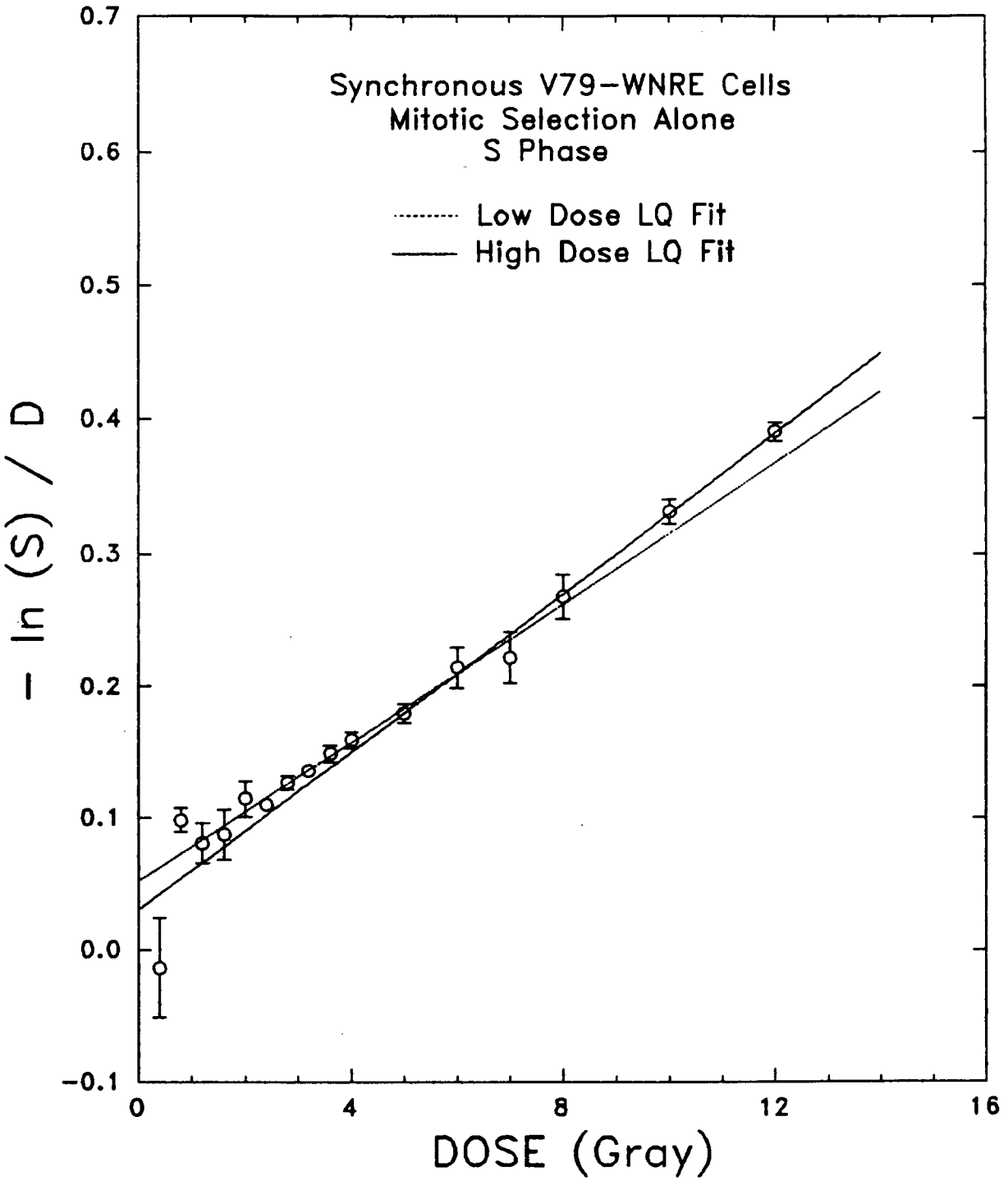

FIGURE 24 : MITOTIC SELECTION S PHASE CELL IRRADIATION - II

Survival data obtained from the average of two experiments of cell populations synchronized by mitotic selection and irradiatied in S phase 6.5 hours after harvest. Experimental conditions were as described in figure 8. Data and separate LQ fits to the low dose (0 to 3.2 Gy) region (------) and high dose (3.2 to 12 Gy) region (————) are plotted in the form - $\ln S/D = \alpha + \beta D$.

3.3.2 Mitotic Selection Followed By A Drug Block

Populations that were synchronized by mitotic selection alone were initially composed of cells from early metaphase to late telophase, representing a spread in time no greater than the length of mitosis (about 30 minutes, Gillespie 1975). In an effort to sharpen the "window" of synchrony, populations were synchronized using the combined techniques of mitotic selection followed by a drug block. The resulting populations resynchronized again at the G1/S border were highly uniform in their age specificity as indicated by the results in sections 3.1.2 and 3.1.3.

3.3.2.1 Mitotic Selection Followed By Hydroxyurea

Radiation survival experiments were conducted on populations initially synchronized by mitotic selection followed by 12 hour exposure to 1 mM hydroxyurea. A 12 hour exposure to HU (or other inhibitory drugs), which corresponds roughly to the cell cycle time of the cells when grown on monolayer, was found suitable by other investigators in producing a homogeneous cohort of cells at the G1/S border with a relatively minor effect on the plating efficiency or the subsequent radiation response (Fox et al 1987). Irradiations were performed 65 to 70 minutes after release from the drug which included about 35 minutes of cell handling during which time it was assumed that little progression through the cell cycle had occurred. The sample represented a population of highly uniform age at the G1/S border or early S as can be seen from figure 5 for the single dose response of cells synchronized by mitotic selection followed by 1 mM hydroxyurea. Data from 7 such experiments have been averaged and fitted to the LQ equation over the full dose range 0 to 12 Gy as shown in figures 25 and 26. The data, fitted separately over the low dose (0-3.2 Gy) and

high dose (3.2-12 Gy) regions as shown in figures 27 and 28, exhibit very little of the structure observed in the response of asynchronous cells.

Statistical analysis of the values for α or β from high and low dose fits to the LQ model clearly indicate that the low dose values of α or β are not significantly different from the high dose values. Results from the analysis are shown in table V. Differences in the low and high dose values of α were determined to be statistically significant at the $P>0.5$ level for both the paired and unpaired t-tests and at the $P=0.95$ level for the W-test. For β, differences in the low and high dose values were also found to be statistically significant at the $P>0.5$ level for the t-tests but only at the $P=0.208$ level for the W-test. These P values reflect an extremely low degree (< 50 %) of confidence that the low and high dose values of α or β represent distributions which are statistically different from each other.

A goodness of fit test consisting of a calculation of the RMS deviation of the logarithm of the actual data from the fitted points of the LQ survival curve was carried out for the low, high and full dose fits. For the full dose fit, the RMS deviation was found to be 0.00325. The deviation differed by only 6.1 % from the value of 0.00345 obtained by fitting the low dose data but by 36 % with the value of 0.00206 obtained by fitting the high dose data. These values for the RMS deviation are considerably smaller than the values obtained from the asynchronous response (0.012 to 0.064).

Similar radiation experiments were conducted on populations that had been initially synchronized by mitotic selection followed by 12 hour exposure to hydroxyurea and irradiated between 2.5 and 3.5 hours after release from the drug, which includes about 35 minutes of non-cycling cell

handling time. According to the single dose irradiation response as a function of cell cycle time for a population synchronized by this method (figure 5), the cells were just past the most radioresistant point in the cell cycle ie. late S/early G2 phase. Data from 3 experiments, one each at 2.5, 3.0 and 3.5 hours after release from the hydroxyurea representing an unperturbed cycling time of 2.0, 2.5 and 3.0 hours respectively, have been averaged and fitted to the LQ equation over the full dose range shown in figures 29 and 30. The data, fitted separately over the low dose (0-3.2 Gy) and high dose (3.2-12 Gy) regions as shown in figures 31 and 32, clearly exhibits substructure in the low dose region.

Statistical analysis of the values for α and β from high and low dose fits to the LQ model clearly indicate the low dose values of α or β are significantly different from the high dose values, as shown in table V. The P values reflect a very high degree of confidence that the low and high dose values of α or β represent distributions which are statistically different from each other.

3.3.2.2 Mitotic Selection Followed By Aphidicolin

Radiation survival experiments were also conducted on populations initially synchronized by mitotic selection followed by a 12 hour exposure to 1 µg/ml aphidicolin. Irradiations were performed 65 to 70 minutes after release from the drug which included about 35 minutes of non-cycling time during cell handling. According to the single dose irradiation response as a function of cell cycle for a population synchronized by this method (figure 5) the cells were irradiated just past the G1/S border in early S phase. Data from 3 identical experiments have been averaged and fitted to the LQ equation over the full dose range shown in figures 33 and 34. The

same data has been fitted separately over the low dose (0-3.2 Gy) and high dose (3.2-12 Gy) regions as shown in figures 35 and 36. The response is very similar to that obtained using hydroxyurea (figures 28 and 29) exhibiting very little of the structure observed in the response of asynchronous cells.

Statistical analysis of the values for alpha or beta from high and low dose fits to the LQ model clearly indicate that the low dose values of alpha or beta are not significantly different from the high dose values. Results are shown in table V. Differences between the low and high dose values of α or β were determined to be statistically significant at the $P>0.5$ level for both the paired and unpaired t-tests and at the $P=0.70$ level for the W-test. These P values reflect an extremely low degree (<50 %) of confidence that the low and high dose values of α or β represent distributions which are statistically different from each other.

Goodness of fit calculations indicated for the full dose fit an RMS deviation of 0.00716 and for the low and high dose fits values of 0.00907 and 0.00334 respectively. These values do not differ greatly from each other and are considerably smaller than the values for the asynchronous fits.

TABLE V
STATISTICAL SIGNIFICANCE OF THE DIFFERENCES BETWEEN THE LOW DOSE AND HIGH DOSE VALUES OF α AND β
SYNCHRONOUS CELL EXPERIMENTS
MITOTIC SELECTION FOLLOWED BY A DRUG BLOCK

	Full Dose Mean	Low Dose Mean	High Dose Mean	P_{pair}	P_{unp}	P_{sr}	P_W
Hydroxyurea G1/S Phase Cells (7 Expts)							
α ($\times 10^{-1}$ Gy^{-1})	2.168	2.131	2.157	> 0.5	> 0.5		0.95
β ($\times 10^{-2}$ Gy^{-2})	3.502	3.757	3.531	> 0.5	> 0.5		0.208
Hydroxyurea S/G2 Phase Cells (3 Expts)							
α ($\times 10^{-1}$ Gy^{-1})	2.826	1.716	2.969	0.0016	0.055		0.05
β ($\times 10^{-2}$ Gy^{-2})	2.238	5.616	2.094	0.0069	<0.001		0.05
Aphidicolin G1/S Phase Cells (3 Expts)							
α ($\times 10^{-1}$ Gy^{-1})	2.378	2.359	2.367	> 0.5	> 0.5		**0.70**
β ($\times 10^{-2}$ Gy^{-2})	3.071	3.224	3.081	> 0.5	> 0.5		0.70

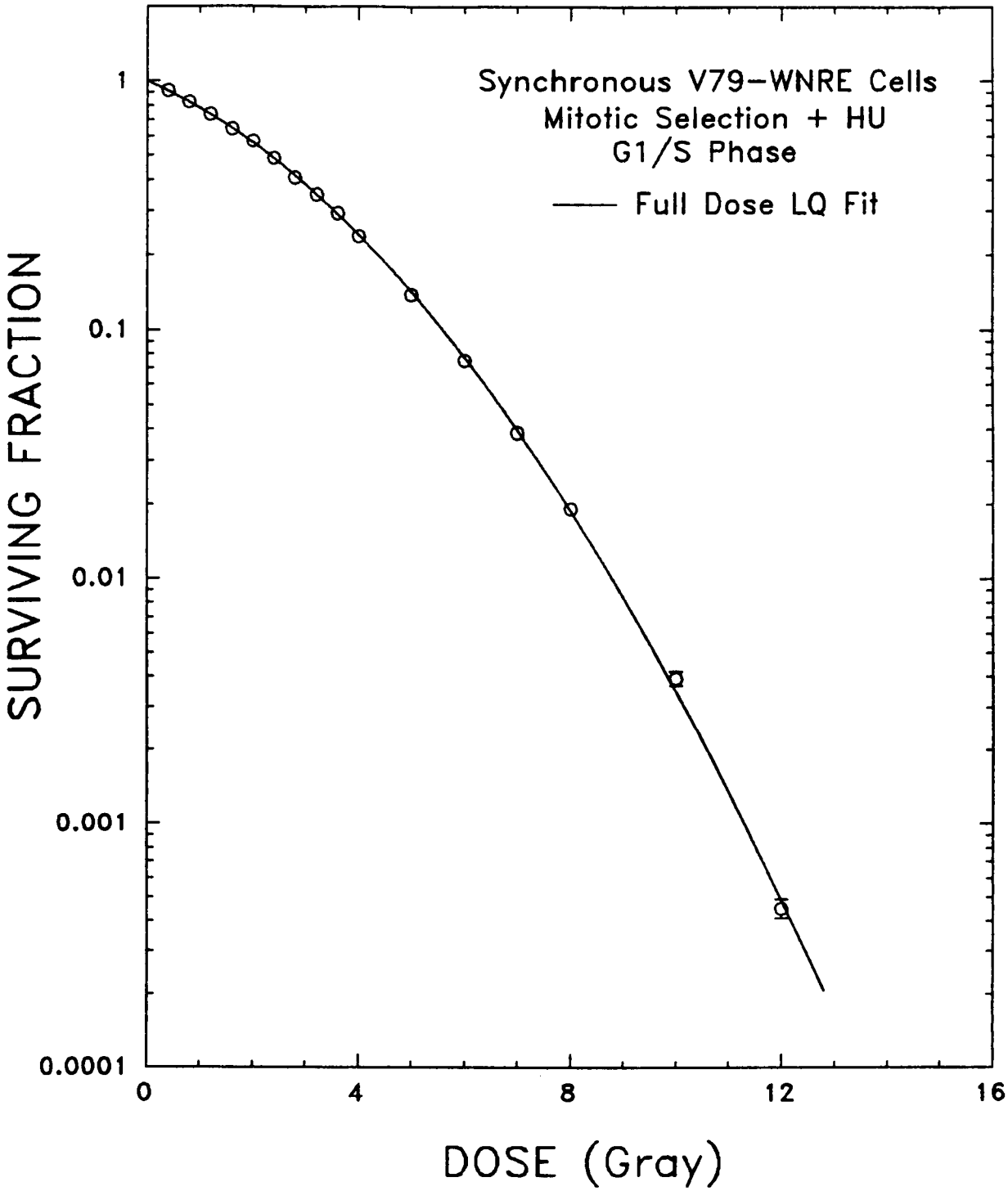

FIGURE 25 : MITOTIC SELECTION + HYDROXYUREA G1/S PHASE - I

Survival data obtained from the average of seven experiments of cell populations synchronized by mitotic selection followed by 12 hour exposure to 1 mM hydroxyurea. Populations were irradiated 30 minutes after release from the drug, just past the G1/S border. Experimental conditions were as described in figure 8. Data and the full dose (0 to 12 Gy) LQ fit are plotted in the form $S = \exp(-\alpha D - \beta D^2)$.

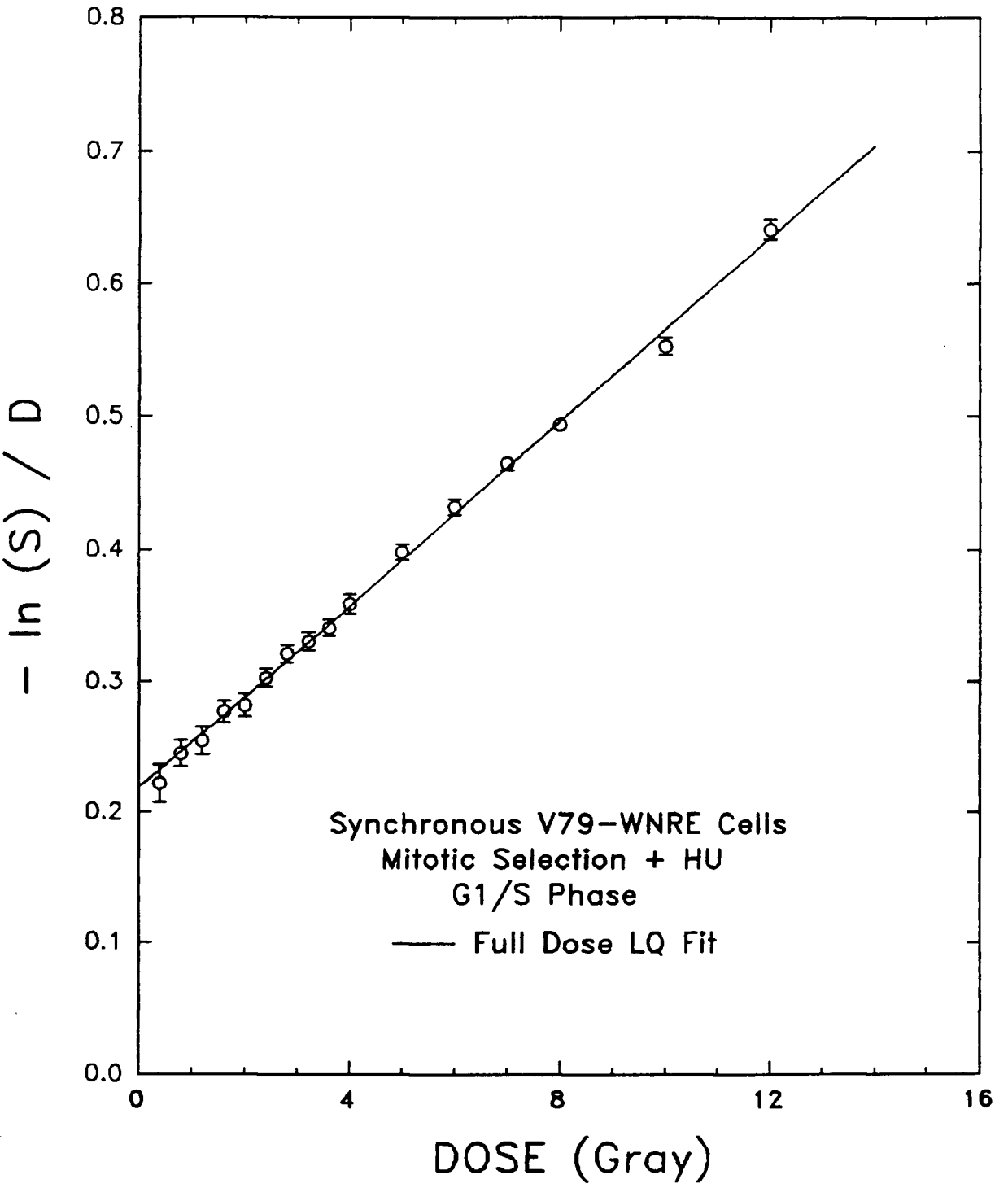

FIGURE 26 : MITOTIC SELECTION + HYDROXYUREA G1/S PHASE - II

Survival data obtained from the average of seven experiments of cell populations synchronized by mitotic selection followed by 12 hour exposure to 1 mM hydroxyurea. Populations were irradiated 30 minutes after release from the drug just past the G1/S border. Experimental conditions were as described in figure 8. Data and the full dose (0 to 12 Gy) LQ fit are plotted in the form $-\ln S/D = \alpha + \beta D$.

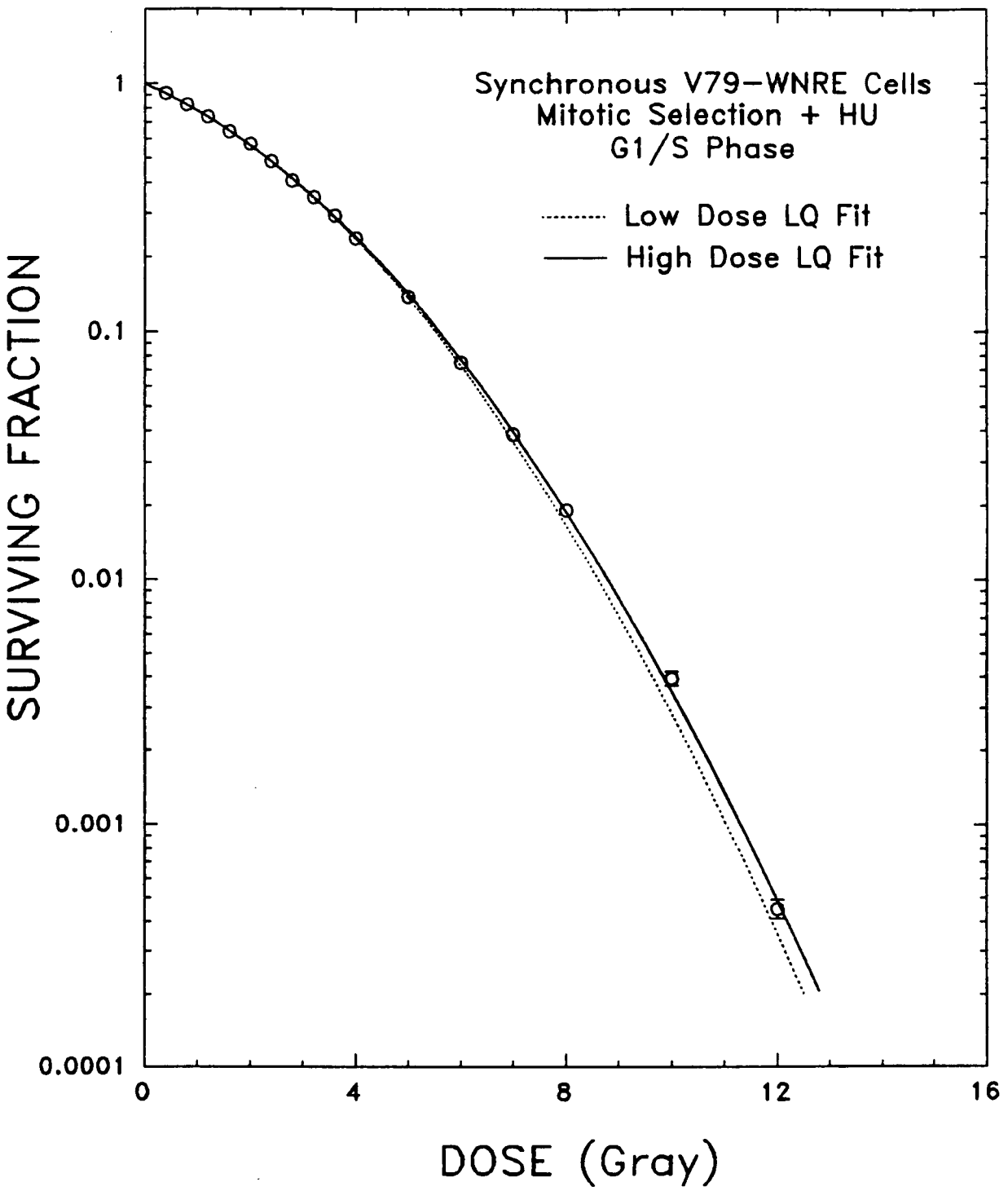

FIGURE 27 : SEPARATE FITS MITOTIC SELECTION + HU G1/S PHASE - I

The same data shown in figure 25 have been fitted separately to the LQ equation over the low dose (0 to 3.2 Gy) region (------) or the high dose (3.2 to 12 Gy) region (————). Data and separate low and high dose LQ fits are plotted in the form $S = \exp(-\alpha D - \beta D^2)$.

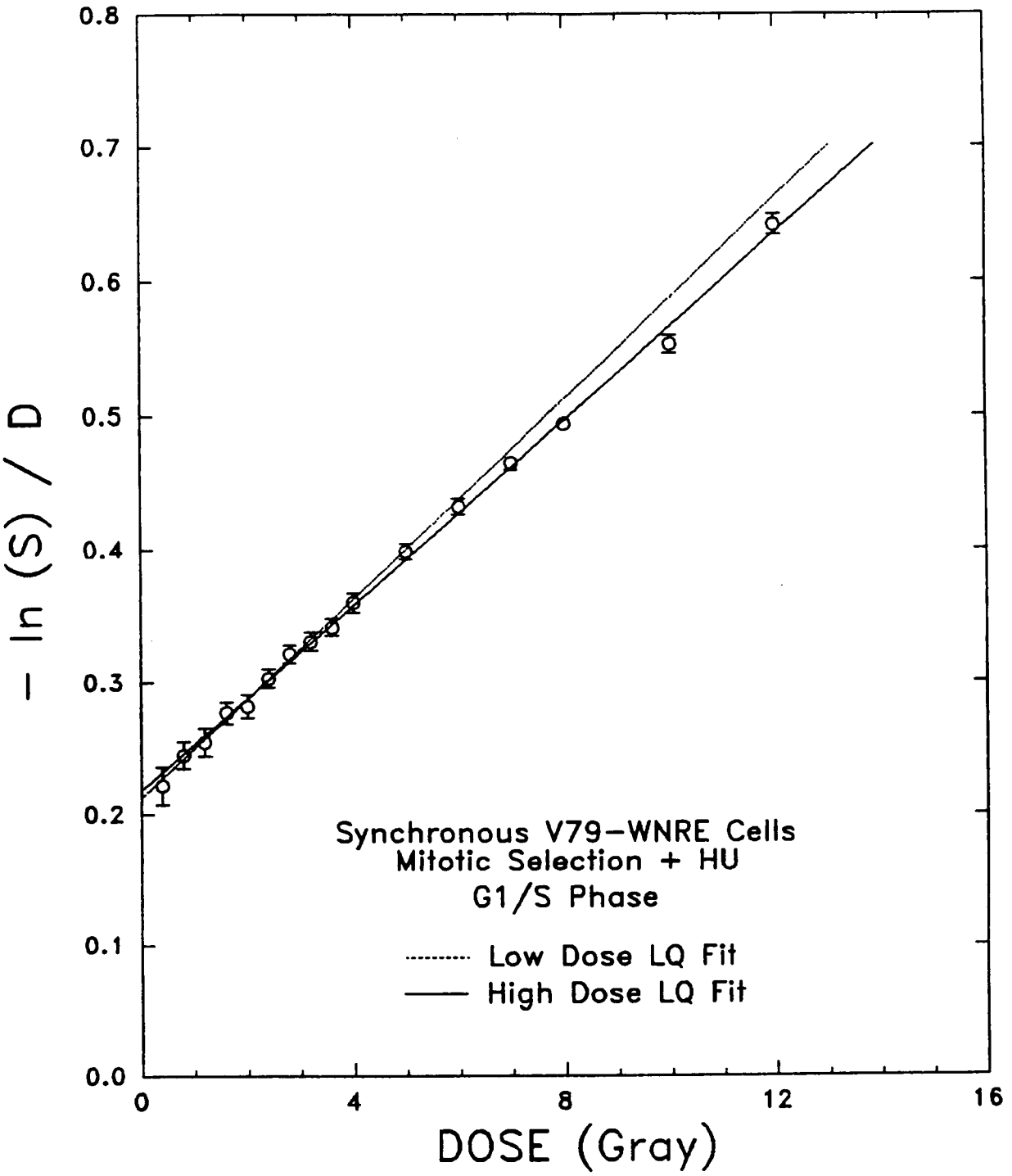

FIGURE 28 : SEPARATE FITS MITOTIC SELECTION + HU G1/S PHASE - II

The same data shown in figure 25 have been fitted separately to the LQ equation over the low dose (0 to 3.2 Gy) region (-------) or the high dose (3.2 to 12 Gy) region (———). Data and separate low and high dose LQ fits are plotted in the form $-\ln S/D = \alpha + \beta D$.

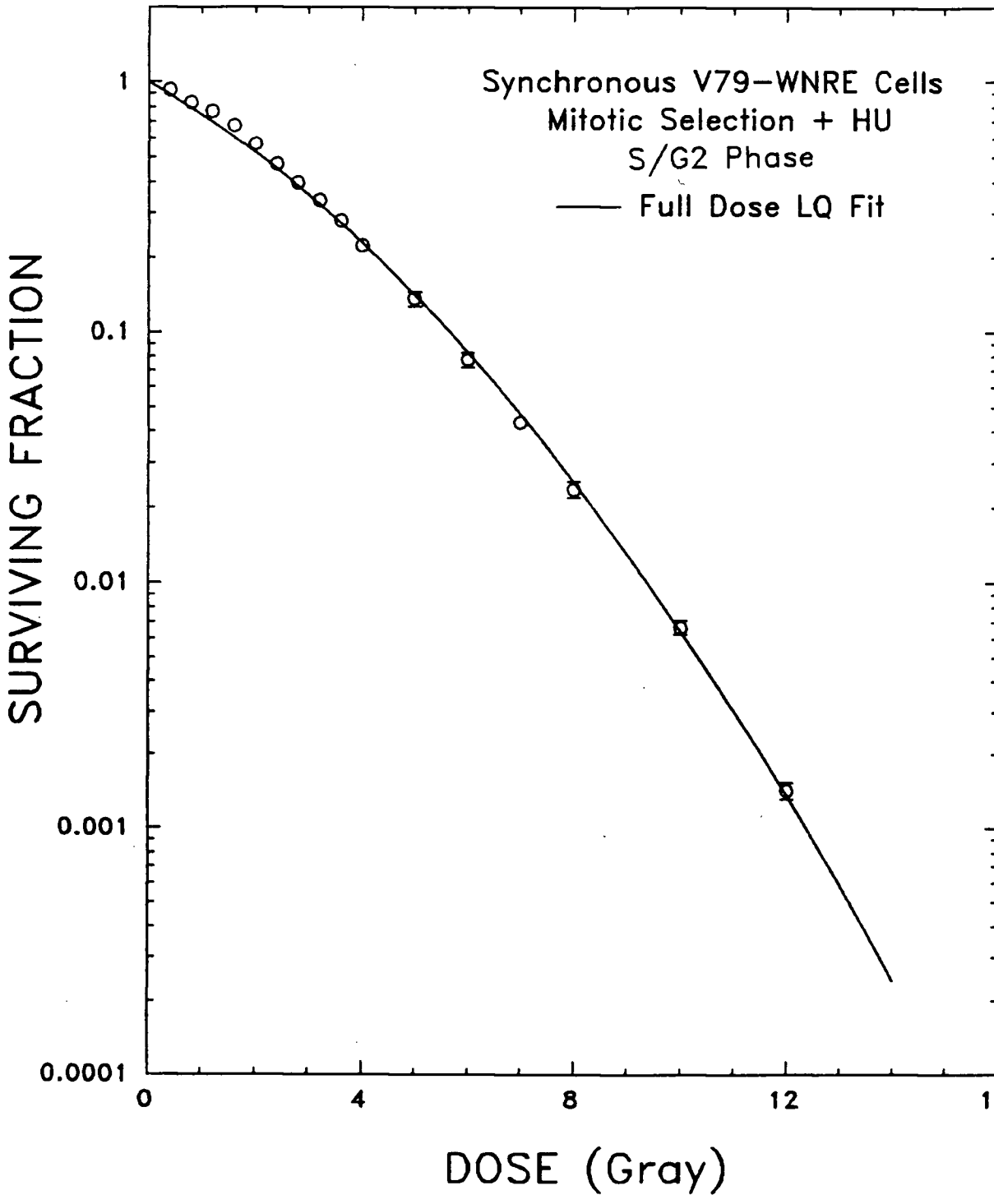

FIGURE 29 : MITOTIC SELECTION + HYDROXYUREA S/G2 PHASE - I

Survival data obtained from the average of three experiments of cell populations synchronized by mitotic selection followed by 12 hour exposure to 1 mM hydroxyurea. Populations were irradiated 2 to 3 hours after release from the drug when they were in late S/early G2 phase. Experimental conditions were as described in figure 8. Data and full dose (0 to 12 Gy) LQ fit are plotted in the form $S = \exp(-\alpha D - \beta D^2)$

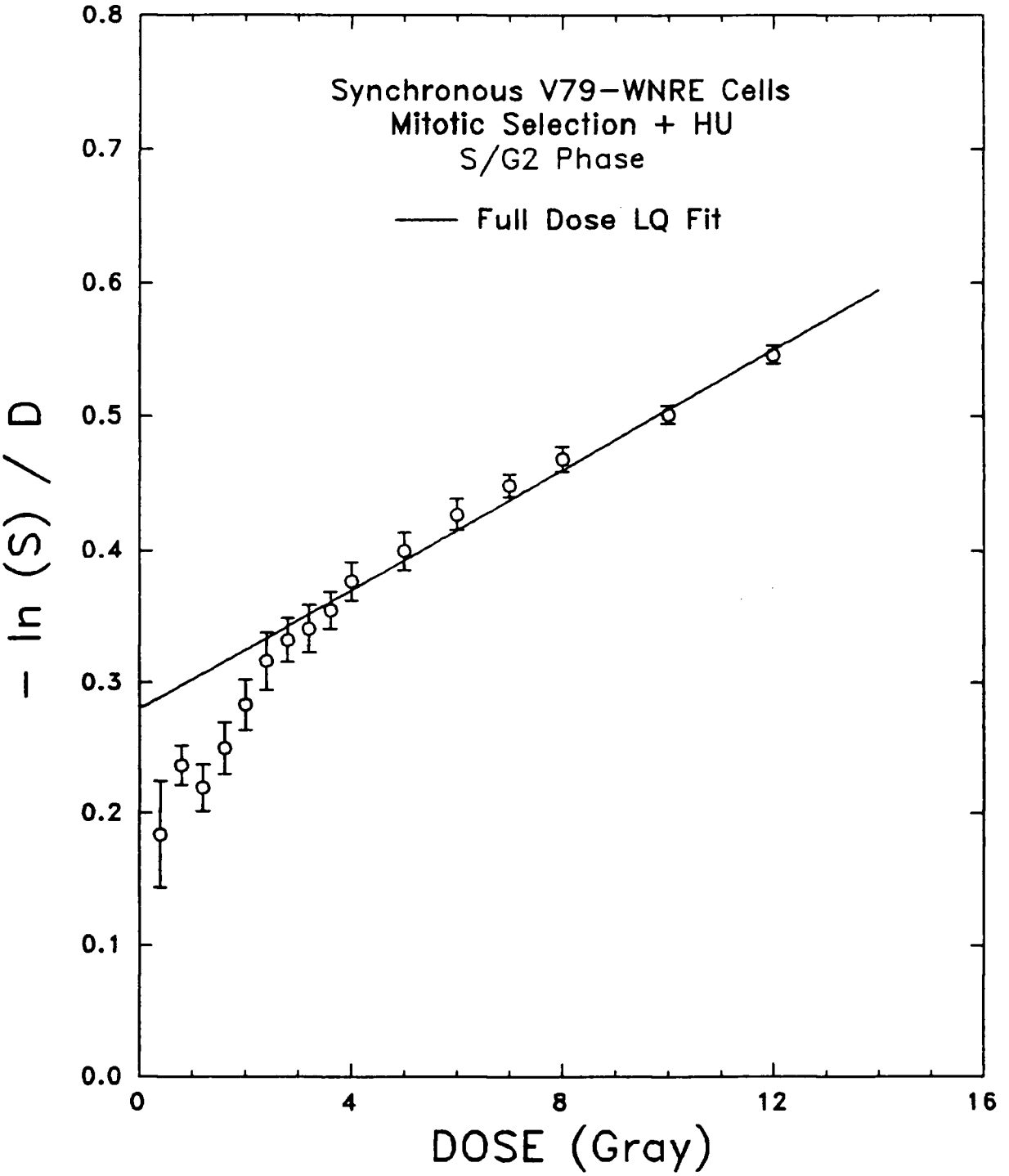

FIGURE 30 : MITOTIC SELECTION + HYDROXYUREA S/G2 PHASE - II

Survival data obtained from the average of three experiments of cell populations synchronized by mitotic selection followed by 12 hour exposure to 1 mM hydroxyurea. Populations were irradiated 2 to 3 hours after release from the drug when they were in late S/early G2 phase. Experimental conditions were as described in figure 8. Data and full dose (0 to 12 Gy) LQ fit are plotted in the form $-\ln(S)/D = \alpha + \beta D$

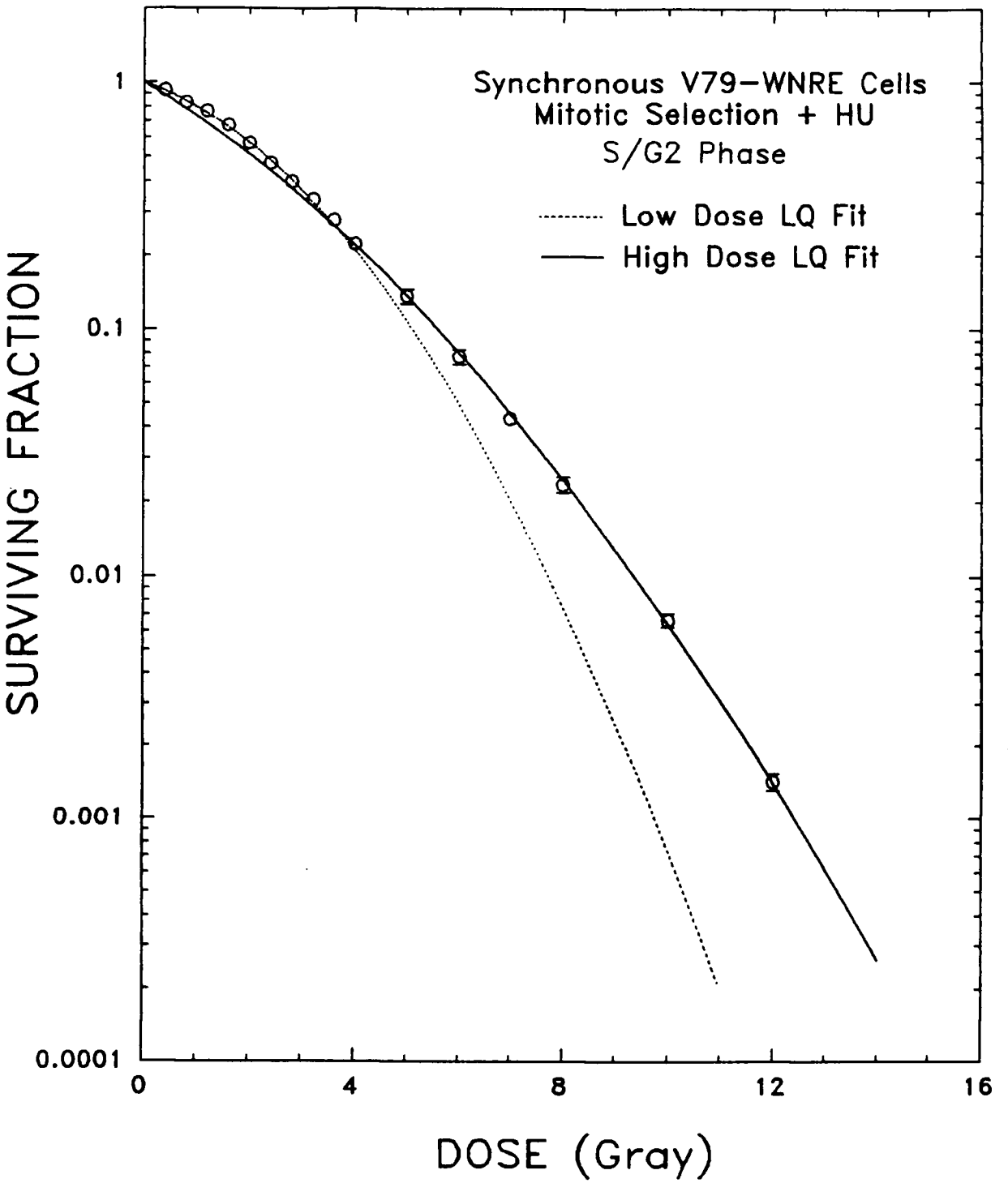

FIGURE 31 : SEPARATE FITS MITOTIC SELECTION + HU S/G2 PHASE - I

The same data shown in figure 29 have been fitted separately to the LQ equation over the low dose (0 to 3.2 Gy) region (------) or the high dose (3.2 to 12 Gy) region (————). Data and separate low and high dose LQ fits and plotted in the form $S = \exp(-\alpha D - \beta D^2)$.

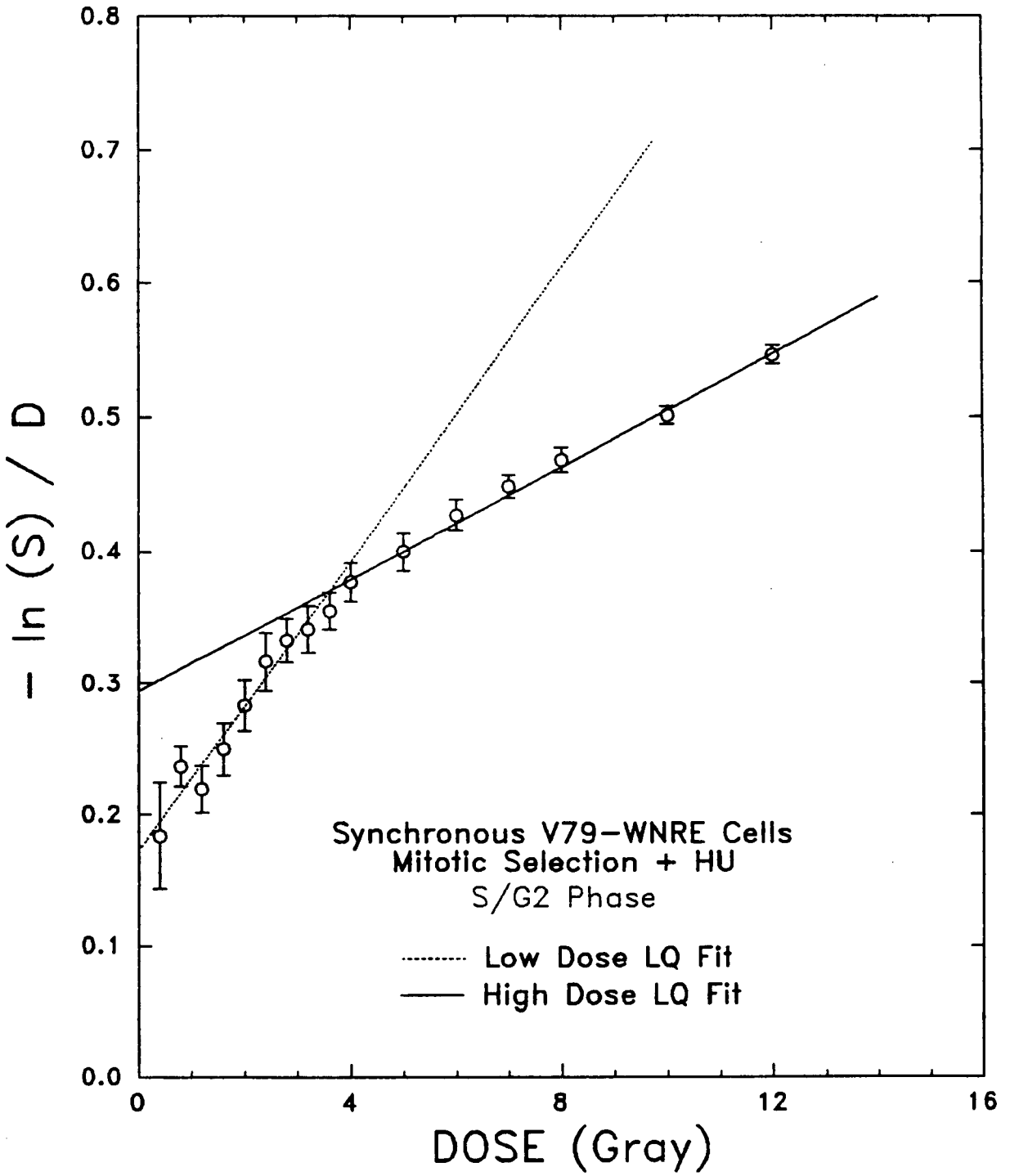

FIGURE 32 : SEPARATE FITS MITOTIC SELECTION + HU S/G2 PHASE - II

The same data shown in figure 29 have been fitted separately to the LQ equation over the low dose (0 to 3.2 Gy) region (------) or the high dose (3.2 to 12 Gy) region (————). Data and separate low and high dose LQ fits and plotted in the form $-\ln(S)/D = \alpha + \beta D$.

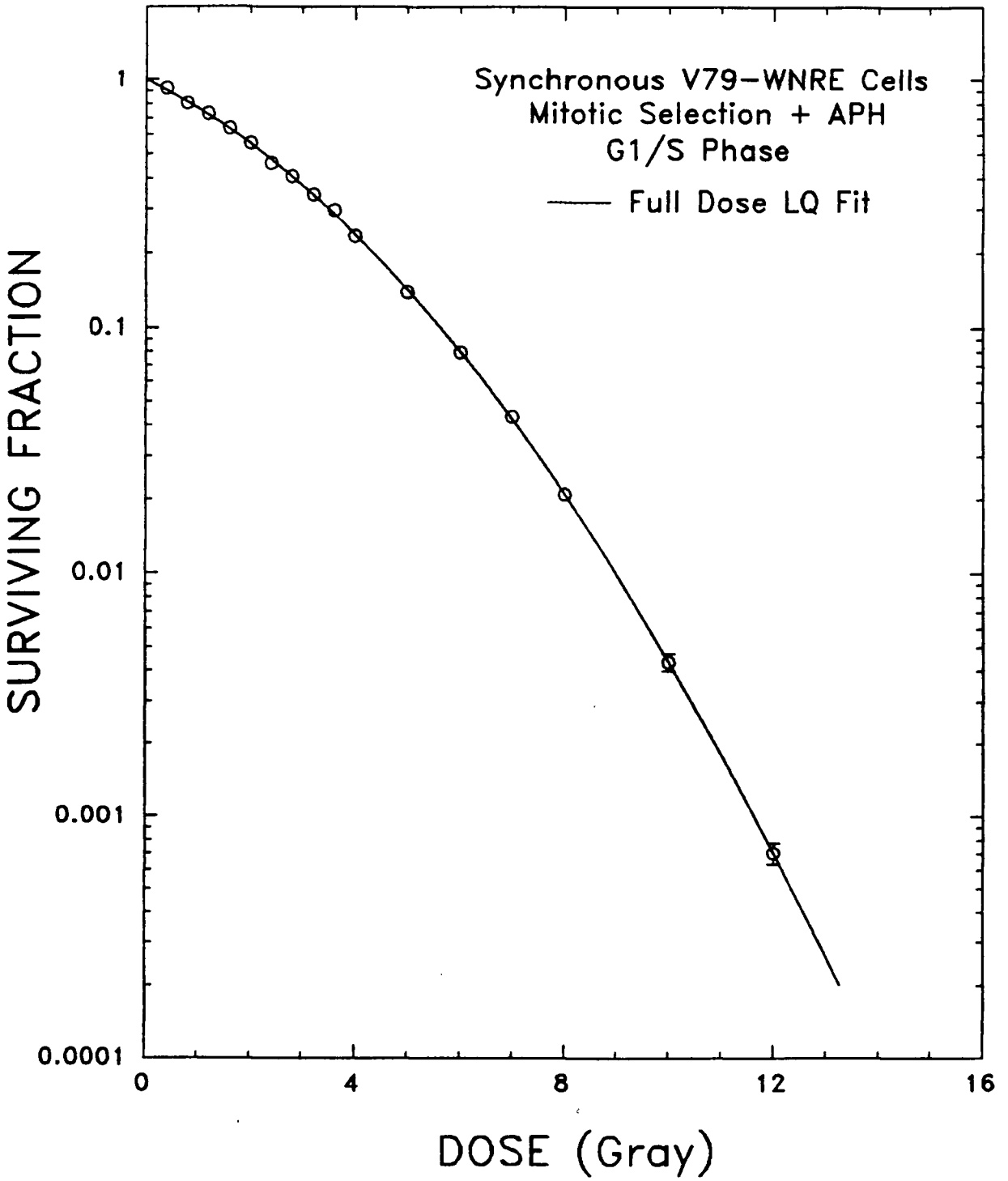

FIGURE 33 : MITOTIC SELECTION + APHIDICOLIN G1/S PHASE - I

Survival data obtained from the average of three experiments of cell populations synchronized by mitotic selection followed by 12 hour exposure to 1 μg/ml aphidicolin. Populations were irradiated 30 minutes after release from the drug just past the G1/S border. Experimental conditions were as described in figure 8. Data and the full dose (0 to 12 Gy) LQ fit are plotted in the form $S = \exp(-\alpha D - \beta D^2)$.

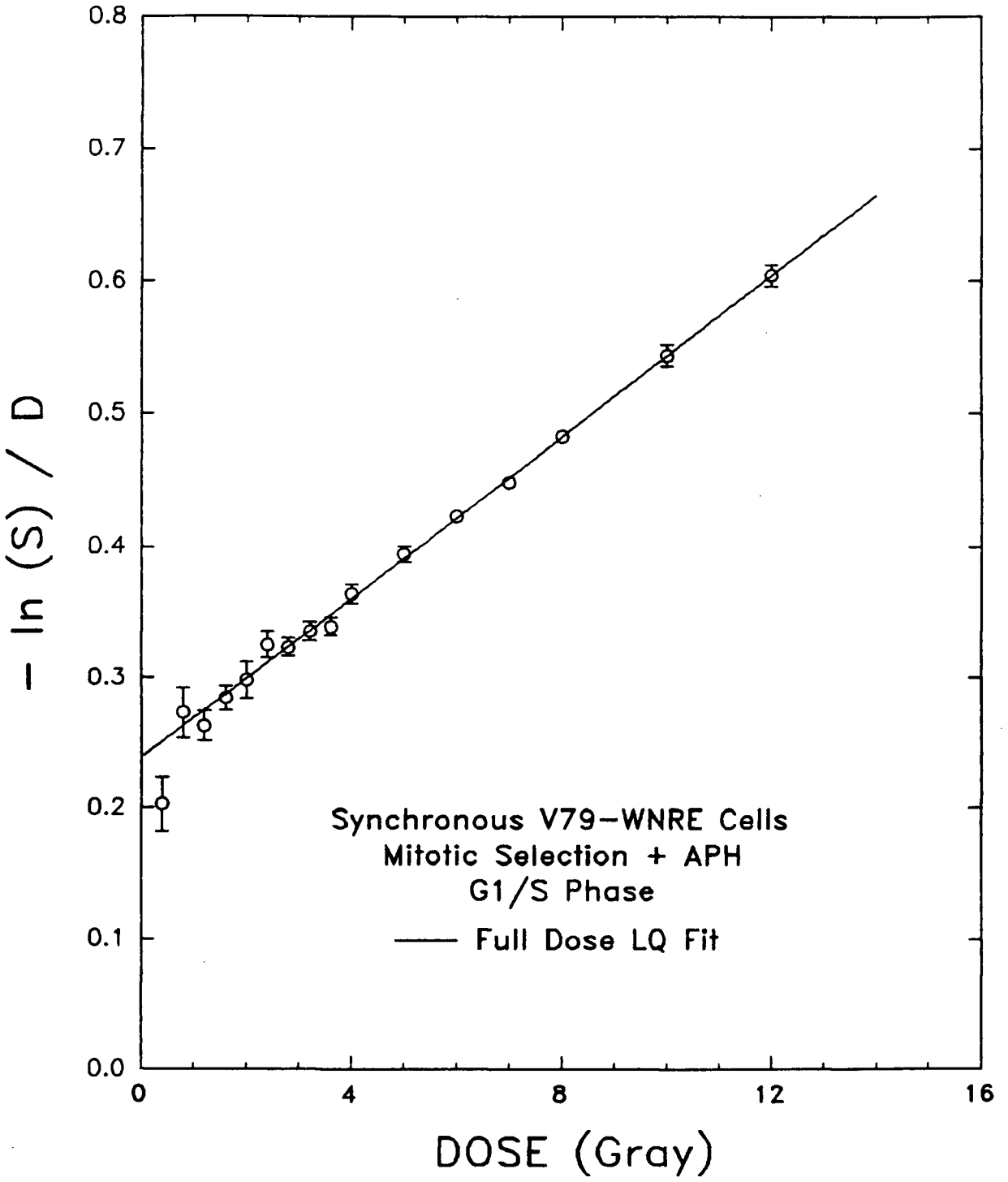

FIGURE 34 : MITOTIC SELECTION + APHIDICOLIN G1/S PHASE - II

Survival data obtained from the average of three experiments of cell populations synchronized by mitotic selection followed by 12 hour exposure to 1 μg/ml aphidicolin. Populations were irradiated 30 minutes after release from the drug just past the G1/S border. Experimental conditions were as described in figure 8. Data and the full dose (0 to 12 Gy) LQ fit are plotted in the form $-\ln S/D = \alpha + \beta D$.

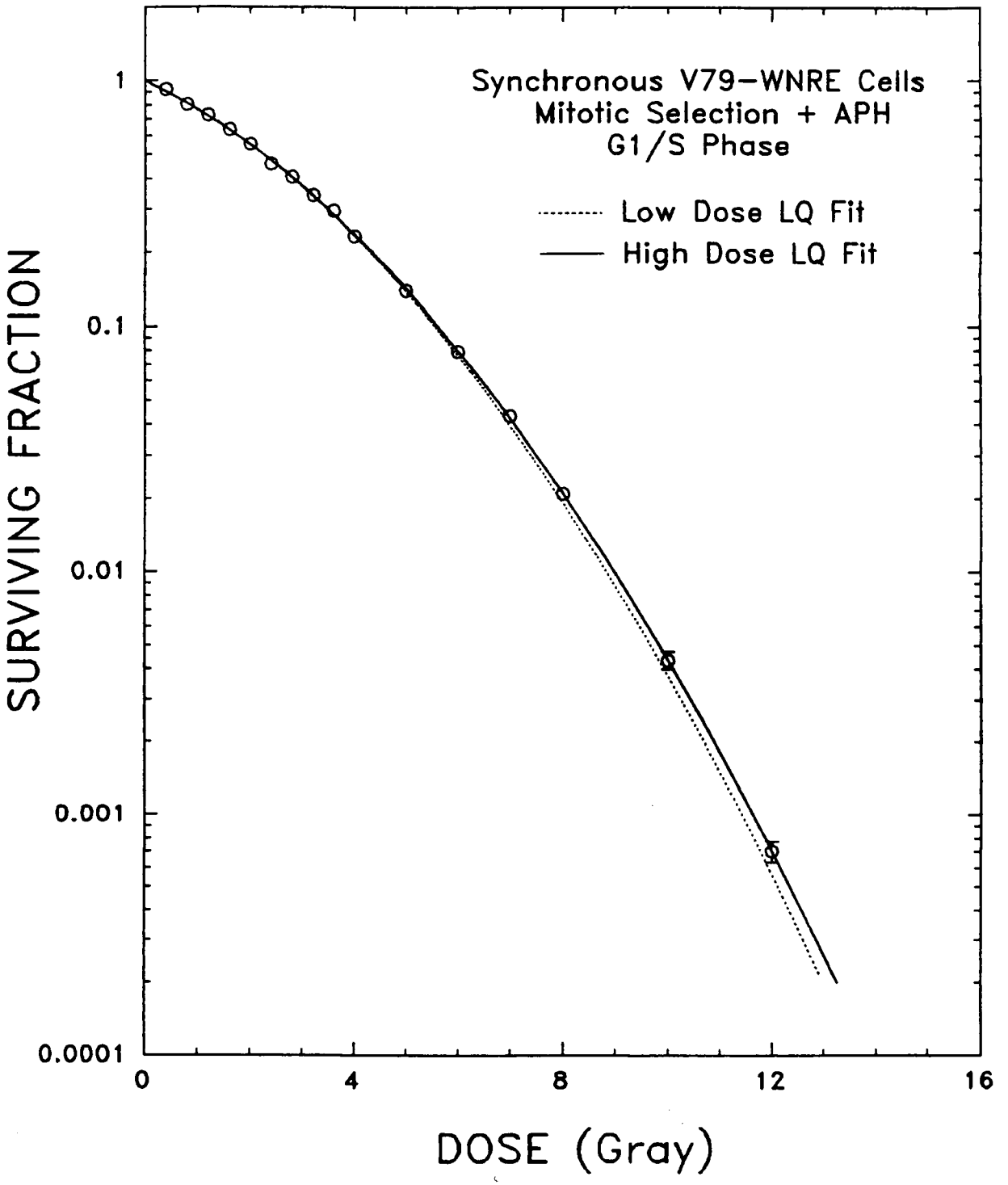

FIGURE 35 : SEPARATE FITS MITOTIC SELECTION + APH G1/S PHASE - I

The same data shown in figure 33 have been fitted separately to the LQ equation over the low dose (0 to 3.2 Gy) region (------) or the high dose (3.2 to 12 Gy) region (————). Data and separate low and high dose LQ fits and plotted in the form $S = \exp(-\alpha D - \beta D^2)$.

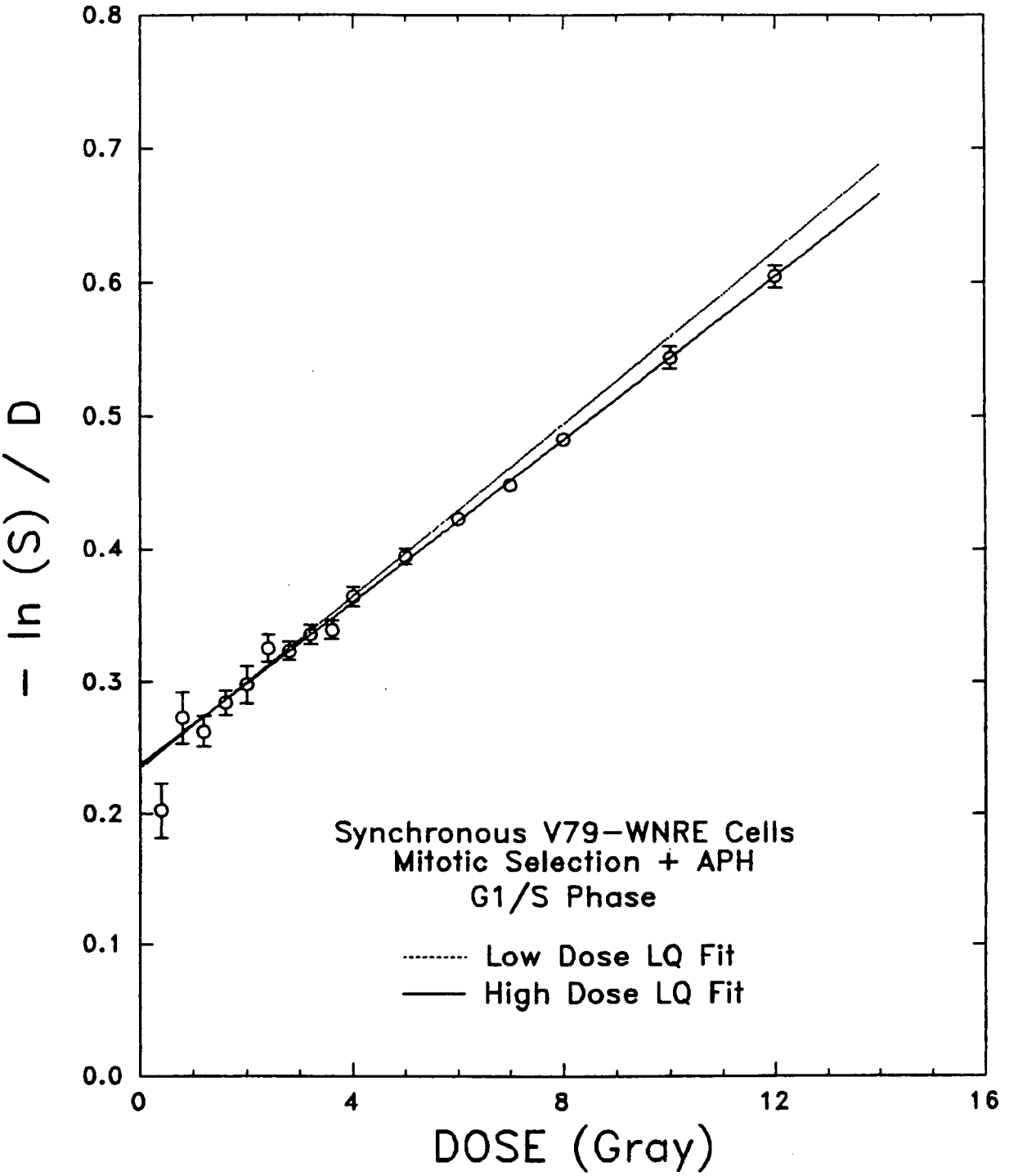

FIGURE 36 : SEPARATE FITS MITOTIC SELECTION + APH G1/S PHASE - II

The same data shown in figure 33 have been fitted separately to the LQ equation over the low dose (0 to 3.2 Gy) region (------) or the high dose (3.2 to 12 Gy) region (————). Data and separate low and high dose LQ fits and plotted in the form $-\ln S/D = \alpha + \beta D$.

4. DISCUSSION

4.1 DEGREE OF SYNCHRONY

In order for results from experiments involving synchronized cells to be meaningful, both the quality (ie. homogeneity at a particular point in the cell cycle) and the position in the cell cycle of the population must be precisely determined. Section 3.1 oulines results on the quality of synchrony of populations synchronized by mitotic selection alone or followed by a 12 hour exposure to hydroxyurea or aphidicolin. Techniques employed to determine the quality and position of the synchronized populations include evaluation of the mitotic index, measurment of the response of the synchronized population to a single dose of radiation as a function of position in the cell cycle (ie. the "age response") and the examination of FACS analyzed histograms of DNA distribution over the cell cycle.

4.1.1 Populations Synchronized By Mitotic Selection Alone

It has been recognized by others (Mitchison 1971, Grdina et al 1984, Nias and Fox 1971) that perhaps the method of choice for obtaining a synchronized population in G1 is mitotic selection alone. Improvements on the original technique of Terasima and Tolmach (1963, 1965) by Klevecz (1972, 1975) have resulted in the ability to obtain large numbers of mitotic or early post-mitotic cells of very high quality. Such capabilities are essential in order to perform radiation survival experments that require a large yield ($3x10^7$) of cells of highly uniform age specificity.

Populations obtained by mitotic selection alone were determined to be well synchronized initially as shown by indices of synchrony for the initial population of between 96.2 % and 97.7 %. Although the number of cells visibly in mitosis is relatively small (8.6 to 41.3 %), the overall population is well synchronized including cells from early metaphase to late telophase/early G1 within a "window" of time no longer than the length of mitosis (about 30 minute, Gillespie 1975). Within a short time the population has moved beyond mitosis and into G1. The uniformity of the population in G1 is observed in two ways. The age response over the cell cycle indicates that during the first 2 hours after synchronization by mitotic selection the population maintained a uniform radiation response. It is during this time (prior to 2 hours) that the G1 irradiations were performed. The slight decrease in survival at T = 1 and 2 hours from the value at T = 0 may have been an artefact arising from an imprecise determination of the control plating efficiency at the T = 0 point. The plating efficiencies (uncorrected for the zero dose plating efficiency) for the T = 0, 1, and 2 hour points are in reality equivalent. The uniformity of the G1 population (within the synchrony "window") may also be observed by the narrow width of the G1 peak in the T=0 histogram of the DNA distribution. Analysis of the histograms revealed that approximately 92.88 % of the cells were contained beneath the G1 peak, as described in section 3.1.3, and that the distribution had a coefficient of variation (CV) of 4.33% indicating a relatively narrow distribution of DNA content for the population.

Further evidence for the quality of the synchronized population may be found by analysis of the cell cycle variation in radiaton response. Figure 5 indicates a difference of just under one full log of survival between the most sensitive (G1) and resistant (late S) points in the cell

cycle when irradiated at 8 Gy. This large difference compares favorably with results of Sinclair and Morton (1965) for V79 cells indicating a similar difference in response between the most sensitive and resistant points. The quality of synchrony appears to decrease as the population moves through S and into G2 and then G1 as indicated by an increase in survival between 10 and 12 hours for the sensitive portion of the response compared to the initial sensitive region at 0 to 2 hours. The population is most highly synchronized, then, during the initial hours after mitotic selection. The response at T=6 to 7 hours, presumably at late S phase, is equivalent in resistance to similar populations released from hydroxyurea or aphidicolin, indicating that the synchrony has not yet decayed too much by that time.

Analysis of the histograms of DNA content suggest a high degree of synchrony, especially for the initial population. At T = 0, 1 or 2 hours the percentage of cells present in G1/S/G2+M (and the corresponding CV) as determined by computer analysis described in section 3.1.3 was 92.88/6.67/0.46 (0.0433), 93.33/6.16/0.51 (0.0465) and 87.52/11.77/0.71 (0.0897). An increase in the tail of the histogram, beginning at T=2 hours indicates the progression of some of the cells through G1 and into S phase. These figures, although only approximate, given the limitations of such an analysis, indicate a high degree of initial synchrony especially during the first 2 hours when the G1 irradiations would have occured. It should be noted that these results were obtained from populations initially cultured in glass roller bottles which exhibited many large clumps of cells on the growth surface which were suspected of contributing non-mitotic contaminants. Improvements in the growth conditions and a switch to plastic bottles resulted in the elimation of the clumping, but populations

obtained from these bottles showed no obvious difference in their radiation responses compared to those from the glass bottles.

4.1.2 Mitotic Selection Followed By A Drug Block

In an effort to sharpen the somewhat wider than desirable "window" of cells obtained by mitotic selection alone, populations were resynchronized at the G1/S border by exposure to hydroxyurea or aphidicolin, which act by different mechanisms to inhibit the synthesis of DNA. This combination of techniques has been used by other investigators especially to obtain highly synchronized populations in G1/S, S and G2 phase (Fox et al 1987).

The quality of the resulting populations was very high, as indicated by the age response over the cell cycle (figure 5), and by the FACS analyzed histograms of DNA distribution, (figure 6). The populations resynchronized by 1 mM hydroxyurea or 1 μg/ml aphidicolin exhibit very similar responses to a single dose (8 Gy) of radiation with both displaying just under one full log survival difference between the most sensitive and resistant points. The responses are very similar also to that obtained for mitotic selection alone showing the same levels of survival at the points of greatest and least resistance, but shifted by a few hours in the position of the peaks. The age response qualitatively indicates that the populations synchronized by mitotic selection followed by 1 mM hydroxyurea or 1 μg/ml aphidicolin are well synchronized. These results are very similar to those obtained by Hall for asynchronous Chinese hamster cells synchronized by a 6 hour treatment with 1.24 mM hydroxyurea and irradiated at 8 Gy following release from the drug. Both results indicate just under one full log survival difference between the most sensitive and resistant points. As

well, both exhibit a survival at the T = 0 point, just following release from the drug at the G1/S border, that is higher than the most sensitive point in the response (Hall 1972, Legrys and Hall 1969).

The histograms of DNA content over the cell cycle also indicate that the synchronized populations are highly uniform in their age specificity when initially released from the drug block, but show broadening of the distribution wihin a short time as indicated by the CV's for the analyzed histograms. The percentage of cells represented by the prominent peak at time T = 0, 1, 2, 3 hours (and the corresponding CV) for populations synchronized by mitotic selection followed by 1 mM hydroxyurea was 95.36% (6.61), 86.88% (6.72), 96.43% (8.61) and 98.27% (7.89). For populations synchronized by mitotic selection followed by 1 µg/ml aphidicolin the results were 93.47% (5.87), 93.22% (6.61), 96.37% (7.72) and 98.91% (8.88). The increasing value of the percentage number of cells beneath the prominent peak would incorrectly appear to indicate a population that has become more uniformly distributed as it passed through S phase. The general increase in the CV would indicate, however, that the population has experienced a broadening of the distribution of cells containing between 2n and 4n number of chronosomes. The increase in percentage under the peak may also result from inclusion of those non-viable cells in S phase killed by the drug pre-treatment.

Irradiations were performed 30 minutes (not including a 30 to 35 minute non-cycling cell handling time) after release from the drug block. The populations were irradiated at their most highly synchronized point as evidenced by the low value of the CV for T = 0 and 1 hours.

4.2 Asynchronous Experiments

The survival response of asynchronously dividing V79-WNRE cells to 250 kVp X-rays strongly suggests the prescence of substructure in the low dose region that can be resolved by separately fitting the low dose (0 to 3.2 Gy for series 1, or 0 to 2 Gy for series 2 experiments) and high dose (3.2 to 12 Gy for series 1, or 2 to 12 Gy for series 2 experiments) data to the linear-quadratic (LQ) model. Figures 10 and 14 show the substructure in the form of a "kink" in the survival curve at between 2 and 3.2 Gy. An even clearer picture is seen when replotting the same data in the linear form of the LQ equation -lnS/D vs. D as seen in figures 11 and 15.

Apart from being able to resolve the substructure in a visual manner, it has also been resolved in a statistical manner. Analysis of the LQ parameters α and β for the separate low and high dose fits indicates that differences in the low and high dose distributions of α or β are statistically significant at the P=0.001 to P=0.067 level for the initial series and at the P=0.001 to 0.11 level for the second series of asynchronous experiments (see table III). The statistical significance of this result is that there is a high degree of confidence that the low and high dose values of α or β represent statistically different distributions and that they are not subsets of the same, larger distribution of α or β values.

As well, a goodness of fit test on the various LQ fits to the data indicates that the data are better characterized by separate low and high dose fits than by a single full dose fit.

Closer examination of figures 11 and 15 may indicate that the data is best characterized not by two, but by three separate fits to the LQ equation over the dose ranges 0 to 2 Gy, 2 to 4 Gy and 4 to 12 Gy.

Figure 37 shows the series 1 asynchronous data fitted separately to the LQ equation over these dose ranges. A 2 to 12 Gy fit is also shown to indicate that a two-component fit from 0 to 2 Gy and 2 to 12 Gy provides poor characterization of the data, particularly in the 2 to 4 Gy range, as shown by an RMS deviation of 0.0281. The three-component fit provides the best fit to the data, as any multi-component fit should as the number of components is increased, with an RMS deviation of 0.0259. This is smaller than the RMS deviation for the two-component (0 to 3 Gy, 3 to 12 Gy) fit of 0.0270 or the full dose fit (0 to 12 Gy) of 0.0346.

The better fit provided by the three-component analysis may indicate the presence of more than 2 subpopulations of cells within the asynchronous population, or it may simply be showing how, in general, any fit to data can be improved by decreasing the number of points fitted per curve (the best fit, of course, being provided by a fit to 2 data points). The appearance of the mid-dose component is likely the result of a mixed population of cells that is influenced mainly by two dominant subpopulations : a sensitive subpopulation, which would primarily influence the low dose (0 to 2 Gy) region of the response, and a resistant subpopulation which would primarily influence the high dose (> 4 Gy) region of the survival response. The mid-dose region (2 to 4 Gy) may then be reflecting contributions from both subpopulations rather than from a third subpopulation of intermediate sensitivity. Perhaps the influence of a G1 subpopulation that is best characterized by the three component SH+MT model (section 4.3.3.2) could result in the appearance of three-component substructure at low dose. The exact nature of this three-component substructure is left to conjecture. Discussion in this thesis, however, will be limited to a two-component analysis of the data.

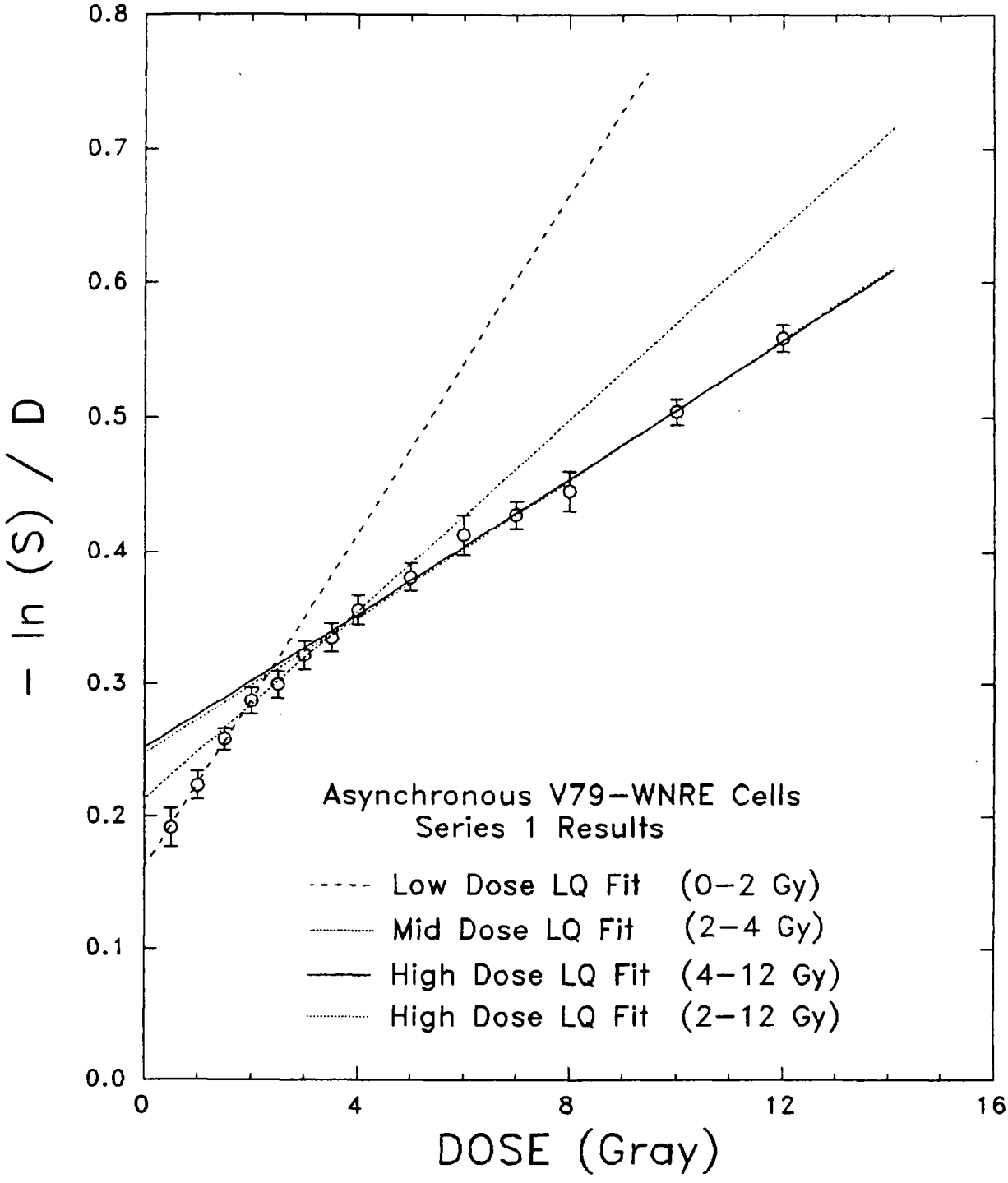

FIGURE 37 : THREE COMPONENT FIT - SERIES 1 ASYNCHRONOUS DATA

The survival data shown in figure 8 for the initial series of asynchronous experiments are shown here fitted over the dose range 0 to 2 Gy, (- - - -), 2 to 4 Gy (·····), 4 to 12 Gy (———) and 2 to 12 Gy (·····) to the LQ model and plotted in the form $-\ln(S)/D = \alpha + \beta D$.

4.3 POSSIBLE CAUSES OF THE SUBSTRUCTURE

Three possible explanations for the apparent substructure in the radiation survival response of asynchronously dividing V79-WNRE may be offered :

1). The apparent substructure may be an experimental artefact.

2). The linear-quadratic model may not be appropriate for characterizing the asynchronous response of V79-WNRE cells, and the LQ model may, in fact, have artificially created the appearance of substructure.

3). The substructure may be the result of differential killing of subpopulations of cells with different radiosensitivities. An asynchronously dividing culture contains populations of cells distributed throughout the cell cycle which, as seen in figure 5, exhibit an extensive variation in radiosensitivity. An asynchronous response is, in reality, a composite of the responses of these subpopulations. The experimental technique and the subsequent results may have been of high enough precision to accurately resolve the effects of the subpopulations on the asynchronous survival.

4.3.1 Hypothesis 1

If the observed substructure were simply an artefact of the experimental procedure used to obtain or analyze the results then we would expect some obvious (or not so obvious) differences to be present in procedures used for the low and high dose data. The fact that the substructure can be described in terms of the parameters α and β in an experimentally consistent manner for individual results (ie. the structure is present and can be described in terms of the LQ parameters from experiment to experiment) and in a statistically reproducible manner for the overall results, would suggest that any experimental artefact would have to be systematic in nature (ie. repeated from experiment to experiment). Variations in the survival assay between the low and high dose samples could produce the observed results. However, the cell sorting assay was used throughout the entire dose range and great care was taken to ensure identical treatment for all of the experimental samples. One obvious difference between the low dose and high dose procedures would relate to the dose increments used to obtain the respective samples. For samples up to 4 Gy, dose increments of 0.5 Gy, for the initial series of asynchronous experiments, or of 0.4 Gy, for all other experiments, were used. Between 4 Gy and 8 Gy, increments of 1 Gy were used, with 2 Gy increments used thereafter to obtain the 10 Gy and 12 Gy samples. Thus one should consider the possibility of some dose-fractionation effect which would tend to produce more cell killing at larger doses where there would be a higher effective dose rate (ie. a larger dose per fraction). Such an effect, which would result in a decrease in survival at larger doses, would actually dilute the appearance of substructure at low dose, rather than creating its appearance. However, the overall irradiation time did not exceed 15

minutes for any of the experiments, making it unlikely that fractionation effects would be significant in such an overall time.

Some differences also did exist in relation to the numbers of cells plated into each petri dish for the low dose and high dose samples. Typically, for asynchronous experiments, under 2500 cells (or enough to produce 500 colonies after 6 days of growth) were plated per petri dish in the dose range 0 to 4 Gy, between 4000 and 20000 cells for samples between 5 Gy and 8 Gy, and 80000 cells for the 10 Gy and 12 Gy samples. The increase in the number of cells plated at higher doses could have resulted in a "feeder effect" that may have acted to provide a more suitable growth environment due to medium conditioning at intermediate levels of plating, or a less suitable growth environment due to nutrient depletion at very high levels of plating. Studies on V79-WNRE cells designed to detect if the cells were sensitive to a feeder effect (results not shown) showed no consistent differences between feeder and non-feeder treated samples. It thus seems unlikely that the observed substructure could be attributed to experimental artefact.

4.3.2 Hypothesis 2

The results of survival studies on asynchronously dividing V79-WNRE cells indicate substructure in the low dose region of the survival in the form of a 'kink' in the survival data at about 3 Gy, as revealed by the series 1 asynchronous experiments, or at about 2 Gy, as revealed by the series 2 asynchronous experiments. The 'kink' is apparent by direct visual inspection of the data presented in the form of surviving fraction vs. dose. In an attempt to characterize the results of asynchronous cells, the data were first fit to the LQ model over the entire experimental dose range (0 to

12 Gy) but the fit was deemed unsuitable in describing the observed substructure as indicated by the obvious visual and large numerical deviation of the fit from the data. Instead of abandoning the LQ model, however, it was applied again separately to the data on either side of the observed 'kink', from 0 to 2 or 3 Gy and from 2 or 3 Gy to 12 Gy. The separate fits to the low and high dose region of the data displayed an improvement in both the visual and numerical deviation of the fit from the data, especially for the low dose data which are of particular interest. The improvement is visually more obvious when the data are replotted in the form -ln(S)/D vs D with separate LQ fits to equation 8 as evidenced by a clear departure of the low dose data from the high dose fits.

The possibility does remain, however, that the LQ model may simply be inadequate in describing precisely the survival response of asynchronously dividing V79-WNRE cells. The appropriateness of the LQ fits may be compared with those provided by other survival curve models (Alper 1980, Chapman 1980).

The multi-target model

$$S = 1 - (1 - e^{-D/D_o})^n \qquad (5)$$

has an initial slope of zero which would clearly not provide an adequate characterization of the data. The three parameter, two component multi-target plus single hit model

$$S = e^{-D/D_1} [1 - (1 - e^{-D/D_o})^n] \qquad (7)$$

accommodates a nonzero slope at zero dose by the introduction of a one-hit term. There is, however, usually not enough information in most experiments to define with any precision all three parameters of the

equation (D_1, D_o, n), resulting in the need to specify one of the parameters in order to reduce the number of independant parameters to two. Both expressions approximate to an exponential equation of the form

$$S = n\, e^{-kD} \qquad (21)$$

at high dose.

The Repair-MisRepair (RMR) model (Tobias et al 1980, 1985)

$$S = e^{-\delta D}\,(\,1 + \delta D/\epsilon\,)^{\epsilon} \qquad (11)$$

in its two parameter form may also be considered.

The data from both series of experiments involving asynchronously dividing V79-WNRE cells were fitted to the linear-quadratic (equation 8), single hit multi target (equation 7) and the repair-misrepair (equation 11) models in order to examine their appropriateness to the data. Results from the fits , shown in table VI, include the best fit parameters for each model as well as the RMS deviations of the fitted function from the data points.

The inadequacy of the RMR and SH+MT models in fitting the data is evident in figures 38 and 39 where they can be seen to consistently underestimate the amount of cell inactivation at low dose. The values of the RMS deviation of the fitted points from the data indicate that the whole data set is best characterized by (in order from best to worst) : composite LQ, full dose LQ, RMR and SH+MT. (The composite LQ is that curve which would result if the low dose data were fitted with the low dose α and β parameters and the high dose data by the high dose parameters.) The continuously bending nature of the survival curve observed for up to the four decades of the response is better accomodated by the LQ expression

than by either of the RMR or SH+MT models indicating that at least the most resistant subpopulation may be best described by the LQ model after the first decade of cell kill. It may be, however, that other subpopulations might be better described by models other than the LQ model, as would appear to be the case for G1 phase cells synchronized by mitotic selection alone (see section 4.3.3).

It would appear unlikely that any single model could explain the substructure observed in the survival response of asynchronously dividing V79-WNRE cells. The best description is found by fitting the low dose and high dose data separately to the LQ expression.

TABLE VI
SURVIVAL MODEL FIT PARAMETERS
ASYNCHRONOUS CELL EXPERIMENTS

SERIES 1 RESULTS

Equation	Parameters	RMS Deviation
$S = \exp(-\alpha D - \beta D^2)$		
Full Dose Fit (0-12 Gy)	α = 0.2447 Gy^{-1} β = 0.02607 Gy^{-2}	0.0346
Low Dose Fit (0-3 Gy)	α = 0.1896 Gy^{-1} β = 0.04447 Gy^{-2}	0.00952
High Dose Fit (3-12 Gy)	α = 0.2494 Gy^{-1} β = 0.02559 Gy^{-2}	0.0331
Two-Component Composite Fit		0.0270
Three-Component Composite Fit		0.0259
$S = e^{(-D/D_1)}\{1 - [1 - e^{(-D/D_o)}]^n\}$		
Full Dose Fit (0-12 Gy)	D_1 = 4.386 Gy D_o = 2.320 Gy n = 4.63	0.119
$S = e^{(-\delta D)}(1 + \delta D/\epsilon)^{\epsilon}$		
Full Dose Fit (0-12 Gy)	δ = 0.8707 Gy^{-1} ϵ = 2.2916	0.108

TABLE VII
SURVIVAL MODEL FIT PARAMETERS
ASYNCHRONOUS CELL EXPERIMENTS

SERIES 2 RESULTS

Equation	Parameters	RMS Deviation
$S = \exp(-\alpha D - \beta D^2)$		
Full Dose Fit (0-12 Gy)	$\alpha = 0.2491$ Gy^{-1} $\beta = 0.02251$ Gy^{-2}	0.0544
Low Dose Fit (0-2 Gy)	$\alpha = 0.2350$ Gy^{-1} $\beta = 0.04175$ Gy^{-2}	0.00471
High Dose Fit (2-12 Gy)	$\alpha = 0.2482$ Gy^{-1} $\beta = 0.02260$ Gy^{-2}	0.0622
Two-Component Composite Fit		0.0524
$S = e^{(-D/D_1)}\{1 - [1 - e^{(-D/D_o)}]^n\}$		
Full Dose Fit (0-12 Gy)	$D_1 = 11.65$ Gy $D_o = 2.01$ Gy $n = 2.934$	0.178
$S = e^{(-\delta D)}(1 + \delta D/\epsilon)^{\epsilon}$		
Full Dose Fit (0-12 Gy)	$\delta = 0.7369$ Gy^{-1} $\epsilon = 1.4179$	0.155

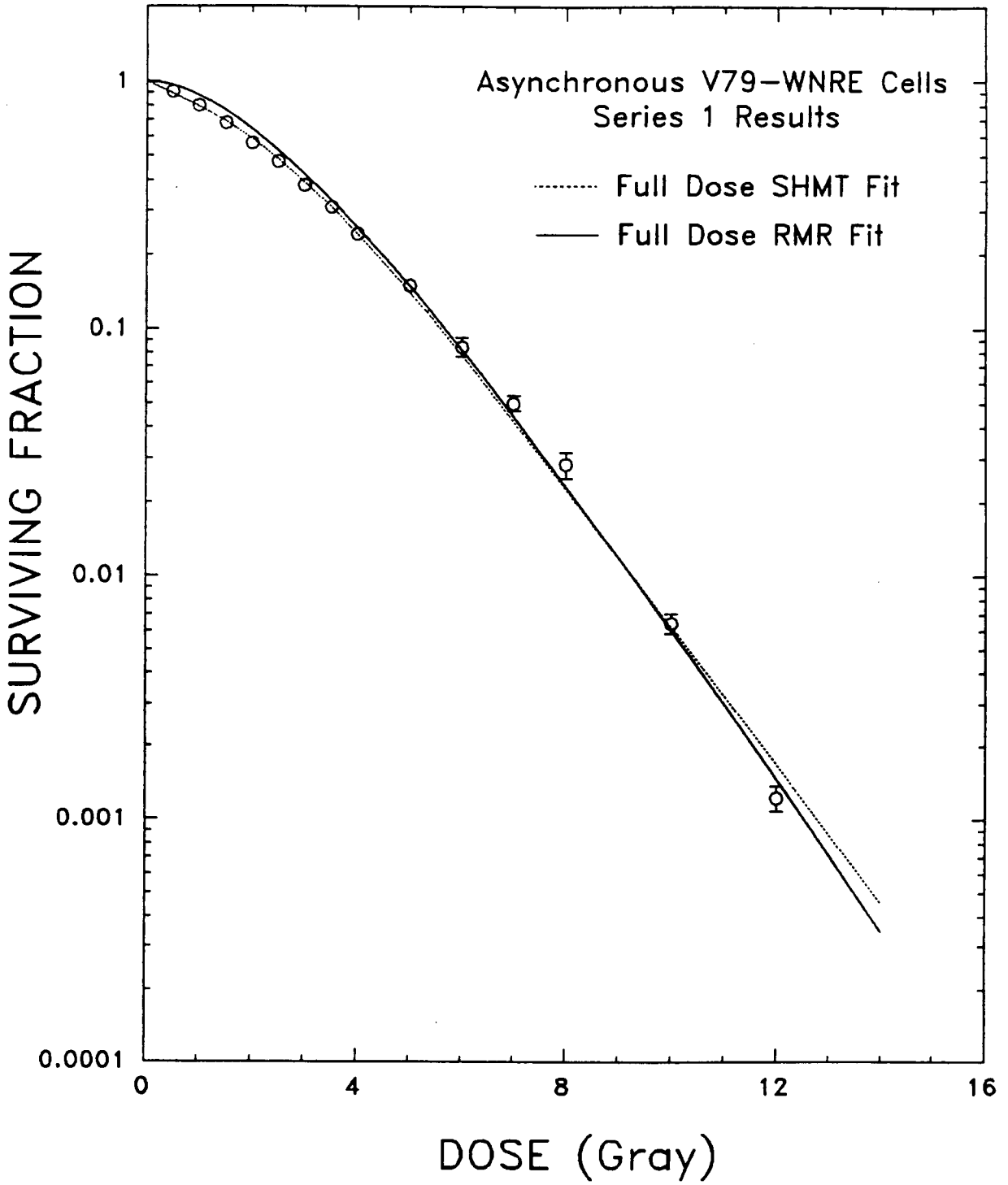

FIGURE 38 : MODEL FITS TO SERIES 1 ASYNCHRONOUS DATA

The survival data shown in figure 8 for the initial series of asynchronous experiments are shown here fitted over the full dose (0 to 12 Gy) region to the two-parameter RMR equation (———) and to the three-parameter SH+MT equation (--------).

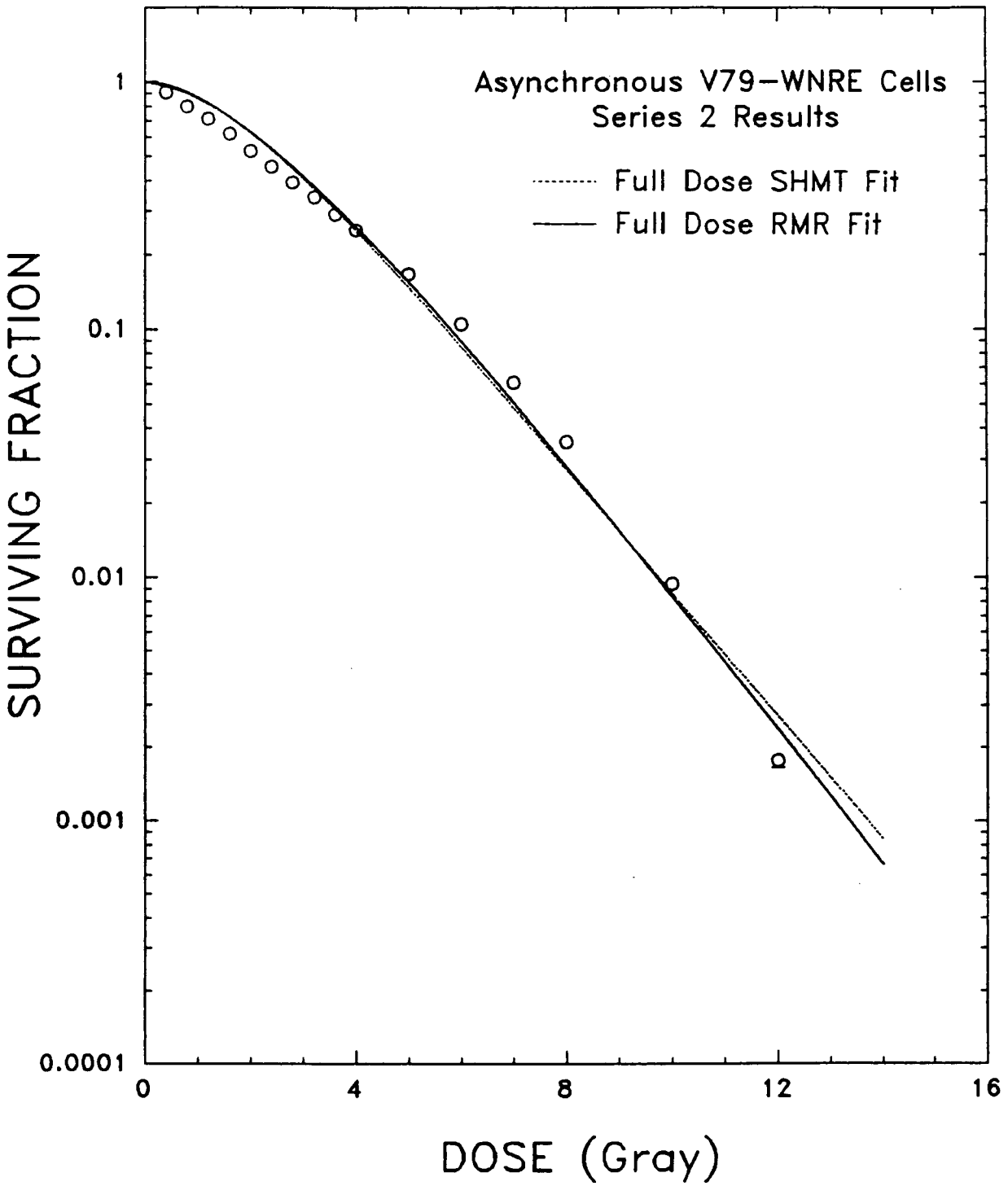

FIGURE 39 : MODEL FITS TO SERIES 2 ASYNCHRONOUS DATA

The survival data shown in figure 14 for the second series of asynchronous experiments are shown here fitted over the full dose (0 to 12 Gy) region to the two-parameter RMR equation (————) and to the three-parameter SH+MT equation (·····).

4.3.3 Hypothesis 3

In order to test hypothesis 3, that the observed substructure was due to differential killing of subpopulations of cells with different radiosensitivities, studies were carried out on more homogeneous populations of synchronized cells. An attempt could have been made to reproduce the substructure by measuring the survival response at several stages of the cell cycle and then synthesizing from those responses the expected asynchronous response, as has been done by Gillespie et al using the response of synchronized populations of V79-379A cells (Gillespie 1975). However, their results indicated large deviations between the synthesized curve and the actual asynchronous data. It is perhaps unrealistic to expect to be able to exactly reproduce the substructure observed in the asynchronous response through such an analysis.

A more direct test of the hypothesis would be to determine if the substructure is absent in the radiation reponse of synchronized cells. If the response of a tightly synchronized population at some phase of the cell cycle failed to exhibit the same kind of substructure then the hypothesis would be supported. The absence of substructure could be indicated by the ability of the data to be characterized adequately by a single LQ expression, and hence appear to fit a single straight line when plotted in the form -ln(S)/D vs D. It could also be indicated by the ability of the data to be characterized adequately by any other single model of cell inactivation, such as those discussed in section 4.3.2, in which case the data may not appear to fit a single straight line when plotted in the form -ln(S)/D vs D since this type of plot tests the data only in terms of the LQ equation.

4.3.3.1 Mitotic Selection Followed By A Drug Block

Experiments were conducted on populations synchronized by mitotic selection followed by a 12 hour exposure to 1 mM hydroxyurea and irradiated after 30 minutes of free cycling time from release of the drug, just past the G1/S border. The results, shown in figures 27 and 28, show a clear absence of the substructure that was present in the asynchronous response. This is indicated by the ability of a single LQ expression to adequately characterize the response as is most evident in figure 26. It is also apparent from statistical analysis of the α and β values for the individual experimental fits that the low dose and high dose parameter values are not significantly different ($P>0.5$). These results, then, are in clear support of hypothesis 3.

Almost identical results were obtained for cells treated similarily to the samples described above except that mitotic selection was followed by a 12 hour exposure to 1 µg/ml aphidicolin instead of hydroxyurea. Figures 33 and 34 for such populations again show a clear absence of substructure indicated by the ability of a single LQ expression to adequately characterize the response. As well, a similar statistical analysis revealed no significant difference between the low dose and high dose values of the LQ parameters α or β ($P>0.5$). These results also support the hypothesis that the substructure in the asynchronous response is due to subpopulations of cells with different cell-cycle dependent radiosensitivities.

Results from populations synchronized by mitotic selection followed by 1 mM hydroxyurea and irradiated after 2 to 3 hours free cycling time upon release from the drug, as shown in figures 31 and 32, indicate the prescence of substructure. The data may be fitted to the RMR and SH+MT

equations, as shown in figure 40, but an even poorer fit to the data is obtained as indicated by RMS deviations of 0.0643 for the RMR fit, 0.0933 for the SH+MT fit, 0.0607 for the global LQ fit, and 0.0328 for the composite LQ fit. The presence of the substructure is somewhat puzzling. As noted earlier, however, the populations irradiated following 2 to 3 hours of free cycling time after release from hydroxyurea may have been partially composed of cells that had rushed through S and into G2 phase, as evidenced by the obvious drop in radiation response between 1 1/2 to 2 hours in figure 5 and by an increase in the coefficient of variation of the DNA histograms for the T = 2 and 3 hour distributions. The substructure may be reflecting the presence of a sensitive G2 population mixed in with the dominant S phase population.

TABLE VIII
SURVIVAL MODEL FIT PARAMETERS
SYNCHRONOUS CELL EXPERIMENTS
MITOTIC SELECTION FOLLOWED BY HYDROXYUREA

G1/S PHASE CELLS

Equation	Parameters	RMS Deviation
$S = \exp(-\alpha D - \beta D^2)$		
Full Dose Fit (0-12 Gy)	α = 0.2186 Gy^{-1} β = 0.03473 Gy^{-2}	0.0396
Low Dose Fit (0-3.2 Gy)	α = 0.2126 Gy^{-1} β = 0.03744 Gy^{-2}	0.00649
High Dose Fit (3.2-12 Gy)	α = 0.2182 Gy^{-1} β = 0.03476 Gy^{-2}	0.0523
Composite Fit		0.0394
$S = e^{(-D/D_1)}\{1 - [1 - e^{(-D/D_o)}]^n\}$		
Full Dose Fit (0-12 Gy)	no convergence in the parameters	
$S = e^{(-\delta D)}(1 + \delta D/\epsilon)^{\epsilon}$		
Full Dose Fit (0-12 Gy)	δ = 1.1953 Gy^{-1} ϵ = 5.2225	0.136

TABLE IX
SURVIVAL MODEL FIT PARAMETERS
SYNCHRONOUS CELL EXPERIMENTS
MITOTIC SELECTION FOLLOWED BY HYDROXYUREA

S/G2 PHASE CELLS

Equation	Parameters	RMS Deviation
$S = \exp(-\alpha D - \beta D^2)$		
Full Dose Fit (0-12 Gy)	α = 0.2800 Gy^{-1} β = 0.02249 Gy^{-2}	0.0607
Low Dose Fit (0-3.2 Gy)	α = 0.1729 Gy^{-1} β = 0.05480 Gy^{-2}	0.0185
High Dose Fit (3.2-12 Gy)	α = 0.2942 Gy^{-1} β = 0.02106 Gy^{-2}	0.0401
Composite Fit		0.0285
$S = e^{(-D/D_1)}\{1 - [1 - e^{(-D/D_o)}]^n\}$		
Full Dose Fit (0-12 Gy)	D1 = 16.077 Gy D2 = 1.805 Gy n = 2.934	0.0933
$S = e^{(-\delta D)}(1 + \delta D/\epsilon)^{\epsilon}$		
Full Dose Fit (0-12 Gy)	δ = 0.7582 Gy^{-1} ϵ = 1.2841	0.0644

TABLE X
SURVIVAL MODEL FIT PARAMETERS
SYNCHRONOUS CELL EXPERIMENTS
MITOTIC SELECTION FOLLOWED BY APHIDICOLIN

G1/S PHASE CELLS

Equation	Parameters	RMS Deviation
$S = \exp(-\alpha D - \beta D^2)$		
Full Dose Fit (0-12 Gy)	$\alpha = 0.2385$ Gy^{-1} $\beta = 0.03048$ Gy^{-2}	0.0158
Low Dose Fit (0-3.2 Gy)	$\alpha = 0.2351$ Gy^{-1} $\beta = 0.03237$ Gy^{-2}	0.0145
High Dose Fit (3.2-12 Gy)	$\alpha = 0.2377$ Gy^{-1} $\beta = 0.03056$ Gy^{-2}	0.0156
Composite Fit		0.0155
$S = e^{(-D/D_1)}\{1 - [1 - e^{(-D/D_o)}]^n\}$		
Full Dose Fit (0-12 Gy)	no convergance in the parameters	
$S = e^{(-\delta D)}(1 + \delta D/\epsilon)^{\epsilon}$		
Full Dose Fit (0-12 Gy)	$\delta = 1.0115$ Gy^{-1} $\epsilon = 3.2764$	0.123

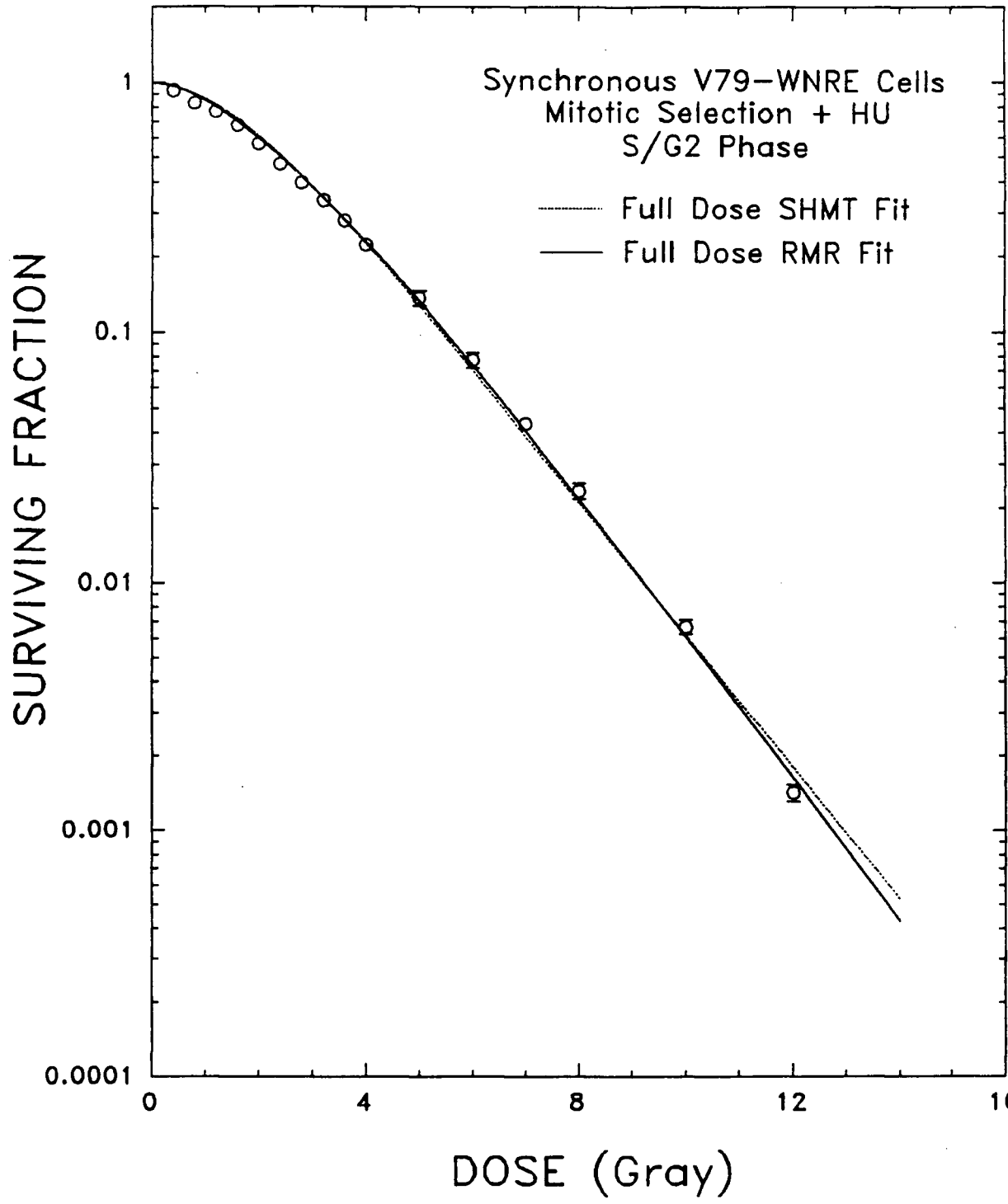

FIGURE 40 : MODEL FITS TO MITOTIC SELECTION + HU S/G2 PHASE DATA

The survival data shown in figure 29, for the average response of populations synchronized by mitotic selection followed by 12 hour exposure to 1 mM hydroxyurea and irradiated 2 to 3 hours after release from the drug, are shown here fitted to the two-parameter RMR (————) and three-parameter SH+MT (- - - - - -) models over the full dose range (0 to 12 Gy).

4.3.3.2 Mitotic Selection Alone

Populations irradiated 30 to 90 minutes of free cycling time after mitotic selection alone (ie G1 phase cells) appear to indicate the presence of substructure in the low dose region of the response as indicated by the separate LQ fits in figures 20 and 21. Before accepting this conclusion it is important to analyze the data in terms of other models of cell inactivation. The same data fitted to the repair-misrepair and the two component, three parameter single hit multi-target models show a substantially better fit than to the linear-quadratic equation as shown in figure 41. Table XI lists the RMS deviations and parameter values of the functions fitted to the data. Simple observation of the G1 phase data clearly indicates a terminal exponential region beyond about 4 Gy. The data, including the terminal exponential, are fit very well by a single SH+MT equation over the full dose range of the data as indicated by a very low RMS deviation of 0.0294. The RMR model fits the data well with an RMS deviation of 0.0363, but does not accomodate the terminal exponential quite as well as the SH+MT equation. The global LQ equation provides the poorest fit with an RMS deviation of 0.157. The substructure that is apparent in figures 20 and 21 is thus most likely an artefact of imposing the LQ expression to data that are best described by another model, in this case the two component SH+MT. This is an example of a hypothesis 2 (section 4.3) type of explanation to describe the presence of substructure in a response ie. that the LQ model has, in fact, artificially created the appearance of substructure in the response of G1 phase cells.

If one tries to reconcile the substructure in the G1 response (figures 20 and 21) using the same approach taken to reconcile the substructure in

the asynchronous response, then the three hypotheses (section 4.3) must be considered.

Hypothesis 1 (the artefact explanation) may be eliminated as a possibility based on the arguements in section 4.3.1.

Hypothesis 3 (the subpopulation explanation) applies only if it is suspected that the G1 population was not of uniform age. Sections 3.1 and 4.1 indicate a high degree of synchrony in the populations, although a small degree of contamination by non-mitotic cells at harvest was always assumed. The possibility does exist that the contaminant subpopulation, if it were more radioresistant than the G1 population, could have increased the overall survival of the population. This would be particularly noticeable at higher dose when most of the sensitive G1 cells would be killed. If the response of a purely homogeneous population of G1 cells did, in reality, follow a single continuously bending LQ function, one could possibly imagine how a small resistant subpopulation could straighten out the tail of the response so that it appeared to follow an exponential at high dose. This does not, however, appear to be a plausible explanation given the uniform age of the G1 population.

It must also be mentioned that the G1 population was comprised of cells within a 30 minute window of time, approximately, in the cell cycle, as explained in sections 3.1.1 and 4.1.1. It is unlikely that within this age distribution that subpopulations at slightly different times in G1 could have produced the observed substructure; the age response of the cells (figure 5) shows very little variation in radiosensitivity within the 1 to 2 hour period after mitotic selection during which time irradiations occured.

The remaining hypothesis, that the substructure is an artefact of an improperly applied LQ fit, has been shown to have some validity in figure 41 where the data are shown to be well characterized by a single SH+MT or RMR fit. This does leave a puzzling result, however, in that it appears as though the fundamental shape of the survival curve has changed as the population of cells traversed the cell cycle from G1, where the response may be described by a SH+MT or RMR model fit, to G1/S phase, where the response is described by a LQ model fit. The results are complicated further if this is interpreted as a change in the mechanisms of cell lethality that underly the different models depending on the position of the population in the cell cycle. Such an interpretation would contradict other studies and would, at the very least, require further investigation (Gillespie 1975).

TABLE XI
SURVIVAL MODEL FIT PARAMETERS
SYNCHRONOUS CELL EXPERIMENTS
MITOTIC SELECTION ALONE

G1 PHASE CELLS

Equation	Parameters	RMS Deviation
$S = \exp(-\alpha D - \beta D^2)$		
Full Dose Fit (0-12 Gy)	$\alpha = 0.4514$ Gy^{-1} $\beta = 0.02168$ Gy^{-2}	0.157
Low Dose Fit (0-3.2 Gy)	$\alpha = 0.2043$ Gy^{-1} $\beta = 0.09231$ Gy^{-2}	0.0217
High Dose Fit (3.2-12 Gy)	$\alpha = 0.4896$ Gy^{-1} $\beta = 0.01786$ Gy^{-2}	0.115
Composite Fit		0.0766
$S = e^{(-D/D_1)}\{1 - [1 - e^{(-D/D_o)}]^n\}$		
Full Dose Fit (0-12 Gy)	$D_1 = 5.882$ Gy $D_o = 1.636$ Gy $n = 2.886$	0.0294
$S = e^{(-\delta D)}(1 + \delta D/\epsilon)^{\epsilon}$		
Full Dose Fit (0-12 Gy)	$\delta = 0.8723$ Gy^{-1} $\epsilon = 0.7965$	0.0363

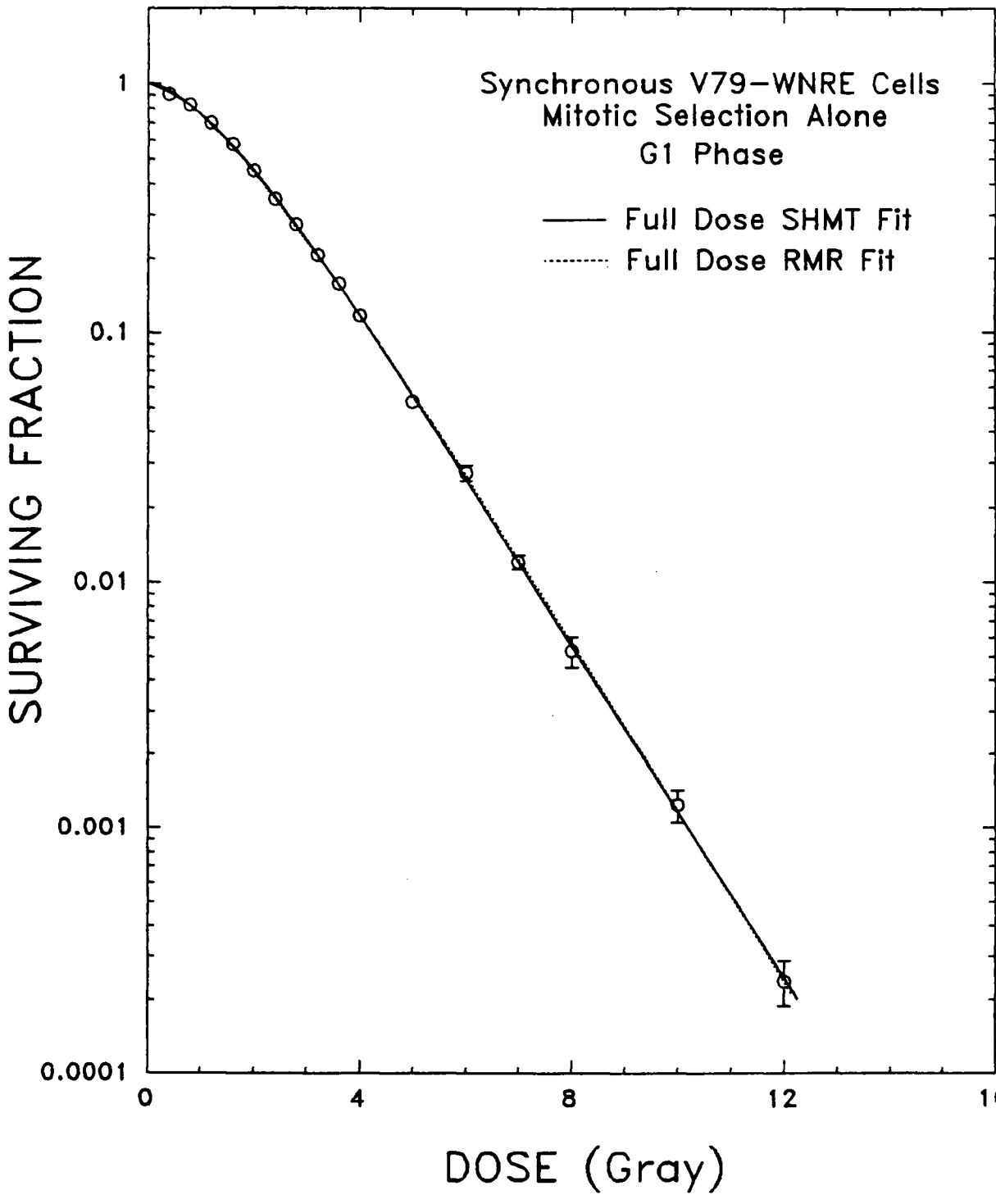

FIGURE 41 : MODEL FITS TO MITOTIC SELECTION G1 PHASE DATA

The survival data shown in figure 18, for the averaged response of populations synchronized by mitotic selection alone and irradiated in G1 phase, are shown here fitted to the two-parameter RMR (- - - - - -) and three-parameter SH+MT (———) models over the full dose range (0 to 12 Gy).

Experiments conducted on S phase cells irradiated 6 hours of free cycling time after mitotic selection are suggestive that the substructure may not be present in such a population. Although, since only two experiments were averaged to obtain the results seen in figures 23 and 24 no confident statement can be made regarding the substructure. The results do appear to indicate a slightly reversed shape to the substructure than previously observed for other cell populations as shown by a larger value of α in the -ln(S)/D vs D plot for the low dose fit compared to the α for the high dose fit. The reason for such a reversal in the substructure appearance may simply be that the data collected from the two experiments is not precise enough to indicate the true nature of the survival response. Another possibility is that the reverse nature of the substructure may be the result of forcing the LQ equation onto data that is actually best represented by an LQ fit in the low to mid doses and then by an exponential thereafter. The data up to 8 Gy appears to be best fitted by a single LQ expression. The divergence of the 10 Gy and 12 Gy points could be indicative of the beginning of a terminal exponential region in the survival curve at high dose. Such a situation is described by Alper where she produces a -ln(S)/D vs D plot for a hypothetical population described at low dose by the LQ equation and terminating with an exponential at high dose, as seen in figure 42 (Alper 1979). Alper raises this discussion in order to illustrate the difficulty in examing the validity of the LQ expression over the full dose range of the data using the -ln(S)/D vs D plot. She makes the point that when data of this type are plotted in the form -ln(S)/D vs D the curve ABCDE would result with an inflection at B (see figure 42). She then states that "the accuracy with which the fractional survival can be determined is unlikely to allow that curve to be distinguished from the straight line ABD, and this method of plotting might

therefore give the impression that the LQ expression was a good description over a dose range almost twice as great as was actually the case" (Alper 1979). Alper states this in support of her idea that the LQ model is simply a low dose approximation to shouldered survival curves (Alper 1980).

Further experimentation over an extended dose range would have to be performed in order to verify this possibility. The continuously bending nature of the high dose region of the asynchronous survival curve, however, would appear to indicate that at least the most radioresistant subpopulation (ie. late S phase) of the asynchronous population would follow the LQ expression. This suggests that the slightly reversed nature of the substructure may be due to experimental imprecision that could only be resolved by increasing the number of like experiments considered.

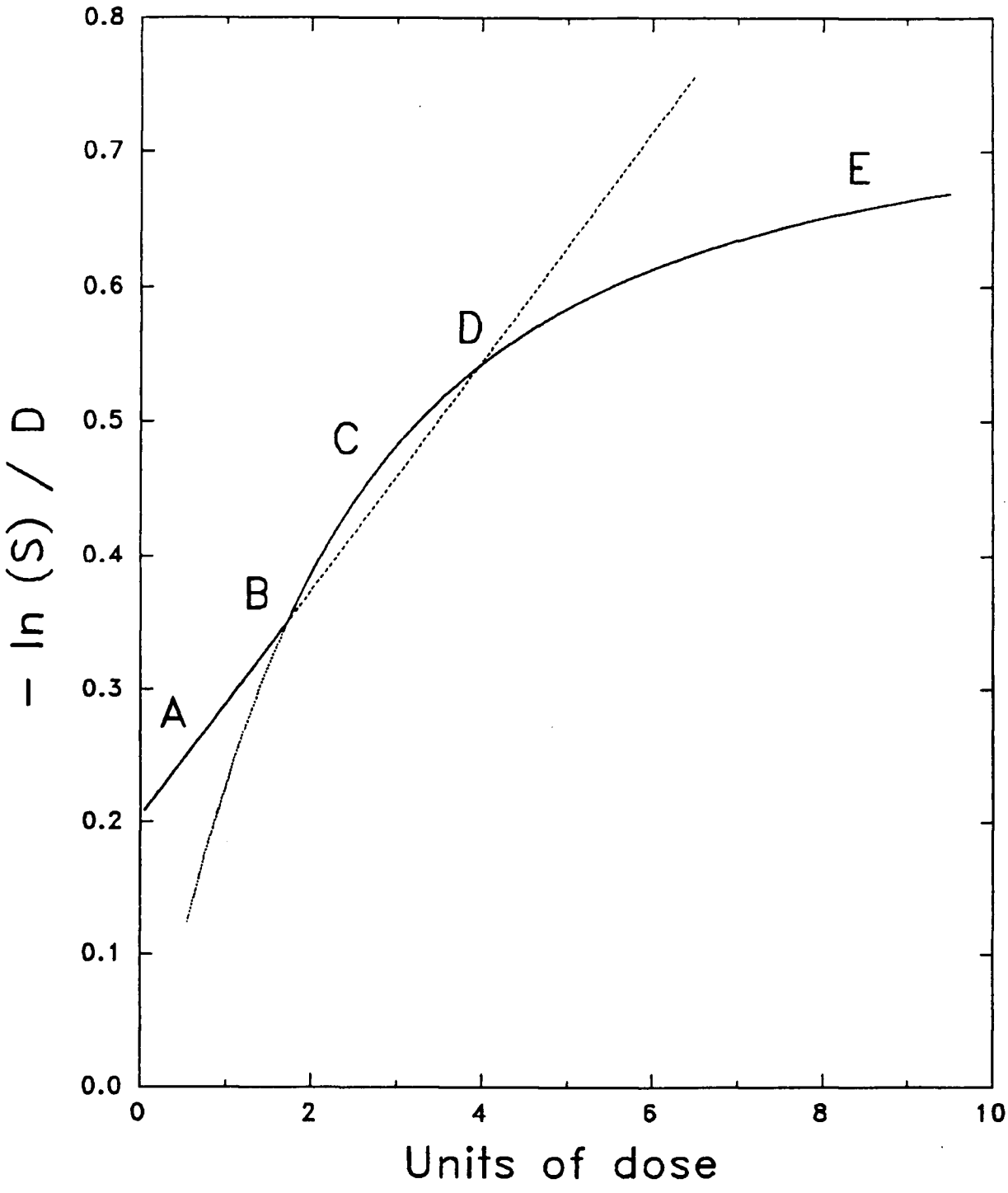

FIGURE 42 : SHOULDERED SURVIVAL PLOT WITH A TERMINAL EXPONENTIAL

A hypothetical -lnS/D vs D plot of data that may be well described by the LQ equation at low dose, but by an exponential at higher doses (the curve ABCDE). According to Alper, departure of the data from the LQ equation $\ln S = -\alpha D - \beta D^2$ (------) used to describe the initial region of a shouldered survival curve may be difficult to detect in the region BCD given the usual limitation of experimental uncertainty.

5. CONCLUSION

The radiation survival response of asynchronously dividing populations of the cell line V79-WNRE indicate substructure in the low dose region that can be best characterized by separately fitting the data within the low and high dose regions to the linear-quadratic equation, $S = \exp(-\alpha D-\beta D^2)$. The structure has been resolved visually by plotting the data in the linear form of the LQ equation as $-\ln(S)/D$ vs D. Further evidence for the presence of the substructure has come from statistical analysis of the linear-quadratic fit parameters α and β obtained by separate low and high dose fits to the LQ equation which has shown that the low dose fit values of α and β are significantly different from the high dose fit values.

The presence of the substructure in the asynchronous response has been shown to result from differential killing of subpopulations of cells with different cycle-dependent radiosensitivities. In particular, the substructure appears to be due to the radiosensitive cell component (G1 and perhaps G2) and the degree to which it is present in the cell population. This was demonstrated by the lack of substructure in the survival response of populations that were double-synchronized by mitotic selection followed by 1 mM hydroxyurea or 1 µg/ml aphidicolin and irradiated while tightly synchronized soon after release from the drug block. Such populations were uniformly composed of cells just past the G1/S border in early S phase. When similar populations were irradiated 2 to 3 hours after release from the drug block, at which time the high degree of synchrony initially present had decayed so that the population was comprised of resistant S phase and sensitive G2 phase cells, the presence of substructure was again apparent in the survival response.

The response of populations synchronized by mitotic selection alone and irradiated in G1 showed very clear evidence of substructure when fitted with the LQ equation, but could be accurately characterized by a single fit to the SH+MT or RMR equations. Once similar populations had sufficiently progressed beyond G1 and into S phase (but not to G2) to eliminate the presence of sensitive cells, the responses of such populations appeared to once again show a lack of substructure and are well described by a single LQ equation.

The results, although somewhat perplexing, appear to indicate a fundamental change in the form of the radiation response or in the makeup of the population as the cells progress from G1, where the response is well characterized by a single fit to the SH+MT or RMR equations, to S phase, where a single fit to the LQ equation has been shown to describe both early S and mid-late S phase populations synchronized by two different techniques. Further investigation is required to accurately determine the nature of the sensitive G2 phase response.

Hence, the substructure at low dose in the radiation survival response of asychronously dividing populations of V79-WNRE cells appears to result from radio-sensitive subpopulations of cells that are not only naturally present in the asynchronous population, but may also (in the case of G1 cells) be better described by different equations for cell inactivation than that used to describe the response of the radio-resistant subpopulations.

APPENDIX A - STATISTICAL METHODS

Statistical methods used in this thesis to examine the presence or absence of substructure in the averaged survival response of a particular population of cells include :

1). Student's t-test, and

2). nonparametric tests.

These tests were applied to the sets of best-fit parameter values α and β of the linear-quadratic (LQ) model, $S = \exp(-\alpha D -\beta D^2)$, obtained by fitting the LQ model to each of the individual responses that were part of a series of experiments. Fits were performed separately to the data points included within the low dose range (0 to 2, 3 or 3.2 Gy), high dose range (2, 3 or 3.2 to 12 Gy) or full dose range (0 to 12 Gy). The set of parameter values, α or β, obtained from the low dose fits were then compared to the parameter values obtained from the high dose fits in order to discover and evaluate differences between the parameter values for the separate fits. Statistical methods were employed in order to determine the level at which differences between the low and high dose parameter samples were statistically significant.

A.1 Students T-Test

Student's t-test may be used to evaluate the level of significance represented by the difference between two samples. The t-test may be applied in two forms for two samples that are either paired or independant (unpaired). In both cases it is assumed that each member of the two samples is normally and independantly distributed.

A.1.1 Paired Analysis

For two samples that are closely related to each other by a variable relevant to the effect being considered, a paired t-test may be used to increase the accuracy of the comparison. The conditions for which a paired analysis is used, however, are not always clearly outlined or obvious.

One may consider a sample consisting of i pairs of normal, independent deviates. The first member of each pair, X_{1i}, may represent the result produced by a procedure that is different from that used to produce the second member, X_{2i}. The differences between the members of each pair may be designated D_i and are assumed to be distributed about a mean μ_D which represents the average difference in the effects of the two procedures over the populaton of which these pairs are a random sample. Deviations of the differences from the mean, $D_i - \mu_D$, are assumed to be normally and independantly distributed with a population mean of zero.

With these assumptions, the sample mean difference $\bar{D}$ may be considered normally distributed about μ_D with standard deviation σ_D of the population of differences. The population standard deviation is usually not known, but it may be approximated by the sample standard deviation, given by

$$S_D = \left[\sum_{i=1}^{n} (D_i - \bar{D})^2 / (n-1) \right]^{\frac{1}{2}}$$

The standard error $\sigma_{\bar{D}} = \sigma_D/\sqrt{n}$ may be approximated by $S_{\bar{D}} = S_D/\sqrt{n}$. The t-statistic may then be defined as an approximation to the standard normal deviate as,

$$t = (\bar{D} - \mu_o)/S_{\bar{D}}$$

This quantity follows Student's t-distribution with (n - 1) degrees of freedom, where n equals the number of pairs.

The t-distribution may be used to test the null hypothesis or to determine confidence intervals for μ_D. A test of significance may be conducted to determine the confidence level at which the null hypothesis is valid ie. that $\mu_D = 0$, implying that the mean difference between the two samples is zero. In this case t may be computed from

$$t = \bar{D}/s_{\bar{D}}$$

For n-1 degrees of freedom, the probability (or P value) that the null hypothesis is valid may be determined from the t-distribution which is usually presented in tabular form. Small P values ($P < 0.05$) indicate rejection of the null hypothesis whereas large values ($P > 0.50$) indicate a high degree of acceptance. Another way of stating this is that the probability P corresponds to the risk associated with the rejection of the null hypothesis.

All P values in this thesis are quoted using a two-tailed test of the mean ie. that deviations from the null hypothesis could occur in either direction.

A.1.2 Unpaired Analysis

When no pairing has been used, the two samples are considered to be independent with means $\bar{X}_1$ and $\bar{X}_2$ that are estimates of the respective population means μ_1 and μ_2. The t-distribution is again the basis of significance tests and confidence intervals concerning the population difference $\mu_1 - \mu_2$. In this case, however, the t-statistic now has the value

$$t' = [(\bar{X}_1 - \bar{X}_2)-(\mu_1 - \mu_2)] / S_{X1-X2}$$

It is assumed that X_1 and X_2 are normally distributed and independent and hence X_1-X_2 is also normally distributed.

The denominator of t', S_{X1-X2}, is a sample estimate of the population standard error of X_1-X_2 given by

$$S_{\bar{X}1} - S_{\bar{X}2} = [\ S^2_{X1}/n_1 \ + \ S^2_{X2}/n_2\ ]^{\frac{1}{2}}$$

where S^2_{X1} and S^2_{X2} are sample estimates of the population standard deviations σ^2_{X1} and σ^2_{X2}, where it is assumed that σ_{X1} does not equal σ_{X2}.

In comparing the means of two independent samples having degrees of freedom given by $\nu_1 = n_1-1$ and $\nu_2 = n_2-1$, the approximate number of degrees of freedom in t' is given by

$$\nu' = (v_1 + v_2)^2 / (v^2_1/ \nu_1 \ + \ v^2_2/ \nu_2)$$

where $v_1 = S^2_{X1}/n_1$ and $v_2 = S^2_{X2}$. The value of ν' was rounded down to the nearest integer when referring to the t-distribution table.

The null hypothesis (ie. $\mu_1 - \mu_2 = 0$) was tested by calculating for t'

$$t' = (X_1-X_2) / [\ (S^2_1/n_1 \ + \ S^2_2/n_2)\ ]^{\frac{1}{2}}$$

For ν' degrees of freedom the probability (P value) that the null hypothesis is valid was then determined from a t-distribution table.

A.2 Nonparametric Tests

The t-test deals with the comparison of the means of the two samples, paired or independent, from populations that are assumed to follow normal distributions. If this assumption is seriously violated, a "nonparametric" technique that is free from any distribution requirements may be applied. Two nonparametric tests are considered is this analysis : the signed-rank test, which corresponds to the paired t-test, and the W-test, which corresponds to the unpaired t-test.

A.2.1 The Signed-Rank Test

The signed-rank test (originated by Wilcoxin) may be applied as a substitute for the t-test in paired samples. To carry out this test, one first ranks the absolute values of the differences, the smallest difference being assigned rank 1. The sign corresponding to the difference is then restored to the ranking. The ranks with negative or positive signs are totalled separately. The test criterion is the smaller of these two totals. This number, sign ignored, may be referred to a table of P values for the signed-rank test (Snedecor, Wonnacott).

The null hypothesis being tested in this case is that the frequency distribution of the original measurements is the same for both members of a pair, but the shape of the distribution does not need to be specified. Consequently, the null hypothesis implies that each rank is equally likely to be + or -. Another way of stating the null hypothesis is that the two underlying populations are identical and hence the objective of the test is to detect whether the two underlying populations are centered differently (Wonnacott).

A.2.2 The Rank-Sum (W) Test

The W-test may be applied as a substitute for the t-test of two independant samples. The null hypothesis being tested is the same as described for the signed-rank test.

To carry out the test, all of the observations (not differences) from both samples are combined and ranked with the smallest observation being assigned rank 1. (The actual values, not absolute, are referenced.) Care must be taken to distinguish the ranks assigned to members of each of the samples. The ranks from each sample are summed and the smaller of the two summed ranks, W, is referred to a table of P values for the rank-sum test to determine the level of significance. Small values of W indicate rejection of the null hypothesis, which implies that one population has a higher median (Snedecor).

6. BIBLIOGRAPHY

AAPM Report No. 18 (1986)
A Primer On Low-Level Ionizing Radiation And Its Biological Effects. American Association Of Physicists In Medicine, American Institute Of Physics, New York.

Alper, T. (1979)
Cellular Radiobiology. Cambridge University Press, Cambridge.

Alper, T. (1980)
Keynote Address : Survival Curve Models. In: Radiation Biology in Cancer Research, R.E. Meyn and H.R. Withers, eds. Raven Press, New York. 3-18.

Ashihara, T. and Baserga, R. (1979)
Cell Synchronization. Methods In Enzymology, 58, 248-262.

Becker, W.M. (1986)
The World Of The Cell. Benjamin/Cummings, Menlo Park.

Bender, M.A. and Gooch, P.C. (1962)
The Kinetics Of X-Ray Survival Of Mammalian Cells *in vitro*. Int. J. Radiat. Biol., 5, 133-145.

The BEIR Report. (1972)
The Effects On Populations Of Exposure To Low Levels Of Ionizing Radiation. National Academy of Sciences, National Research Council.

BEIR III Report. National Academy of Sciences. Committee on the Biological Effects of Ionizing Radiations. (1980)
The Effects On Populations Of Exposure To Low Levels Of Ionizing Radiation : 1980. National Academy Press, Washington, D. C.

Blakely, E.A., Chang, P.Y. and Lommel, L. (1985)
Cell-Cycle-Dependent Recovery From Heavy-Ion Damage In G_1-Phase Cells. Radiat. Res., 104, S145-S157.

Brosing, J.W. (1983)
Measurements Of Cell Survival At Low Doses Of Radiation. Ph.D. Thesis, University of British Columbia.

Chadwick, K.H. and Leenhouts, H.P. (1973)
A Molecular Theory Of Cell Survival. Physics Med. Biol., 18, 78-87.

Chadwick, K.H. and Leenhouts, H.P. (1981)
The Molecular Theory Of Radiation Biology. Springer-Verlag, Berlin.

Chapman, J.D., Todd, P. and Sturrock, J. (1970)
X-Ray Survival Of Cultured Chinese Hamster Cells Resuming Growth After Plateau Phase. Radiat. Res., 42, 590-600.

Chapman, J.D., Reuvers, A.P., Borsa, J., Petkau, A. and McCalla, D.R. (1972)
Nitrofurans As Radiosensitizers Of Hypoxic Mammalian Cells. Cancer Res., 32, 2630-2632.

Chapman, J.D., Gillespie, C.J., Reuvers, A.P. and Dugle, D.L. (1975)
The Inactivation Of Chinese Hamster Cells By X-Rays : The Effects Of Chemical Modifiers On Single- and Double-Events. Radiat. Res., 64, 365-375.

Chapman, J.D. (1980)
Biophysical Models Of Mammalian Cell Inactivation By Radiation. In: Radiation Biology in Cancer Research, R.E. Meyn and H.R. Withers, eds. Raven Press, New York. 21-32.

Deacon, J., Peckham, M.J. and Steel, G.G. (1984)
The Radioresponsiveness Of Human Tumors And The Initial Slope Of The Cell Survival Curve. Radiother. Oncol., 2, 317-323.

Douglas, B.G. and Fowler, J.F. (1975)
Fractionation Schedules And A Quadratic Dose-Effect Relationship. Br. J. Radiol., 48, 502-504.

Durand, R.E. (1986)
Use Of A Cell Sorter For Assays Of Cell Clonogenicity. Cancer Res., 46, 2775-2778.

Elkind, M.M. and Sutton, H. (1959)
X-Ray Damage And Recovery In Mammalian Cells In Culture. Nature, 184, 1293-1295.

Elkind , M.M. and Sutton, H. (1960)
Radiation Response Of Mammalian Cells Grown In Culture. 1. Repair Of X-Ray Damage Of Surviving Chinese Hamster Cells. Radiat. Res., 13, 556-593.

Elkind, M.M. and Whitmore, G.F. (1967)
The Radiobiology Of Cultured Mammalian Cells. Gordon and Breach, New York.

Fertil, B., Malaise, E.P. (1981)
Inherent Cellular Radiosensitivity As a Basic Concept For Human Tumor Radiotherapy. Int. J. Radiat. Oncol. Biol. Phys., 7, 621-629.

Fertil, B., Dertinger, H., Courdi, A. and Malaise, E.P. (1984)
Mean Inactivation Dose : A Useful Concept For Intercomparison Of Human Cell Survival Curves. Radiat. Res., 99, 73-84.

Fertil, B., Malaise, E.P. (1985)
Intrinsic Radiosensitivity Of Human Cell Lines Is Correlated With Radioresponsiveness Of Human Tumors : Analysis Of 101 Published Survival Curves. Int. J. Radiat. Oncol. Biol. Phys., 11, 1699-1707.

Freshney, R.I. (1983)
Culture Of Animal Cells : A Manual Of Basic Technique. Alan R. Liss Inc., New York.

Fricke, H. and Hart, E.J. (1966)
Chemical Dosimetry. In : Radiation Dosimetry, Volume II, Instrumentation. F.H. Attix and W.C. Roesch eds. Academic Press, New York, 126.

Fried, J., Perez, A.G. and Clarkson, B. (1980)
Quantitative Analysis Of Cell Cycle Progression Of Synchronous Cells By Flow Cytometry. Exp. Cell Res., 126, 63-74.

Fowler, J.F. (1987)
Principles Of Fractionation In Radiotherapy. In : Radiobiology In Radiotherapy, N.M. Bleehen, ed. Springer-Verlag, London. 53-58.

Fox, M.H., Read, R.A. and Bedford, J.S. (1987)
Comparison Of Synchronized Chinese Hamster Ovary Cells Obtained By Mitotic Shake-Off, Hydroxyurea, Aphidicolin or Methotrexate. Cytometry, 8, 315-320.

Gillespie, C.J., Chapman, J.D., Reuvers, A.P. and Dugle, D.L. (1975a)
The Inactivation Of Chinese Hamster Cells By X-Rays : Synchronized and Exponential Cell Populations. Radiat. Res., 64, 353-364.

Gillespie, C.J., Chapman, J.D., Reuvers, A.P. and Dugle, D.L. (1975b)
Survival Of X-Irradiated Hamster Cells : Analysis In Terms Of the Chadwick-Leenhouts Model. In : Cell Survival After Low Doses Of Radiation : Theoretical and Clinical Implications, T. Alper, ed. The Institute of Physics and John Wiley and Sons, London. 25-33.

Goodhead, D.T. (1980)
Models Of Radiation Inactivation And Mutagenesis. In: Radiation Biology in Cancer Research, R.E. Meyn and H.R. Withers, eds. Raven Press, New York. 231-247.

Grdina, D.J., Meistrich, M.L., Meyn, R.E., Johnson, T.S. and White, R.A. (1984)
Cell Synchrony Techniques. I. A Comparison Of Methods. Cell Tissue Kinetics, 17, 223-236.

Hall, E.J. (1972)
The Effect Of Hypoxia On The Repair Of Sublethal Radiation Damage In Cultured Mammalian Cells. Radiat. Res., 49, 405-415.

Hall, E.J. (1988)
Radiobiology For The Radiologist. J.B. Lippincott Company, Philadelphia.

Howard, A. and Pelc, S.R. (1953)
Synthesis Of Deoxyribonucleic Acid In Normal And Irradiated Cells And Its Relation To Chromosome Breakage. Heredity, 6, 261-273.

Ikegami, S., Taguchi, T., Ohashi, M., Oguro, M., Nagano, H., Mano, Y., (1978)
Aphidicolin Prevents Mitotic Cell Division By Interfering With The Activity Of DNA Polymerase-α. Nature, 275, 458-459.

Iliakis, G., Nusse, M. and Bryant,P. (1982)
Effects Of Aphidicolin On Cell Proliferation, Repair Of Potentially Lethal Damage And Repair Of DNA Strand Breaks In Ehrlich Ascites Tumour Cells Exposed To X-Rays. Int. J. Radiat. Biol., 42, 417-434.

Iliakis, G., Pantelias, G., Okayasu, R. and Seaner, R. (1989)
Comparative Studies On Repair Inhibition By AraA, AraC And Aphidicolin Of Radiation Induced DNA And Chromosome Damage In Rodent Cells : Comparison With Fixation Of PLD. Int. J. Rad. Oncol. Biol. Phys., 16, 1261-1265.

Johns, H.E. & Cunningham, J.R. (1983)
The Physics of Radiology. Charles C. Thomas, Springfield.

Kellerer, A.M. and Rossi, H.H. (1972)
The Theory Of Dual Radiation Action. Current Topics Radiat. Res., 8, 85-158.

Kellerer, A.M. and Rossi, H.H. (1978)
A General Formulation Of Dual Radiation Action. Radiat. Res., 75, 471-488.

Klevecz, R.R. (1972)
An Automated System For Cell Cycle Analysis. Anal. Biochem., 49, 407-415.

Klevecz, R.R. (1975)
Temporary Structure Of S Phase Analyzed Using An Automated Synchrony System. Biotech. and Bioeng., 17, 675-694.

Legrys, G.A. and Hall, E.J. (1969)
The Oxygen Effect And X-Ray Sensitivity In Synchronously Dividing Cultures Of Chinese Hamster Cells. Radiat. Res., 37, 161-172.

Lewis, E.B. (1957)
Leukemia and Ionizing Radiation. Science, 125(3255), 965-972.

Malaise, E.P., Fertil, B., Deschavanne, P.J., Chavaudra, N., and Brock, W.A. (1987)
Initial Slope Of Radiation Survival Curves Is Characteristic Of The Origin Of Primary And Established Cultures Of Human Tumor Cells And Fibroblasts. Radiat. Res., 111, 319-333.

Mazia, D. (1961)
The Cell Cycle. Science, xx, 55-64.

Mitchison, J.M. (1971)
Biology Of The Cell Cycle. Cambridge University Press, Cambridge.

McCulloch, E.A. and Till, J.E. (1962)
The Sensitivity Of Cells From Normal Mouse Bone Marrow To Gamma Radiation *in vitro* and *in vivo*. Radiat. Res., 16, 822-832.

Monahan, J.J. and Hall, R.H. (1974)
Magnesium Acetate Treatment Of Roller Bottles For The Preparation Of Uniform Cell Monolayers. Prep. Biochem., 4, 353-358.

National Cancer Institute Of Canada (1989)
National Cancer Institute Of Canada : Canadian Cancer Statistics 1989, Toronto.

Nias, A.H.W. and Fox, M. (1971)
Synchronziation Of Mammalian Cells With Respect To The Mitotic Cycle. Cell Tissue Kinet., 4,375-398.

Ngo, F.Q.H., Blakely, E.A., Tobias, C.A., Chang, P.Y. and Lommel, L. (1988)
Sequential Exposures Of Mammalian Cells To Low- and High-LET Radiations : II. As A Function Of Cell-Cycle Stages. Radiat. Res., 115, 54-69.

Pedrali-Noy, G. and Spadari, S. (1979)
Effect Of Aphidicolin On Viral And Human DNA Polymerases. Biochem. Biophys. Res. Comm., 88, 1194-1202.

Pedrali-Noy, G. and Spadari, S. (1980)
Aphidicolin Allows A Rapid and Simple Evaluation Of DNA-Repair Synthesis In Damaged Human Cells. Mutation Research, 70, 389-394.

Petersen, D.F., Anderson, E.C. and Tobey, R.A. (1968)
Mitotic Cells As A Source Of Synchronized Cultures. Meth. Cell Physiol., 3, 347-370.

Prescott, D.M. (1978)
The Reproduction Of Eukaryotic Cells. Carolina Biological Supply Company, Burlington, N.C.

Puck, T.T. and Marcus, P.I. (1956)
Action Of X-Rays On Mammalian Cells. J. Exp. Med., 103, 653-666.

Ritenour, E.R. (1984)
Overview Of The Hazards Of Low-Level Exposure To Radiation In : Health Effects Of Low-Level Radiation, W.R. Hendee ed. Appleton-Century-Crofts, East Norwalk, Conn. 13-22.

Sinclair, W.K. (1966)
The Shape Of Radiation Survival Curves Of Mammalian Cells Cultured *in vitro*. In: Biophysical Aspects of Radiation Quality, I.A.E.A., Vienna. 21-48.

Sinclair, W.K. (1967)
Hydroxyurea : Effects On Chinese Hamster Cells Grown In Culture. Cancer Research, 27, 297-308.

Sinclair, W.K. and Morton, R.A. (1963)
Variations In X-Ray Response During The Division Cycle Of Partially Synchronized Chinese Hamster Cells In Culture. Nature, 199, 1158-1160.

Sinclair, W.K. and Morton, R.A. (1965)
X-Ray and Ultraviolet Sensitivity Of Synchronized Chinese Hamster Cells At Various Stages Of The Cell Cycle. Biophys. J., 5, 1-25.

Skarsgard, L.D. and Harrison, I. (1990a)
Dose Dependance Of The Oxygen Enhancement Ratio (OER) In Radiation Inactivation Of V79 Cells. Radiat. Res. (submitted).

Skarsgard, L.D., Harrison, I. and Durand, R.E. (1990b)
The Radiation Response Of Asynchronous Cells At Low Dose: Evidence Of Substructure. Radiat. Res. (submitted).

Skarsgard, L.D. and Wilson, D.J. (1990c)
Survival At Low Dose In Asynchronous And Partially Synchronized V79-171 Cells. Radiat. Res. (submitted).

Snedecor, G.W. (1980)
Statistical Methods. Iowa State University Press, Ames Iowa.

Steel, G.G., McMillan, T.J. and Peacock, J.H. (1989)
The Picture Has Changed In The 1980s. Int. J. Radiat. Biol., 56, 525-537.

Stubblefield, E. (1968)
Synchronization Methods For Mammalian Cell Cultures. Meth. Cell Phys., 3, 25-43.

Stryer, L. (1988)
Biochemistry. W. H. Freeman and Company, New York.

Terasima, T. and Tolmach, L.J. (1961)
Changes In X-Ray Sensitivity Of HeLa Cells During The Division Cycle. Nature, 190, 1210-1211.

Terasima, T. and Tolmach, L.J. (1963)
Growth and Nucleic Acid Synthesis In Synchronously Dividing Populations Of HeLa Cells. Exp. Cell Res., 30, 344-362.

Tobias, C.A., Blakely, E.A., Ngo, F.Q.H. and Yang, T.C.H. (1980)
The Repair-Misrepair Model Of Cell Survival. In: Radiation Biology in Cancer Research, R.E. Meyn and H.R. Withers, eds. Raven Press, New York. 195-230.

Tobias, C.A. (1985)
The Repair-Misrepair Model In Radiobiology : Comparison To Other Models. Radiat. Res., 104, S77-S95.

UNSCEAR (1982)
Report of the United Nations Scientific Committee on the Effects of Atomic Radiation, General Assembly document, 37th Session, Supplement No. 45 (A/37/45). United Nations, New York.

Wheatley, D. (1982)
Cell Growth and Division. E. Arnold, London

Willmer, E.N. (1964)
Cells and Tissues In Culture : Methods, Biology and Physiology. Academic Press, London.

Wonnacott, T.H. and Wonnacott, R.J. (1977)
Introductory Statistics. John Wiley and Sons, New York.

Yu, C.K. and Sinclair, W.K. (1967)
Mitotic Delay and Chromosomal Aberrations Induced By X-Rays In Synchronized Chinese Hamster Cells *In Vitro*. J. Nat. Canc. Inst., 39, 619-622.